

A FUZZY METHOD FOR MODELING AND FORECASTING HUMAN POPULATION



by

Duygun Fatih Demirel

Submitted to Graduate School of Natural and Applied Sciences
in Partial Fulfillment of the Requirements
for the Degree of Doctor of Philosophy in
Systems Engineering

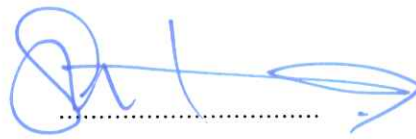
Yeditepe University

2019

A FUZZY METHOD FOR MODELING AND FORECASTING HUMAN POPULATION

APPROVED BY:

Prof. Dr. Melek Başak
(Thesis Supervisor)
(Yeditepe University)



Prof. Dr. Linet Özdamar
(Yeditepe University)



Prof. Dr. Temel Öncan
(Galatasaray University)



Assoc. Prof. Dr. Serol Bulkan
(Marmara University)



Assist. Prof. Dr. Zeynep Ocak
(Yeditepe University)



DATE OF APPROVAL: .../.../2019

ACKNOWLEDGEMENTS

First, I would like to thank my advisor Prof. Dr. Melek Başak, for her trust in me and I would like her to know how deeply grateful and appreciated I am for her precious support, and guidance she has given me throughout this research. My research has become more attractive and successful by means of her advices and motivations.

Also, I am so grateful for all help, Prof. Dr. Linet Özdamar and Assoc. Prof. Dr. Serol Bulkan who offer advices as my thesis committee members.

I would like to thank Prof. Dr. Ali Taylan Ula, Assoc. Prof. Dr. Dilek Tüzün Aksu and Assist. Prof. Dr. Semih Yalçındağ for their support and contribution during the modeling phase of my study.

Moreover, I would like to express my sincere gratitude to TUBITAK (Scientific and Technological Research Council of Turkey) – BİDEB (Scientist Support Directorate) for their financial support.

Finally and for most, I am grateful to my precious family for their limitless support and encouragement throughout my life and their share in whatever I have achieved till now.

ABSTRACT

A FUZZY METHOD FOR MODELING AND FORECASTING HUMAN POPULATION

Human population modeling and forecasting are significant issues in development planning and financial and public decision making. Age-specific population estimates of immediate future or long-term forecasts shape the policies in allocating the resources among public and private investments and the future population. In literature, population estimation is generally based on deterministic or stochastic models for the three vital demographic indicators: mortality, fertility, and migration. The existing deterministic and stochastic models for demographic modeling and forecasting rely on strict assumptions which may sometimes be difficult to satisfy.

Considering the above mentioned issues, a fuzzy bi-level method for modeling and forecasting age-specific demographic indicators is proposed in this thesis study. The bi-level structure embedded in the model makes use of the well-known Lee-Carter method as well as fuzzy regression, singular value decomposition technique, unconstrained nonlinear optimization, and hierarchical clustering approaches; and reflects the general characteristics of the country of concern together with the distinct demographic behaviors of the age groups. Time series models through Bayesian approach are fitted to the time-variant fuzzy parameters obtained via the proposed fuzzy bi-level method to forecast future demographic values. Finally, the future mortality, fertility, and migration forecasts are aggregated within a novel fuzzy population estimation model based on the conventional cohort component method. The proposed novel method is applied on age-specific mortality, fertility, and migration data of Finland, and the future demographic values and population levels are forecasted. In addition, the outputs of the proposed fuzzy method are compared with the outputs of an existing Bayesian method. The numerical findings display that the proposed fuzzy method yields superior forecasts within narrower prediction intervals compared to the existing Bayesian approach, therefore, it can be viewed as an efficient method for modeling and forecasting age specific demographic values and the future population.

ÖZET

İNSAN NÜFUSU MODELLEMESİ VE TAHMİNİ İÇİN BULANIK BİR YÖNTEM

İnsan nüfusu modellemesi ve tahmini kalkınma planları ile ekonomik ve kamusal kararlarda önemli bir yer teşkil etmektedir. Öyle ki, geleceğe dönük yaşa bağlı nüfus tahminleri özel teşebbüs ve kamu kaynaklarının gelecek nüfusa aktarımı ve dağıtımını şekillendiren politikaları etkilemektedir. Literatürde nüfus tahminleri genel olarak üç temel demografik unsur olarak ifade edilen ölüm, doğum ve göç değerlerinin deterministik ve stokastik yöntemlerle modellenmesine dayanır. Ancak, hem deterministik hem de stokastik modellerin karşılanması zor olan bir takım varsayımlara dayandıkları bilinmektedir.

Bu çalışmada, yukarıda bahsedilen durumları göz önünde bulundurarak demografik unsurları modellemek ve gelecek değerleri tahmin etmek amacıyla iki seviyeli yaşa özel bir bulanık yöntem önerilmektedir. Modele gömülü olan iki seviyeli yapı literatürde sıkça karşılaşılan Lee-Carter metoduna dayanmakta olup bulanık regresyon, tekil değer ayrışımı, kısıtsız doğrusal olmayan programlama ve hiyerarşik kümeleme yöntemlerini kullanmaktadır. Bu iki seviyeli yapı ile ilgilenilen ülkenin genel özelliklerinin demografik unsurlar üzerine etkileriyle birlikte yaş gruplarının farklı demografik davranışları da yansıtılmaktadır. Demografik unsurların gelecek değerlerini tahmin etmek amacıyla bulanık yöntemden elde edilen parametreler üzerine Bayesgil bir yaklaşımla zaman serisi modelleri oluşturulmuştur. Tahmin edilen gelecek ölüm, doğum ve göç değerleri yeni ve özgün bir bulanık nüfus modeli ile birleştirilmiş, böylece gelecek nüfus değerlerinin tahminine yönelik bir bulanık nüfus modeli ortaya konmuştur. Önerilen özgün yöntem Finlandiya'ya ait ölüm, doğum ve göç verileri üzerine uygulanmış ve geleceğe dönük nüfus seviyeleri tahmin edilmiştir. Ayrıca önerilen yöntemden elde edilen sonuçlar literatürde yer alan Bayesgil bir yöntemin sonuçlarıyla kıyaslanmıştır. Sayısal bulgular önerilen yöntemin var olan yönteme kıyasla daha dar tahmin aralıklarında daha doğru sonuçlar verdiğini göstermekte, böylece önerilen bulanık yöntemin yaşa özel demografik unsurlar ve nüfus değerlerini modellemek ve tahmin etmek için etkili bir yaklaşım olabileceğini ortaya koymaktadır.

TABLE OF CONTENTS

ACKNOWLEDGEMENTS	iii
ABSTRACT.....	iv
ÖZET	v
LIST OF FIGURES	x
LIST OF TABLES	xiii
LIST OF SYMBOLS/ABBREVIATIONS.....	xv
1. INTRODUCTION	1
1.1. CONTENT OF THE STUDY	1
2. MODELS IN AGE-SPECIFIC DEMOGRAPHIC FORECASTING	3
2.1. MORTALITY MODELING AND FORECASTING APPROACHES.....	4
2.1.1. Lee-Carter Model and Its Variants	4
2.1.1.1. Renshaw-Haberman Model	6
2.1.1.2. Multiple Population Models	6
2.1.1.3. Hyndman-Ullah Model.....	8
2.1.2. Cairns-Blake-Dowd Model and Its Variants	9
2.1.3. Time Series Extrapolation of Age-Specific Mortality Rates	10
2.2. FERTILITY MODELING AND FORECASTING APPROACHES	12
2.2.1. Curve Fitting Approaches	12
2.2.1.1. Hadwiger Model	13
2.2.1.2. Coale-Trussel Model	14
2.2.1.3. Peristera-Kostaki Model	14
2.2.2. Relational Models	15
2.2.3. Spline Models	17
2.2.4. Other Approaches	18

2.2.4.1.	Logistic Models	19
2.2.4.2.	Simple Nonparametric Methods.....	19
2.2.4.3.	Dimension Reduction Methods	20
2.3.	MIGRATION MODELING AND FORECASTING APPROACHES	22
2.3.1.	Model Migration Schedules.....	22
2.3.2.	Logit Models.....	26
2.3.3.	Bayesian Approaches.....	29
2.4.	COHORT COMPONENT METHOD	31
2.4.1.	Estimating the Population at Age Five and Over	32
2.4.2.	Estimating the Population Below Age Five.....	33
2.4.3.	Other Demographic Outcomes	35
2.4.4.	Applications Areas.....	38
2.5.	LESLIE MATRIX.....	39
3.	MOTIVATION FOR THE STUDY	41
3.1.	CONTRIBUTIONS AND RESEARCH AIMS OF THE STUDY	42
3.2.	A SUMMARY OF THE PROPOSED METHOD.....	43
4.	METHODOLOGY	45
4.1.	PRELIMINARIES	45
4.1.1.	Fuzzy Set Theory and Related Terminology.....	45
4.1.2.	Singular Value Decomposition.....	48
4.2.	FUZZY LEE-CARTER MODEL	48
4.3.	BI-LEVEL FUZZY AGE SPECIFIC DEMOGRAPHIC MODEL	49
4.3.1.	Level-I: Modeling Country Profile.....	51
4.3.1.1.	Fuzzification Phase	51
4.3.1.2.	Estimation Phase.....	53

4.3.2. Level-II: Modeling Age-Cluster Factor.....	56
4.3.3. Forecasting Future Migration Values	58
4.4. MODELING AND FORECASTING THE POPULATION	60
5. NUMERICAL FINDINGS.....	63
5.1. MORTALITY RESULTS	66
5.1.1. Mortality Data	66
5.1.2. Validity of FMM Modeling Results	69
5.1.3. Comparison of FMM and KSM	70
5.1.4. Mortality Modeling Results of FMM and BMM	73
5.1.5. Mortality Forecasting Results of FMM and BMM	75
5.2. FERTILITY RESULTS	78
5.2.1. Fertility Data.....	78
5.2.2. Fertility Modeling Results	80
5.2.3. Fertility Forecasting Results	82
5.3. MIGRATION RESULTS.....	85
5.3.1. Migration Data.....	85
5.3.2. Migration Modeling Results.....	91
5.3.3. Migration Forecasting Results.....	96
5.3.4. Sensitivity Analysis	99
5.4. POPULATION FORECASTS	101
5.4.1. Error Comparisons.....	103
5.4.2. Age Distributions.....	106
6. DISCUSSION AND FUTURE PERSPECTIVES	109
6.1. ON RESULTS FOR DEMOGRAPHIC COMPONENTS	109
6.2. ON POPULATION FORECASTS	111

6.3. FURTHER RESEARCH AREAS..... 113

7. CONCLUSION 116

REFERENCES 118

APPENDIX A..... 132

APPENDIX B 135

APPENDIX C 140

APPENDIX D..... 144



LIST OF FIGURES

Figure 2.1. The standard model migration schedule	23
Figure 4.1. Triangular fuzzy number with α -cut.....	46
Figure 4.2. Reflection, extension, contraction and shrinkage operations of NM algorithm	55
Figure 5.1. Observed mortality rates, females	67
Figure 5.2. Observed mortality rates, males	67
Figure 5.3. Observed ln-mortality rates, females.....	68
Figure 5.4 Observed ln-mortality rates, males.....	68
Figure 5.5. Fitting mortality rates for age group [20,25), females: FMM versus KSM	71
Figure 5.6. Fitting mortality rates for age group [20,25), males: FMM versus KSM	72
Figure 5.7. Mortality modeling estimates for age group [20,25), females, using 1940-1999 data: FMM versus BMM	73
Figure 5.8. Mortality modeling estimates for age group [20,25), males, using 1940-1999 data: FMM versus BMM	74
Figure 5.9. Mortality forecasts for age group [20,25), females	76
Figure 5.10. Mortality forecasts for age group [20,25), males	76
Figure 5.11. Observed fertility rates	78

Figure 5.12. Observed ln-fertility rates.....	79
Figure 5.13. Fertility modeling estimates for age group [20,25), using 1940-1999 data: FMM versus BMM	81
Figure 5.14. Fertility forecasts for age group [20,25).....	83
Figure 5.15. Observed emigration counts, females	86
Figure 5.16. Observed emigration counts, males.....	87
Figure 5.17. Observed immigration counts, females	87
Figure 5.18. Observed immigration counts, males	88
Figure 5.19. Observed ln-emigration counts, females	89
Figure 5.20. Observed ln-emigration counts, males	89
Figure 5.21. Observed ln-immigration counts, females.....	90
Figure 5.22. Observed ln-immigration counts, males.....	90
Figure 5.23. Emigration modeling estimates for age group [20,25), females, using 1990- 2010 data: FMM with Level I versus BMM.....	94
Figure 5.24. Emigration modeling estimates for age group [20,25), females, using 1990- 2010 data: bi-level FMM versus BMM	95
Figure 5.25. Emigration forecasts for age group [20,25), females	97
Figure 5.26. Observed versus forecasted population for Finland, 1995	102

Figure 5.27. Observed versus forecasted population for Finland, 2010.....	103
Figure 5.28. Forecasted population for Finland, 2025.....	103
Figure 5.29. Distributions of the age group populations	106
Figure 5.30. Percentage changes in distribution of young-age-population	107
Figure 5.31. Percentage changes in distribution of working-age-population	107
Figure 5.32. Percentage changes in distribution of old-age-population	108

LIST OF TABLES

Table 5.1. Summary of total population statistics of Finland.....	64
Table 5.2. Age-specific distribution of Finland in year 2015.....	65
Table 5.3. Results of paired fuzzy sample differences tests for the equality of actual mortality values and FMM estimates.....	70
Table 5.4. MAPE between actual and fitted mortality values for 1940-1999 period obtained via KSM and FMM.....	72
Table 5.5. MAPE between actual and fitted mortality values for 1940-1999 period obtained via BMM and FMM.....	74
Table 5.6. Forecast analysis of actual and forecasted mortality values for 2000-2014 period	77
Table 5.7. Mortality forecast interval comparisons for the BMM and the FMM.....	77
Table 5.8. Results of paired fuzzy sample differences tests for the equality of actual fertility values and FMM estimates	81
Table 5.9. MAPE between actual and fitted fertility values for 1940-1999 period obtained via BMM and FMM.....	82
Table 5.10. Forecast analysis of actual and forecasted fertility values for 2000-2014 period	84
Table 5.11. Fertility forecast interval comparisons for the BMM and the FMM.....	84

Table 5.12. MAPE between actual and fitted migration values for 1990-2010 period obtained via different dissimilarity proportions (p) in Level II of FMM method	91
Table 5.13. Results of paired fuzzy sample differences tests for the equality of actual migration values and FMM estimates.....	92
Table 5.14. MAPE between actual and fitted migration values for 1990-2010 period obtained via BMM and FMM.....	93
Table 5.15. The models used in forecasting future k_t , δ_t , and $r_{i,t}$ values.....	96
Table 5.16. Forecast analysis between actual and forecasted migration values for 2011-2016 period	98
Table 5.17. Prediction and fuzzy interval comparisons for the BMM and the FMM	98
Table 5.18. Summary of sensitivity analyses conducted on variance magnitudes of prior distributions used in the BMM	100
Table 5.19. Expost analysis for BMM population forecasts.....	104
Table 5.20. Expost analysis for FMM population forecasts	104
Table 5.21. Population forecasts via BMM and FMM.....	105
Table 6.1. Summary of eigenvalues extracted via SVD in Level-I modeling phase.....	110

LIST OF SYMBOLS/ABBREVIATIONS

a	Center of a triangular fuzzy number
a_x	Age specific constant
\tilde{A}	Fuzzy number
\tilde{A}_x	Fuzzy age-specific parameter
b_x	Age specific constant
\tilde{B}_x	Fuzzy age-specific parameter
$\tilde{C}_{i,x,t}$	Age group class i
D_{LR}	Diamond distance
E	Hyperplane
$E[X]$	Expectation of random variable X
$\tilde{E}_{x,t}^s$	Fuzzy emigration count for sex s and age x at time t
\exp	Exponential function
f_t	Time variant fuzzification index
$\tilde{F}_{x,t}^s$	Fuzzy fertility rate for sex s and age x at time t
g_t	Function mapping $\bar{m}_{x,t}$ to f_t
h	Level of fuzziness
H	Forecast horizon
\mathbf{I}	Identity matrix
$\tilde{I}_{x,t}^s$	Fuzzy immigration count for sex s and age x at time t
k_t	Time-variant demographic index
\tilde{K}_t	Fuzzy time-variant demographic index
l	Spread of a symmetric triangular fuzzy number
L	Left
l_A	Left spread of a triangular fuzzy number
\ln	Natural logarithm
m	Slope of a function
$m_{x,t}$	Value of demographic indicator for age group x at time period t
$\vec{m}_{x,t}$	Vector of demographic indicator rates
M_j	Time series model j

N	Normal distribution
\tilde{N}_t	Fuzzy population at time t
n_j	Number of parameters in model j
p	Dissimilarity proportion
$p(M_j)$	Prior probability for model M_j
$p(M_j x)$	Posterior probability for model M_j given observation x
R	Right
\mathbb{R}	Set of real numbers/real line
r_A	Right spread of a triangular fuzzy number
s	Sex group index
S_{ij}	Slope similarity index between age groups i and j
$\tilde{S}_{x,t}^s$	Fuzzy survival rate for sex s and age x at time t
t	Time index
T	Triangular norm
T_W	Weakest T norm
\oplus_{T_W}	Weakest T norm based addition
\otimes_{T_W}	Weakest T norm based multiplication
\ominus_{T_W}	Weakest T norm based subtraction
U	Set of universe
Var	Variance
x	Age group index
$Y_{x,t}$	Observed ln -demographic indicator rate of age group x at time t
$\tilde{Y}_{x,t}$	Fuzzy ln -demographic indicator rate of age group x at time t
Z	Decomposition matrix
γ_{t-x}	Cohort factor
$\mu_{\tilde{A}}$	Membership function of a fuzzy subset \tilde{A}
\sim	Fuzzy sign/distribution sign
ε	Error term
θ_j	Moving average parameter of model j
σ	Standard deviation

φ_j	Autoregressive parameter of model j
AR	Autoregressive model
ARIMA	Autoregressive integrated moving average
ARMA	Autoregressive moving average
ASFR	Age-specific fertility rate
ASMR	Age-specific mortality rate
BMM	Bayesian method for modeling age specific demographic indicators
CBD	Cairns-Blake-Dowd model
CT	Coale-Trussel model
<i>et al.</i>	et alii (and all others)
etc.	et cetera
EU	European Union
FCPA	Functional principle component analysis
FLC	Fuzzy Lee-Carter
FMM	Fuzzy method for modeling age specific demographic indicators
GLM	Generalized linear model
HU	Hyndman-Ullah method
KSM	Koissi and Shapiro's fuzzy mortality modeling method
LC	Lee-Carter
LC(2)	Lee-Carter II model
LP	Linear programming
MA	Moving average
MAPE	Mean absolute percentage errors
max	Maximum
MCMC	Markov Chain Monte Carlo
min	Minimum
MMS	Model migration schedule
OP	Old-age population
OECD	Organisation for Economic Co-operation and Development
OLS	Ordinary least squares
PK	Peristera-Kostaki model
PK2	Peristera-Kostaki model II

PLA	Piecewise linear approximation
Pop	Population
RGH	Russolillo-Giordano-Haberman model
RH	Renshaw-Haberman model
RH2	Renshaw-Haberman model II
RW	Random walk model
SRB	Sex ratio at birth
SVD	Singular value decomposition
TFR	Total fertility rate
UK	United Kingdom
UN	United Nations
US	United States
USA	United States of America
WP	Working-age population
YP	Young-age population

1. INTRODUCTION

It is known that population modeling and forecasting play significant roles in strategy development and decision making in diverse sectors. Population modeling and demography analysis find application areas in projecting and forecasting life expectancies, age distributions, unemployment rates, labor force compositions, household consumptions and etc. Together with fertility and migration rates, mortality rates constitute the vital demographic indicators of population dynamics [1]. Age-specific population estimates of immediate future or long-term forecasts based on these vital demographic indicators shape the policies in allocating the resources among public and private investments and the future population [2]. The outputs of the models obtained from fertility, mortality and migration elements form the basis for medium or long term planning in various areas such as labor market [3], public financing [4], insurance and pensions sector [5,6], education system [2], healthcare services [7], city planning [8] and etc.

The research on human mortality and fertility is abundant but the demographic studies have omitted migration until recently [9]. However, population movements play significant roles in demography, economy, politics and sociology and culture in countries. Thus, modeling and forecasting international migration has become an attractive research topic, especially for countries with negative or almost zero natural population growth, where the role of migrants in shaping the socioeconomic structure is important [10]. The growing number of studies on international migration modeling mainly focuses on explaining the determinants of migration phenomenon as well as providing reasonable future predictions on migration levels or rates.

1.1. CONTENT OF THE STUDY

In this study, a fuzzy method for modeling and forecasting age-and-sex-specific population is proposed. This method includes modeling and forecasting mortality, fertility and migration rates and aggregating the forecasted rates with an initial population to generate future fuzzy population forecasts. The fuzzy modeling approach incorporates fuzzy regression with minimum fuzzification criterion as well as unconstrained nonlinear

optimization. For migration modeling, an additional level of fuzzy factors is included in the model in which a hierarchical clustering approach is used in estimating the age-and-time specific fuzzy parameters. This bi-level structure enables the model to cover the variations due to country-specific factors as well as age group clusters. The fuzzy model outputs for each demographic indicator are then employed in Bayesian time series models for forecasting the future mortality, fertility, and migration values. Finally, the forecasts are combined to obtain age specific population estimates for the upcoming years.

The main research question in the study is to see the performance of the hybrid fuzzy set theoretical approach and Bayesian techniques for modeling and forecasting population. The proposed method is implemented on Finland mortality and fertility data for 1940-2000 mortality and fertility data and migration data for 1990-2010 period as an exemplary data set to give annual forecasts for 2011-2025 period. The rest of the paper is designed as follows: the existing literature is re-evaluated in Section 2, and the motivation, scope and main deliverables of the study is provided in Section 3. The proposed method is given in Section 4, whereas the application results for Finland are analyzed in Section 5. The study is concluded with the discussion and future work in Section 6 and the conclusion in Section 7.

2. MODELS IN AGE-SPECIFIC DEMOGRAPHIC FORECASTING

Population modeling and estimations are performed via diverse methodologies which can basically be grouped as population projection methods and population forecasting methods. The projection methods simply rely on deterministic scenarios for different components of mortality, fertility and migration value combinations [11]. Setting the values of these components generally requires formation of a group of experts. In contrast, population forecasting makes use of historical data to obtain a future population estimate using a stochastic approach which takes component un-certainties into account. In fact, stochastic modeling methods have a significant area in demographic forecasting since they provide estimations for the vital demographic indicators together with forecast intervals for them [11].

The choice of the age-specific population forecasting model and the appropriate method to deal with it depends on several issues such as data availability, purpose, length of forecast, fit and forecast accuracies and etc. [11]. Cairns *et al.* [12] summarized the model selection criteria for mortality forecasting; which can be extended to include the two other components, fertility and migration, in population forecasting. They assert that a good model should provide consistency with historical data and trends and should generate biologically feasible results (e.g. the model should ensure positivity for forecasts of demographic rates or counts).

Let $m_{x,t}$ be an age-specific demographic rate for age group x at time period t . This demographic rate can be defined as the ratio of number of demographic events for age group x at time period t to the population at risk for that age group at the same time period. For example age-specific mortality rate for a certain region corresponds to the number of deaths for age group x at time period t over the population of age group x at time period t in that region. Actually, the population at risk refers to the population that is open to experience a demographic event of mortality, fertility, immigration or emigration. If the population at risk is set to unity, then the demographic rate becomes a demographic count.

Since population forecasting is based on age-specific mortality, fertility and migration rates, in this section, models used in age-specific forecasting are examined. The commonly

used models are evaluated under separate subsections for the three demographic components: mortality (Section 2.1), fertility (Section 2.2) and migration (Section 2.3). However, it is worth mentioning that some of the models can be used for forecasting more than one single demographic component. In addition to the mortality, fertility and migration modeling approaches, commonly used cohort component method in which mortality, fertility and migration values are integrated to estimate a population with age-specific characteristics is examined in Section 2.4. Last but not least, the Leslie matrix formulation for estimating a population through age-specific demographic components is given in Section 2.5.

2.1. MORTALITY MODELING AND FORECASTING APPROACHES

The almost linear decline in trends followed by age-specific mortality rates (ASMR) in most of the developed and developing countries allow modeling and forecasting human mortality by extrapolating the past trends into future. In majority of the existing approaches, the observed rates are transformed into logarithmic scale to ensure the nonnegativity and visualize the fluctuations and the almost linear structures in mortality trends for most of the ages [13]. In this perspective, the simplest approach is the direct linear extrapolation [14]. Let $m_{x,t}$ be the mortality rate for age group x at time t , which corresponds to ASMR. By direct linear extrapolation, the natural logarithm of $m_{x,t}$ can be modeled as:

$$\ln m_{x,t} = a_x + b_x t + \varepsilon_{x,t} \quad (2.1)$$

where a_x is the intercept, b_x is the regression coefficient and $\varepsilon_{x,t}$ is the error term distributed normally with mean zero and a small variance. Equ. (2.1) treats ASMR as a linear function of time, therefore, its usage is limited in cases of fluctuations in mortality trends.

2.1.1. Lee-Carter Model and Its Variants

Thanks to the regularities in ASMR, the utilization of dimension reduction techniques based on principal components is common for modeling human mortality [7]. Among the

methods similar to principal components, the log-bilinear model proposed by Lee and Carter [15] is very popular. This is because, Lee-Carter (LC) model provides a simple procedure to extract the dominant temporal factor embedded in the mortality data as follows:

$$\ln m_{x,t} = a_x + b_x k_t + \varepsilon_{x,t} \quad (2.2)$$

where a_x and b_x are the age-specific regression coefficients, and k_t is the time-varying mortality index. The error term $\varepsilon_{x,t}$ represents the variations in data that cannot be explained by the model. $\varepsilon_{x,t}$ is normally distributed with a mean value of zero and a small constant variance, which leads to the homoscedasticity assumption of the model. The values of the unknown model parameters and the mortality indices k_t 's in Equ. (2.2) are estimated via singular value decomposition (SVD) technique, in which a data matrix Z , composed of $\ln m_{x,t}$ values purified from the average age impact, is decomposed into its singular values and their corresponding right and left eigenvectors. The most dominant singular value and its associated eigenvectors are then used to give estimates for the unknown model parameters and mortality indices.

Due to its simplicity and ability to reflect the alike declining mortality trends among different age groups, LC model has been widely used in modeling ASMR for most of the developed and developing countries [16]. Several extensions of LC model are available in demographic literature, and these extensions are applied not only for mortality modeling, but also for fertility [13] and migration [17] modeling as well. In such models, once the time-varying k_t values are extracted based on observed mortality data, the future values can be forecasted using univariate time series models such as random walk (RW) or autoregressive integrated moving average models. The future forecasts of k_t are then employed within Equ. (2.2) to give future forecasts of ASMRs.

In Lee-Miller variant of LC model [18] a reduced fitting period is used to mitigate the bias in forecasts based on more data. This model also does not treat the age-specific parameter b_x as a fixed value; instead, b_x changes by time in accordance with the changes in mortality index k_t . Booth-Maindonald-Smith variant of LC model [19] also concentrates on the selection of best fitting period based on goodness of fit criteria with the assumption of a linear k_t .

2.1.1.1. Renshaw-Haberman Model

In cases where using only a single factor extracted via SVD does not meet the model capability requirements, Lee [20] and Renshaw and Haberman [21] suggest including a second factor into the LC model, which is named as LC(2) model:

$$\ln m_{x,t} = a_x + b_x^{(1)}k_t^{(1)} + b_x^{(2)}k_t^{(2)} + \varepsilon_{x,t} \quad (2.3)$$

where a_x , $b_x^{(1)}$, and $b_x^{(2)}$ are the age-specific parameters to be estimated, $k_t^{(1)}$ and $k_t^{(2)}$ are the time-varying mortality indices associated with the first and second most dominant singular values extracted via SVD.

Renshaw and Haberman [22] further include a cohort effect factor into LC model to diminish the unexplained variances in mortality data through reflecting the separate changes in individual cohorts by time. The Renshaw-Haberman (RH) model is as follows:

$$\ln m_{x,t} = a_x + b_x^{(1)}k_t + b_x^{(2)}\gamma_{t-x} + \varepsilon_{x,t} \quad (2.4)$$

where a_x , $b_x^{(1)}$, and $b_x^{(2)}$ are the age-specific parameters to be estimated, k_t is the time-varying mortality index, and γ_{t-x} is the cohort effect (cohort = time period – age group). Another version of RH model, namely RH2 model removes the regression coefficient from the original RH model as:

$$\ln m_{x,t} = a_x + b_x k_t + \gamma_{t-x} + \varepsilon_{x,t} \quad (2.5)$$

2.1.1.2. Multiple Population Models

The determination of which model to implement is due to data-driven manners such as minimizing the fitting or forecast errors. For a population composed of several groups or segments with distinct mortality behaviors, Russolillo *et al.* [23] introduce a factor index to modify the mortality for each group. The Russolillo-Giordano-Haberman (RGH) model proposed by Russolillo *et al.* [23] is as follows:

$$\ln m_{x,t,i} = a_x + b_x k_t I_i + \varepsilon_{x,t,i} \quad (2.6)$$

Here, $\ln m_{x,t,i}$ denotes the natural logarithm of mortality rate for age x at time t for population group i , and I_i is the factor index that modifies mortality for group i members. Debón *et al.* [24] modify RGH model by adding a separate factor index instead of multiplying it with the age-specific mortality factor $b_x k_t$ as:

$$\ln m_{x,t,i} = a_x + b_x k_t + I_i + \varepsilon_{x,t,i} \quad (2.7)$$

The models in Equ. (2.6) and Equ. (2.7) are applied to model the ASMR for small populations within a larger population and they result in more accurate forecast and fitting errors when compared to other LC model variants for such data.

Considering mortality characteristics for multiple populations at a time, Li-Lee model [25] extends the LC model so that mortality patterns in all populations are influenced by a mutual factor as:

$$\ln m_{x,t} = a_x + b_x k_t + B_x K_t + \varepsilon_{x,t} \quad (2.8)$$

Here, a_x , b_x , and B_x denote the age-specific parameters to be estimated, K_t refers to the time-specific common trend factor for a set of populations whereas k_t denote the time-variant mortality factor for a member population of this set. Li and Hardy [26] further propose another two-population model, in which the trend for a smaller population is treated as a function of the trend for a larger population. In Li and Hardy model, the mortality index k_t in Equ. (2.2) is expressed as:

$$k_t = \alpha + \beta k_t^* + \varepsilon_t \quad (2.9)$$

where k_t and k_t^* represent the trend factor for a smaller and a larger population respectively. The mentioned smaller and larger population pairs may be a city and a country or a country and a region of the world. Dowd *et al.* [27] further exploit the trend factors in two-population mortality models by using an error correction model linking the trend for the smaller population to the trend for the larger population as:

$$k_t^* = k_{t-1}^* + \mu^* + \varepsilon_{t-1}^* \quad (2.10)$$

$$\Delta k_t = \phi(k_{t-1} - k_{t-1}^*) + \mu + C\varepsilon_t^* + \varepsilon_t \quad (2.11)$$

Using a state-space framework, de Jong and Tickle [28] propose a modified LC model in which a design matrix X is included as:

$$\ln m_{x,t} = Xa + Xbk_t + \varepsilon_t \quad (2.12)$$

The design matrix X in Equ. (2.12) is formed in such a way that k_t has dependent impact at each age, allowing the representation of age-across effects in mortality trends.

2.1.1.3. Hyndman-Ullah Model

Hyndman and Ullah [2] propose a functional data method to model the ASMRs. In their model, denoted as HU, ASMR are first smoothed using penalized regression spline with concavity constraint as follows:

$$\ln m_{x,t} = f_t(x) + \sigma_t(x)\varepsilon_{x,t}, \quad x = 1, 2, \dots, p, \quad t = 1, 2, \dots, n \quad (2.13)$$

Here, $f_t(x)$ is a continuous smooth function; $\sigma_t(x)$ allows the presence of heteroscedastic error by representing the noise to vary with age x in time t . The mean smooth function of age x , denoted by $a(x)$ can be expressed as weighted sum of $f_t(x)$ s as:

$$a(x) = \sum_{t=1}^n w_t f_t(x) \quad (2.14)$$

where the weight w_t can either be $1/n$, representing equal weights, or $\lambda(1-\lambda)^{n-t}$, representing a set of geometrically decaying weights. Here, the value of weight parameter λ is determined through a data driven approach based on minimizing the total forecast error. Next, the set of curves $\{w_t[f_t(x) - a(x)]; t = 1, 2, \dots, n\}$ is decomposed into orthogonal functional components and their uncorrelated scores similar to the approach in LC model as:

$$\ln m_{x,t} = a(x) + \sum_{j=1}^J b_j(x)k_{t,j} + e_t(x) \quad (2.15)$$

where $b_j(x)$ is the j^{th} equally or geometrically decaying weighted principal component, $k_{t,j}$ is the time varying j^{th} uncorrelated principal component score and $e_t(x)$ is the error

function with mean zero. Here, J is the number of extracted principal components. The h -step-ahead point and interval forecasts for ASMR are predicted by including univariate time series forecasts of $k_{t,j}$.

Mitchell *et al.* [29] criticize the LC model and its variants as they model the level of mortality rates which misinterpret the temporal correlations between age groups, even for models including cohort factor which try to model dependencies between age groups using a downward trending temporal factor. However, the simplicity of LC model and its variants make them frequently be used in mortality modeling and forecasting.

2.1.2. Cairns-Blake-Dowd Model and Its Variants

Another family of dimension reduction methods for modeling ASMR is the Cairns-Blake-Dowd (CBD) model and its variants. Proposed by Cairns *et al.* [30], CBD models include a number of time and cohort factors, where the number of time factors and the decision to include a cohort factor depend on data to be modeled. Four variants of CBD model are as follows:

$$\ln m_{x,t} = k_t^{(1)} + (x - \bar{x})k_t^{(2)} + \varepsilon_{x,t} \quad (2.16)$$

$$\ln m_{x,t} = k_t^{(1)} + (x - \bar{x})k_t^{(2)} + \gamma_{t-x} + \varepsilon_{x,t} \quad (2.17)$$

$$\ln m_{x,t} = k_t^{(1)} + (x - \bar{x})k_t^{(2)} + b_x k_t^{(3)} + \gamma_{t-x} + \varepsilon_{x,t} \quad (2.18)$$

$$\ln m_{x,t} = k_t^{(1)} + (x - \bar{x})k_t^{(2)} + (x_c - x)\gamma_{t-x} + \varepsilon_{x,t} \quad (2.19)$$

Here, $k_t^{(1)}$, $k_t^{(2)}$, and $k_t^{(3)}$ are the time factors, γ_{t-x} is the cohort factor linking age group x and time t , \bar{x} is the mean age group in data, and x_c is a predetermined constant. The coefficient term b_x for the third time factor $k_t^{(3)}$ equals to the following expression:

$$b_x = (x - \bar{x})^2 - \frac{1}{p} \sum_{i=x_1}^p (i - \bar{x})^2 \quad (2.20)$$

where $x = x_1, x_2, \dots, x_p$; and $t=1, 2, \dots, n$. Plat [31] suggests using modified versions for the CBD models described in Equ. (2.16) to Equ. (2.17), which are expressed as:

$$\ln m_{x,t} = a_x + k_t^{(1)} + (\bar{x} - x)k_t^{(2)} + (\bar{x} - x)^+ k_t^{(3)} + \varepsilon_{x,t} \quad (2.21)$$

$$\ln m_{x,t} = a_x + k_t^{(1)} + (\bar{x} - x)k_t^{(2)} + (\bar{x} - x)^+ k_t^{(3)} + \gamma_{t-x} + \varepsilon_{x,t} \quad (2.22)$$

$$\ln m_{x,t} = a_x + k_t^{(1)} + (\bar{x} - x)k_t^{(2)} + (\bar{x} - x)^+ k_t^{(3)} + b_x k_t^{(4)} + \gamma_{t-x} + \varepsilon_{x,t} \quad (2.23)$$

$$\ln m_{x,t} = a_x + k_t^{(1)} + (\bar{x} - x)k_t^{(2)} + (\bar{x} - x)^+ k_t^{(3)} + (x_c - x)\gamma_{t-x} + \varepsilon_{x,t} \quad (2.24)$$

where $(\bar{x} - x)^+$ corresponds to $\max\{(\bar{x} - x), 0\}$, ensuring nonnegativity. The main differences between CBD and Plat models is that Plat models include an intercept coefficient a_x , which can be viewed as the mean mortality trend for age group x , and the coefficient $(x - \bar{x})$ is reversed into $(\bar{x} - x)$. In addition, one more time factor is included in each equation for Plat models. Both CBD and Plat models are generalized linear models (GLM) and they can be fitted using GLM facilities in standard packages. Haberman and Renshaw [32] compared CBD and Plat models with LC, RH, and RH2 models for England and Wales male mortality data and found that Plat models described in Equ. (2.23) and Equ. (2.24), and RH2 model in Equ. (2.5) outperform the other models for this data set.

2.1.3. Time Series Extrapolation of Age-Specific Mortality Rates

Time series extrapolation of age-specific demographic rates, including ASMR, is also quite common in demographic literature. Apart from the parametric and semiparametric models, univariate time series models are the simplest approach in analyzing the age specific demographic rates [33]. Alho and Spencer [34] provide a detailed summary of time series models utilized in demographic forecasting. Being one of the most naïve linear extrapolation model a random walk model with drift term relates age-specific demographic rate for age group x at time $t+1$ with its value at time t as:

$$m_{x,t+1} = c + m_{x,t} + \varepsilon_{x,t+1} \quad t = 1, 2, \dots, n-1, \quad x = x_1, x_2, \dots, x_p \quad (2.25)$$

where $m_{x,t}$ is the age-specific demographic rate to be analyzed, c is the drift term and $\varepsilon_{x,t}$ is the error term which corresponds to a normally distributed random variable with mean zero. The h -step ahead point and interval forecasts are given by [35]:

$$\hat{m}_{x,n+h|n} = E[m_{x,n+h} | m_{x,1}, m_{x,2}, \dots, m_{x,n}] = hc + m_{x,n} \quad (2.26)$$

$$\text{Var}(\hat{m}_{x,n+h|n}) = \text{Var}[m_{x,n+h} | m_{x,1}, m_{x,2}, \dots, m_{x,n}] = \text{Var}[m_{x,n}] + \text{Var}[e_{x,n+h}] \quad (2.27)$$

where E and Var refer to expected value and variance respectively. If the drift term c in Equ. (2.25) is zero, then the expression represents a random walk model without drift. A $100(1-\alpha)\%$ prediction interval for the h -step ahead forecast $m_{x,t+h}$ is constructed as

$$\hat{m}_{x,n+h|n} \pm z_\alpha \sqrt{\text{Var}(\hat{m}_{x,n+h|n})}, \text{ where } z_\alpha \text{ is the } (1-\alpha/2) \text{ standard normal quantile.}$$

Autoregressive integrated moving average (ARIMA) models are also common in demographic forecasting. The model assumes a stationary time series which does not reflect a trend over time. Otherwise, stationarity is achieved through differencing the nonstationary time series so that an optimal autoregressive moving average, ARMA(p, q), model is constructed. Here, p and q refer to the orders of autoregressive (AR) and moving average (MA) components [36]. The ASMR (or other age-specific demographic rates) can be extrapolated by applying ARMA(p, q) model to each age group separately as:

$$m_{x,t+1} - \mu = \sum_{i=1}^p \phi_i (m_{x,t-i} - \mu) + \varepsilon_{x,t} + \sum_{j=1}^q \theta_j \varepsilon_{x,t-j}, \quad t = \max(p, q) + 1, \dots, n \quad (2.28)$$

where μ is the mean value of a time series, $\phi_1, \phi_2, \dots, \phi_p$ are the coefficients of the AR components, and $\theta_1, \theta_2, \dots, \theta_q$ are the coefficients of the MA components. The error term $\varepsilon_{x,t}$ is normally distributed with mean zero and an estimated variance σ_ε^2 . One step ahead point and interval forecasts are obtained through):

$$\hat{m}_{x,n+1|n} = E[m_{x,n+1} | m_{x,1}, m_{x,2}, \dots, m_{x,n}] = \hat{\mu} + \sum_{i=1}^p \hat{\phi}_i (m_{x,n+1-i} - \hat{\mu}) \quad (2.29)$$

$$\text{Var}(\hat{m}_{x,n+1|n}) = \text{Var}[m_{x,n+1} | m_{x,1}, m_{x,2}, \dots, m_{x,n}] = \hat{\sigma}_\varepsilon^2 (1 + \hat{\theta}_1^2 + \hat{\theta}_2^2 + \dots + \hat{\theta}_q^2) \quad (2.30)$$

where E and Var refer to expected value and variance respectively. The iterative application of Equ. (2.29) and Equ. (2.30) generates h -step ahead forecasts, and the related $100(1-\alpha)\%$ prediction interval can be achieved like random walk process.

Despite its common usage and simplicity, Rueda and Rodriguez [33] argue that analyzing each age group separately through univariate time series may not result in plausible outcomes. On the other hand, methods such as LC and CBD models and their variants capture the smooth shape of the demographic rates over age, hence, yielding more consistent and accurate forecasts.

2.2. FERTILITY MODELING AND FORECASTING APPROACHES

Age-specific human fertility modeling and forecasting concentrates mainly on modeling age-specific fertility rates (ASFR) or fertility schedules/fertility curves. ASFR for age group x at time t , denoted by $f_{x,t}$, can be defined as the ratio of number of births given by female population of age x in time period t and the mid-period female population of age group x . Fertility rates for a set of age groups at a certain time period constitute fertility schedules or fertility curves in demographic literature [37]. Various fertility models exist in literature, which can be analyzed in three groups as curve fitting approaches (i), relational models (ii), spline models (iii) and quantum-tempo decomposition approaches and other methods (iv).

Unlike the dominance of dimension reduction methods common in mortality modeling, the majority of the fertility models are based on parametric or semiparametric curve fitting approaches. However, the interpretation of model parameters in curve fitting approaches is limited in most of the cases.

2.2.1. Curve Fitting Approaches

Despite the lack of parameter interpretation, due to its simplicity curve fitting based on well-known statistical distributions is quite common in not only age-specific fertility modeling but also in mortality and migration fitting. Let f_x denote the fertility rate at age x of the mother. Hoem *et al.* [38] make use of the beta distribution to model fertility schedules as:

$$f_x = R \frac{\Gamma(A+B)}{\Gamma(A)\Gamma(B)} (\beta - \alpha)^{-(A+B-1)} (x - \alpha)^{A-1} (\beta - x)^{B-1} \quad (2.31)$$

where Γ is the gamma function, α and β are the minimum and maximum age limits of fertility; and A and B are related to mean and variance of fertility rates. Here, R represents the level of fertility. A similar model, the gamma model is defined as [38,39]:

$$f_x = R \frac{1}{\Gamma(A)B^A} (x-\alpha)^{A-1} \exp\left\{-\left(\frac{x-\alpha}{B}\right)\right\} \quad (2.32)$$

Here, although the parameters A and B are associated with mean and variance of the model, their relation with these concepts are not in a simple linear way. Hence, these parameters cannot be directly explained in demographic context. More recently, de Iaco and Maggio [40] propose a dynamic version of this Gamma model to fit ASFR in Italy by adding a temporal dimension in addition to the age axes. Such extensions of age specific demographic schedules to include a time component enable the fitting models to generate future forecasts in an easier way.

2.2.1.1. Hadwiger Model

Hadwiger model [41] is also one of the oldest and frequently used to model fertility schedules. The Hadwiger model is:

$$f_x = \frac{ab}{c} \left(\frac{c}{x}\right)^{\frac{3}{2}} \exp\left\{-b^2 \left(\frac{c}{x} + \frac{x}{c} - 2\right)\right\} \quad (2.33)$$

where a , b , and c are to be estimated. Here, the values of a , b , and c are not directly interpretable, which is the main drawback of the Hadwiger model. However, in several studies it is noted that a is associated with total fertility level, b is related to the height of the curve, c is related to mean age at motherhood, and $\frac{ab}{c}$ is associated with the modal ASFR [42]. Despite the difficulties encountered in interpreting the parameters in Equ. (2.32), Hadwiger model enjoys the superiorities in terms of number of parameters included and computational complexity. Chandola *et al.* [43] introduce an additional term into the Hadwiger model to provide accurate fits for distorted distributions. They believe that the Hadwiger mixture model is capable of fitting the humped fertility distributions for some

countries like the UK, the USA and Ireland by taking the combination of two separate age distributions as:

$$f_x = m \left(\frac{b_1}{c_1} \right) \left(\frac{c_1}{x} \right)^{\frac{3}{2}} \exp \left\{ -b_1^2 \left(\frac{c_1 + \frac{x}{c_1} - 2}{x} \right) \right\} + (1-m) \left(\frac{b_2}{c_2} \right) \left(\frac{c_2}{x} \right)^{\frac{3}{2}} \exp \left\{ -b_2^2 \left(\frac{c_2 + \frac{x}{c_2} - 2}{x} \right) \right\} \quad (2.34)$$

where m denotes the mixture parameter reflecting the relative size of two component distributions that are believed to be included in a single fertility schedule.

2.2.1.2. Coale-Trussel Model

Another commonly used curve fitting approach is the Coale-Trussel (CT) model [44], which is defined as:

$$f_x = G_0 \left(\frac{x - \mu}{\sigma} \right) n(x) \exp \{ \alpha + \beta v(x) \} \quad (2.35)$$

where $n(x)$ is the age pattern of fertility, $v(x)$ is a fixed pattern of fertility control by age, $\alpha = \log(cm)$, $\beta = m$, and μ and σ are the mean and standard deviation of age at first birth. The parameter m embedded in α reflects the level of natural fertility whereas the parameter c in β represents the degree of fertility control. G_0 in CT model is a standard nuptiality schedule representing the probability that a woman who will ever join a union has done so by age x . In fact, CT model is a relational model which expresses ASFR as a product of two model age schedules: a nuptiality schedule and a marital fertility schedule. Thus, the estimated ASFR by CT model are indeed based on the assumption that marital fertility is a good representative of ASFR. However, this assumption has turned out to be misleading especially since 1980, as childbearing without marriage has been increasing unavoidably [37]; which is viewed as one of the main weaknesses of CT model.

2.2.1.3. Peristera-Kostaki Model

Further changes in fertility curves of various countries in recent years have required a more flexible model such as Peristera and Kostaki (PK) model [45]. The PK model appears like the bell curve but it is asymmetric in sense that the spread before and after the peak differs.

The distorted age-specific fertility patterns in countries such as the UK, Ireland, and Spain can be fitted by PK model as:

$$f_x = c \exp \left\{ - \left(\frac{x - \mu}{\sigma(x)} \right)^2 \right\} \quad (2.36)$$

where c is associated with total fertility rate (TFR), μ is the mean age of fertility, and $\sigma(x)$ is the standard deviation of age of fertility. Here, $\sigma_x = \sigma_{11}$ if $x \leq \mu$ and $\sigma_x = \sigma_{12}$ otherwise; where σ_{11} and σ_{12} are proxy for the spread of the distribution before and after its peak value.

2.2.2. Relational Models

For fitting fertility curves with distortions or bimodal structure due to fluctuations such as high fertility at a young age, Peristera and Kostaki [45] further proposed a modified version of the PK model, namely PK2 model, by adding a second term as:

$$f_x = c_1 \exp \left\{ - \left(\frac{x - \mu_1}{\sigma_1(x)} \right)^2 \right\} + c_2 \exp \left\{ - \left(\frac{x - \mu_2}{\sigma_2(x)} \right)^2 \right\} \quad (2.37)$$

where c_1 and c_2 are related to the fertility level at the first and second peak, μ_1 and μ_2 are related to the mean age of the two subpopulations, and $\sigma_1(x)$ and $\sigma_2(x)$ are associated with the spreads around the two peaks. Although both PK and PK2 models work well in fitting distorted fertility curves, they still lack the complete interpretability of parameters which is common in parametric curve fitting approaches.

In general, the parameters in relational models imply the extent of the deviations from a model age schedule for a particular country in terms of a demographic rate. Originally proposed for modeling mortality, Gompertz model [46] provides one of the oldest relational models that can be applied for modeling fertility schedules. Gompertz model for modeling fertility schedules is as [47]:

$$f_x = Ka \exp \left\{ \left(\frac{-a}{b} e^{-bx} - bx \right) \right\} \quad (2.38)$$

where K is the completed total fertility over all ages, a is a location parameter, which determines the location of the schedule along the age axis for a given b , and b is a time scale parameter indicating the speed of the process. Goldstein [47] notes that a large value for location parameter a presents a compressed distribution with small variance whilst a small b indicates a slow time-scale of the process. Gompertz distribution generates plausible fits for the fertility rates except at extreme ages [42]. To mitigate the distortions from the smooth structure in fertility schedules additional terms are included into Equ. (38) as:

$$f_x = Ka \exp \left\{ \left(\frac{-a}{b} e^{-bx} - bx \right) \right\} g(x) \quad (2.39)$$

where the function $g(x)$ is set to unity before age 33 and take the value zero after age 43. The function takes values that are linearly declining in between ages 33 and 43, thus, $g(x)$ can be viewed as an infertility effect. The model in Equ. (2.39) is said to improve the fitting capability of Gompertz model at older ages and has the advantage of possessing a conceivable biological foundation and behavioral interpretation.

Similar to the model displayed in Equ. (2.39), Gupta and Pasupuleti [37] define a model that provides behavioral interpretation. Their model is given below as:

$$f_{x,t} = rt^a \left(a - \frac{t}{49} \right)^b \quad (2.40)$$

where r is a coefficient to be estimated, a is a parameter associated with exposure to marriage or sexual union, and b is related to fertility control level and biological impotency.

A broader relational model in which fertility rates are linked to any age schedule that is capable of mimicking the overall age patterns of fertility to be fitted is proposed by Brass [48]. Brass model makes use of the log-log transformation in Gompertz distribution to relate two schedules linearly as:

$$Q_x = \alpha + \beta Q_x^* \quad (2.41)$$

Here, $Q_x = -\ln(-\ln f_x)$ and $Q_x^* = -\ln(-\ln f_x^*)$; in which f_x is the ASFR to be fitted and f_x^* represents the fertility rates based on a standard age schedule. The location and spread parameters α and β are estimated through ordinary least squares (OLS) method. Zeng *et al.* [49] assert that several age curves can be utilized as the standard age schedule f_x^* , such as observed rates of another country, as long as they are in accordance with the data to be fitted. In addition, Zeng *et al.* [49] claim that the location and spread parameters in Equ. (2.41) should vary by time to enable projections for the demographic rates. The simplicity of the Brass model leads to its wide utilization for demographic modeling once an appropriate standard age schedule is on hand, however, the goodness of fit frequently depends on the selected standard age schedule. This can be seen as one of the major weaknesses of relational models.

2.2.3. Spline Models

De Beer [42] claims that relating two age schedules with two parameters as in Equ. (2.41) may not be adequate to provide reasonable fits in some cases. By introducing more parameters, de Beer [42] develops a model, namely TOPALS, in which the age patterns in ratios of ASFR of a country and fertility rates based on a standard age schedule are described by a linear spline function as:

$$r_x = a + b_0(x - m) + \sum_{j=1}^n b_j(x - m - k_j)D_j \quad (2.42)$$

where r_x is the age-specific ratio defined by f_x / f_x^* , m is the minimum age included in fertility curve, k_j are the knots, that is, the ages at which the adjacent linear segments are connected. Moreover, n represents the number of knots, and a and b_j are the parameters to be estimated. Here, D_j is an adjustment term with value zero if $x - m \leq k_j$ and with value one otherwise. The knots can be fixed *a priori* based on visual inspection which enables the utilization of OLS method in estimating the unknown model parameters. In contrast, they can be determined in such a way that the fit of the linear spline to the observed ASFR is optimal. This alternative way of knot selection requires a nonlinear estimation approach

in which the objective would be minimizing the distance between the fitted and observed rates.

De Beer [42] asserts that it may be more convenient to use a nonparametric approach, such as fitting via splines, for smoothing age patterns of demographic rates rather than specifying a parametric curve fitting model. This is because the configuration of a nonparametric model is not fixed in advance, specified based on a data driven approach instead. Here, it is worth mentioning that nonparametric does not refer to models with no parameters. Actually, the number of parameters included is not predetermined and they do not require demographic interpretations.

The utilization of spline models to fit demographic rates is not a new approach indeed. McNeil *et al.* [50] use quadratic splines for interpolating demographic data whilst Hoem and Rennermalm [51] and Hoem *et al.* [38] suggest applying cubic splines. Schmertmann [52] and de Beer [42] define the quadratic and cubic splines to be applied in terms of fertility modeling context as:

$$f_x = a + b(x - m) + \sum_{j=1}^n c_j (x - m - k_j)^2 D_j \quad (2.43)$$

$$f_x = a + b(x - m) + c(x - m)^2 + \sum_{j=1}^n d_j (x - m - k_j)^3 D_j \quad (2.44)$$

where a , b , c , c_j and d_j are parameters to be estimated. The difference of linear splines and the models given in Equ. (2.43) and Equ. (2.44) is that the latter two partition the age schedule to be fitted into segments of quadratic or cubic curves instead of the lines expressed in Equ. (2.42). Whether linear, quadratic, or cubic; the spline model describes the distribution of fertility schedule based on the ages at which the schedule reaches certain characteristics.

2.2.4. Other Approaches

Considering the lack of clear interpretation of coefficient values in spline modeling, Kostaki *et al.* [53] propose using support vector machines for fitting fertility schedules.

However, the implementation of support vector machines requires a significant computational effort when compared to splines and spline models are capable of generating fits as accurate as support vector machines. Thus, de Beer [42] advocates the utilization of splines against the more complex support vector machines.

2.2.4.1. Logistic Models

Alho and Spencer [34] provide logistic models that can be applied to model the fertility patterns of different age groups. Conditional to a fixed moment in time, a logistic model enables fitting fertility schedules through simple approach with an orthogonal matrix design. Let $B_{x,t}$ be the number of births to females of age x at time period t . The logistic models assume that $B_{x,t}$ are generated by a Poisson process with intensity $\rho_{x,t}$. The basic r -dimensional logistic model can be expressed as [33]:

$$\log \left[\frac{\rho_{x,t}}{1 - (\rho_{x,t})} \right] = A_x \boldsymbol{\beta}_t \quad (2.45)$$

where $\boldsymbol{\beta}_t = (\beta_{0t}, \beta_{1t}, \dots, \beta_{rt})$ is the parameter vector and A_x is a predetermined design matrix with orthogonal columns defined as a function of the power of age x . Alho and Spencer [34] report that the number of the dimension r to be included depends on the fertility data analyzed, but three or four parameters are usually adequate to provide reasonable fits for the developed countries [54]. Durbin and Koopman [55] formulate the parameter series in Equ. (2.45) within a framework of state-space models. The state-space model enables the various sources of uncertainty to be integrated, thus, allowing the confidence intervals for forecasted fertility rates conveniently.

2.2.4.2. Simple Nonparametric Methods

More simple nonparametric methods such as fitting age specific demographic rates via polynomial or exponential models are also available in literature. Nasir *et al.* [56] compares n^{th} degree polynomial models and a family of exponential models in terms of

fitting capabilities for fertility component. For a fixed moment in time, the polynomial model they use is:

$$f_x = b_0 + \sum_{j=1}^p b_j z^j + \varepsilon_x \quad (2.46)$$

where z is the mid age group, b_0 is a constant, b_j is the coefficient of the term z^j , and ε_x is the error term. The exponential family refers to models with exponential or logarithmic functions. Some of the exponential models have the capability to possess an inflection point and a maximum or minimum value based on the functional structure they have. The exponential family of models used by Nasir *et al.* [56] are:

$$f_x = b_0 \exp(b_1 z) \quad (2.47)$$

$$f_x = b_0 \exp\left(\frac{b_1}{z}\right) \quad (2.48)$$

$$f_x = b_0 + b_1 \ln z \quad (2.49)$$

$$f_x = \frac{1}{b_0 + b_1 \ln z} \quad (2.50)$$

$$f_x = \exp\left(b_0 + \frac{b_1}{z} + b_2 \ln z\right) \quad (2.51)$$

The models displayed above are namely the exponential model (Equ. (2.47)), modified exponential model (Equ. (2.48)), logarithmic model (Equ. (2.49)), reciprocal logarithmic model (Equ. (2.50)), and vapor pressure model (Equ. (2.51)).

2.2.4.3. Dimension Reduction Methods

Apart from the parametric or semiparametric curve fitting approaches and the nonparametric polynomial, logistic or exponential models; dimension reduction based methods such as the LC model (defined in Equ. (2.2)) and HU model (defined in Equ. (2.15)) together with their variants are also applicable in age-specific fertility modeling [13,17,57]. The principal component analysis based approaches minimize the loss of

information while reducing dimensionality and can be viewed as a nonparametric technique to deal with age-specific demographic components. Basically, these methods are preferred against parametric approaches in cases where the parametric assumptions are failed to be satisfied. Many researchers favor dimension reduction methods in demographic forecasting because these methods provide means to follow a data-driven procedure [35].

Considering the above mentioned properties of dimension reduction techniques, Ramsay and Silverman [58] apply functional principal component analysis (FPCA) model on function based demographic processes as:

$$M(x,t) = \mu(x,t) + \sum_{r=1}^R Z_r \gamma_r(x,t) \quad (2.52)$$

where $M(x,t)$ denote a demographic process as a function of space (age) and time, $\mu(x,t)$ is the mean of the process $M(x,t)$, R is the rank of matrix M , and Z_r are the random coefficients. Here, γ_r is an orthonormal basis of a two dimensional space that consists of the covariance operator of $M(x,t)$. Through FPCA, the first K terms for $Z_r \gamma_r(x,t)$ constitutes the K -dimensional representation of $M(x,t)$; and the unexplained variance becomes minimum for the optimal value of K to be extracted.

The model given in Equ. (2.46) analyzes the joint impacts of age and time on the demographic process but ignores their marginal effects. Furthermore the model requires performing nonparametric regression analysis to estimate the covariance operator, which is computationally time consuming due to dimensionality issues. Chen *et al.* [59] enhance Equ. (2.52) by including eigenfunctions in single dimensions.

Pantazis and Clark [60] suggest utilizing SVD as a dimension reduction method to capture the shape of the fertility schedules. Rearranging the original structure of the decomposed matrix, the age specific fertility schedule for country c in time period t , denoted by $\mathbf{f}_{c,t}$, can be modeled as:

$$\mathbf{f}_{c,t} = \sum_{i=1}^3 \mathbf{v}_{c,t}^{(i)} s^{(i)} \mathbf{u}^{(i)} \quad (2.53)$$

Where $s^{(i)}$ is the i^{th} greatest singular value and $\mathbf{u}^{(i)}$ and $\mathbf{v}_{c,t}^{(i)}$ are its corresponding left and right singular vectors. According to Pantazis and Clark [60], the $v^{(i)}$ weights, which are the

elements of right singular vectors can be interpreted. They claim that $v^{(1)}$ controls the level of fertility, $v^{(2)}$ is associated with comparative levels of fertility at young and old ages, and $v^{(3)}$ is related to the amount of peak in the age schedule.

Similar to mortality forecasting, univariate time series models are also commonly applied in ASFR forecasting. Shang [35] compares random walk and ARIMA models with HU methods and shows that the univariate models have worse performances in terms of forecast accuracies. Shang relates this issue to the smoothing of fertility rates performed in HU methods. Furthermore, univariate time series methods extrapolate the past data without considering any possible nonlinear structure. However, dimension reduction approaches forecast the future fertility patterns in terms of principal components and their associated scores, hence yielding more plausible forecasts.

2.3. MIGRATION MODELING AND FORECASTING APPROACHES

The majority of the migration modeling literature concentrates on theoretically explaining the migration phenomenon through several factors and projecting the total migrant stocks or bilateral migration flows without considering the age structure of the migrants. However, inclusion of age characteristics in migration analysis is vital in demographic modeling [61]. The age and sex patterns of migration are essential in cohort component population projections [62], thus, should not be omitted.

2.3.1. Model Migration Schedules

Several researchers emphasize the regularities in migration age profiles across regions and time [63–66]. Based on the observed regularities, migration intensities reach to a peak level in the young adult ages as a result of young adults' tendencies to move due to factors associated with employment, education, marriages, and etc. This peak level is followed by a decline as age increases, mainly because of stability in socioeconomic and family factors. Some migration age profiles exhibit a secondary peak in retirement ages due to movements of couples to convenient locations [67]. Migration profiles for children display alike behavior to their parents as high migration intensities are observed for infants and toddlers whose parents, most of the time, are young adults with high mobility characteristics. The

migration age profile for teenagers exhibit a decline mimicking their parents who also become less mobile and this trend continues up until they become young adults.

Considering this relatively stable structure of age-specific migration profiles, Rogers and Castro [65] introduced a parameterized model migration schedule (MMS) in which the age-specific migration curve is fitted through a multi-exponential model. The standard MMS is composed of the addition of five component curves as [68]:

$$\hat{m}(x) = c + \hat{m}_1(x) + \hat{m}_2(x) + \hat{m}_3(x) + \hat{m}_4(x) \quad (2.54)$$

where $\hat{m}(x)$ is the migration intensity of age x , $\hat{m}_1(x)$ is the single negative exponential childhood curve, $\hat{m}_2(x)$ is the left skewed unimodal labor force curve, $\hat{m}_3(x)$ is the almost bell shaped retirement curve, $\hat{m}_4(x)$ is the single exponential elderly curve, and c is the constant improving the fit.

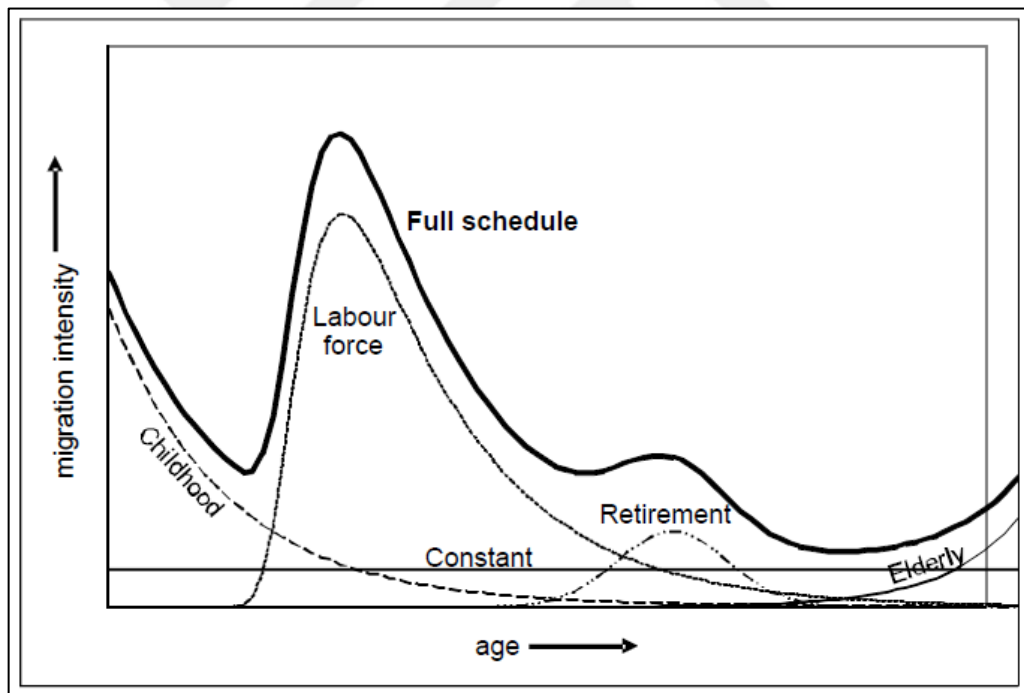


Figure 2.1. The standard model migration schedule [68]

The standard MMS with the five component curves is illustrated in Figure 2.1. Algebraically, Equ. (2.54) is a 13-parameter multi-exponential model expressed as:

$$\begin{aligned} \hat{m}(x) = & c + a_1 \exp(-\alpha_1 x) + a_2 \exp\{-\alpha_2(x - \mu_2) - \exp[-\lambda_2(x - \mu_2)]\} \\ & + a_3 \exp\{-\alpha_3(x - \mu_3) - \exp[-\lambda_3(x - \mu_3)]\} + a_4 \exp(-\alpha_4 x) \end{aligned} \quad (2.55)$$

where a_i is the height of curve $\hat{m}_i(x)$, $i=1, \dots, 4$; α_i is the rate of descent of curve $\hat{m}_i(x)$, $i=1, \dots, 4$; λ_2 and λ_3 are rates of ascents of curves $\hat{m}_2(x)$ and $\hat{m}_3(x)$, and μ_2 and μ_3 are rates of ascents of curves $\hat{m}_2(x)$ and $\hat{m}_3(x)$.

Since its introduction, MMSs have become a major approach in analyzing the migration age patterns. Their primary application is focused on specification of age patterns in case of missing or questionable data [69,70]. MMSs enable comparative analyses of migration age patterns [71] and provide data reduction by representing a large number of migration intensities through a small number of parameters [72]. In addition, the future migration profiles are projected through analyzing time series of model parameters [73].

In most of the cases, the retirement and/or elderly curves of MMS are omitted if age profiles do not display a peaks after the labor force curve; thus, the thirteen parameter standard MMS is transformed into a multi-exponential model with seven or eleven parameters. Wilson [67] includes an additional curve to represent the patterns at late teenage which cannot be captured via the standard MMS. The student curve $\hat{m}_5(x)$ proposed by Wilson [67] is a double exponential function expressed as:

$$\hat{m}_5(x) = a_5 \exp\{-\alpha_5(x - \mu_5) - \exp[-\lambda_5(x - \mu_5)]\} \quad (2.56)$$

in which the parameters are interpreted as it is done for Equ. (2.55). With the addition of Equ. (2.56) into Equ. (2.55) an eighteen parameter MMS is obtained. A further modification is made by replacing the double exponential retirement function by the PK model described in Equ. (2.36) [67,74]. Such a modification enhances the fitting capability of MMSs in some cases by resolving parameter instabilities. As a disadvantage the PK function is symmetrical which may not be appropriate for representing the retirement curve, but it is reported that this symmetry is tolerable for most circumstances [67] as the original retirement curve is also relatively bell shaped.

Implementing MMS to observed data requires nonlinear regression approaches which often rely on initial parameter estimation. Rogers *et al.* [75] propose simpler linear methods to fit the multi-exponential model schedules that can be used in most applications. They express

the set of component curves as a weighted linear combination of density functions dedicated to each component.

MMSs restrict migration age patterns to follow a prototypical shape which may not adequately represent the observed age patterns in developing or under-developed regions. Furthermore, the difficulties in specifying the optimal component curves to integrate weaken the estimation capabilities of MMSs [76,77]. Moreover Rogers *et al.* [75] report that the estimates are highly sensitive to initial parameter values. These problems result in a necessity to determine the set of component curves and parameter initialization following a trial and error manner. Utilization of non-parametric approaches such as cubic splines and kernel regression may prevent such problematic issues. These models do not constrain the age profiles to conform to a predetermined prototypical shape [78] and provide simpler implementations that are relatively less sensitive to subjective prior assumptions [61].

Rogers *et al.* [79] applied cubic splines to smooth the migration intensities assuming that cubic splines generate better fits than the MMSs as they intensely utilize the local information with probably more number of parameters. Cubic splines are linear combinations of third degree polynomial functions that are connected at several knots. Bernard and Bell [61] use the following *b*-spline model to smooth migration age profiles:

$$B(x; s_1, s_2, \dots, s_{k+2}) = (k+1) \sum_{j=1}^{k+2} \left[\prod_{1 \leq m \leq k+2, m \neq j} (s_m - s_j) \right]^{-1} P_k(x; s_j) \quad (2.57)$$

where k is the degree of the polynomial, which is three for cubic splines and:

$$P_k(x; s_j) = \begin{cases} (x - s)^k, & x \geq s \\ 0, & x < s \end{cases} \quad (2.58)$$

Despite their fitting capabilities, cubic splines are sensitive to the number and the locations of knots they include [80]. Knots may be determined by simple approaches such as scatter plot analyses [81] and model fit criteria [82], or through computationally intensive adaptive data-driven techniques [83]. However, in migration context, the number of knots is generally fixed and their locations are distributed at quinquennial intervals [61].

Another non-parametric method used in age-specific migration modeling is the kernel regression. Kernel regression has been implemented to fit age-specific fertility and mortality rates [84,85], and is proposed to smooth age-specific migration data by Bernard and Bell [61]. A kernel regression model for estimating the migration intensities as a function of ages 5 to 90 is:

$$\hat{m}(x) = \frac{\sum_{a=5}^{90} \varphi \left[\frac{x-a}{h} \right] m_a}{\sum_{a=5}^{90} \varphi \left[\frac{x-a}{h} \right]} \quad (2.59)$$

Here, φ is a normal density function which assigns more weight to the observed migration intensities close to age x . The choice of bandwidth parameter h , $h>0$, is critical as large bandwidths while the choice of kernel function is not that significant for the performance of the model [86].

Recently, Bernard and Bell [61] compared cubic splines, kernel regression and MMSs in terms of their performances in smoothing migration age profiles. They found that MMSs result in better fits when predetermined shape of the schedule is capable of capturing the true age distribution and it is possible to specify the set of component curves to be included accurately. When the above mentioned requirements are not satisfied kernel regression or cubic splines provide more satisfactory outputs.

2.3.2. Logit Models

Applications of model schedules in fitting migration age patterns is more limited when compared to utilizations of model schedules for representing age-specific fertility and mortality data. This is mainly because, in contrast to fertility and mortality, which are expressed in terms of a single population, migration is related to both origin and destination populations. Thus, Rogers *et al.* [79] claim that concentrating only on age patterns is not appropriate for migration modeling; one should also take the spatial patterns into account. Such point of view constitutes the basis for a different family of modeling approaches that aim to capture both the age-specific and origin-destination specific

structures in migration flows. Rogers *et al.* [87] use logit models for this purpose. They define the age-specific migration flows as conditional survivorship proportions:

$$\bar{S}_{ij}(x) = \frac{n_{ij}(x)}{n_{i+}(x)}, \quad i \neq j \quad (2.60)$$

where $\bar{S}_{ij}(x)$ is the proportion of emigrants of age x originating from place i to destination j , $n_{ij}(x)$ is the number of emigrants of age x originating from place i to destination j , and $n_{i+}(x)$ is the number of individuals of age x that are present at place i at the beginning of migration interval. The proportion displayed in Equ (2.60) can be decomposed into two elements: the generation (level) element $\bar{S}_i(x)$, and the distribution element $\bar{S}_{j|i}(x)$ as:

$$\bar{S}_{ij}(x) = \frac{\sum_{j \neq i} n_{ij}(x)}{n_{i+}(x)} \frac{n_{ij}(x)}{\sum_{j \neq i} n_{ij}(x)} = \bar{S}_i(x) \bar{S}_{j|i}(x) \quad (2.61)$$

where $j|i$ denotes the conditional term and $\sum_j \bar{S}_{j|i}(x) = 1$. Such decomposition is necessary to characterize the migration patterns that are convoluted through the mixture of inhabitants and migrants. Here, a saturated binomial logit model is utilized to elucidate the proportion of emigrants from each origin and a saturated multinomial logit model is employed to portray the proportion of those that are migrating to each destination given the emigrants from each origin.

Let the predicted values $\hat{\theta}_{ij}(x)$ denote the possibility of migrating from origin i to destination j with respect to a reference destination k . The saturated logit model for generation component is then:

$$\hat{\theta}_i(x) = \frac{\bar{S}_i(x)}{1 - \bar{S}_i(x)} = v v_i^O v^A(x) v_i^{OA}(x) \quad (2.62)$$

where v are the parameters to estimate and superscripts O and A represents origin and age respectively. The model in Equ (2.62) estimates the possibilities of being a migrant to being an inhabitant for origin i . The saturated multinomial model for the distribution element is described as:

$$\hat{\theta}_{j|i}(x) = \frac{\bar{S}_{j|i}(x)}{\bar{S}_{k|i}(x)} = v_{j|i} v_{j|i}^A(x) \quad (2.63)$$

The model displayed in Equ. (2.63) predicts the odds of migrating to destination j given the origin i at age x relative to reference destination k . A similar procedure is followed by Raymer *et al.* [88] to describe the age and spatial characteristics of migration in Italy. For this task, a multiplicative component model based on a saturated log-linear model is defined to describe the migration flows between origin i and destination j at age x , $n_{ij}(x)$, as follows:

$$n_{ij}(x) = (T)(O_i)(D_j)(OD_{ij}) \quad (2.64)$$

The model in Equ. (2.64) includes four elements: T is an overall element depicting the migration level, O is an origin element standing for pushes from each origin point i , D is a destination element standing for pulls to each point j , and OD is a bi-lateral origin-destination interaction element. In its additive log-linear form, Equ. (2.64) can be rewritten:

$$\ln n_{ij}(x) = \lambda + \lambda_i^O + \lambda_j^D + \lambda_{ij}^{OD} \quad (2.65)$$

or in its multiplicative form:

$$n_{ij}(x) = \tau \tau_i^O \tau_j^D \tau_{ij}^{OD} \quad (2.66)$$

Equ. (2.66) can be modified to include an age dimension A as:

$$n_{ij}(x) = \tau \tau_i^O \tau_j^D \tau^A(x) \tau_{ij}^{OD} \tau_i^{OA}(x) \tau_j^{DA}(x) \tau_{ij}^{ODA}(x) \quad (2.67)$$

Raymer and Rogers [89] enhanced Equ. (2.66) by including an offset term to the unsaturated version of the log-linear model as:

$$n_{ij}(x) = n_{ij}^*(x) \tau \tau_i^O \tau_j^D \tau^A(x) \quad (2.68)$$

where the unsaturated model incorporates only the main effects origin, destination and age; and the offset $n_{ij}^*(x)$ is a matrix with auxiliary information such as a past table of migration flows. Thus, the predicted flow values are based on imposed age-specific and

spatial regularities hidden in the offset. Such modifications enable the model to be used when complete or adequate data are not readily available. This idea has already been applied in Rogers *et al.* [90] with an output of a migration flow table that displays the level of a current period by adopting the spatial characteristics of the offset.

2.3.3. Bayesian Approaches

Recently, apart from MMSs and age-specific and spatial logit models, Azose and Raftery [91] fit Bayesian hierarchical first order autoregressive, AR(1), model to net migration rates for all countries. Their novel method is composed of three levels for modeling the migration rate $r_{c,t}$ in country c at time period t as:

$$\text{Level 1} \left\{ \begin{array}{l} r_{c,t} - \mu_c = \phi_c (r_{c,t-1} - \mu_c) + \varepsilon_{c,t} \\ \varepsilon_{c,t} \sim N(0, \sigma_c^2) \end{array} \right. \quad (2.69)$$

$$\text{Level 2} \left\{ \begin{array}{l} \phi_c \sim U(0,1) \\ \mu_c \sim N(\lambda, \tau^2) \\ \sigma_c^2 \sim IG(a,b) \end{array} \right. \quad (2.70)$$

$$\text{Level 3} \left\{ \begin{array}{l} a \sim U(0,10) \\ b | a \sim U(0,100(a-1)) \\ \lambda \sim U(-100,100) \\ \tau \sim U(0,100) \end{array} \right. \quad (2.71)$$

where $X \sim N(\mu, \sigma^2)$ denotes a random variable having a normal distribution with mean μ and variance σ^2 . $U(c,d)$ denotes a uniform distribution between the interval $[c,d]$, and $IG(a,b)$ denotes an inverse gamma distribution. After obtaining posterior distributions for the model parameters through Markov Chain Monte Carlo (MCMC) simulation with Gibbs sampling, migration rates are converted into migration counts. Next, the projected

migration counts for country c at time period t are further decomposed into age and sex components via MMSs.

Another Bayesian modeling framework is suggested by Wiśniowski *et al.* [92] for estimating the age and sex patterns and their linkage with the origin-destination components of migration between European countries. Let z_{odast}^k denote the flows (counts) from country o to country d of sex s at age group a during time period t reported by the sending S or receiving R country, where $k \in \{S, R\}$. It is assumed that:

$$z_{odast}^k \sim \text{multinomial}(z_{od+++}^k, \boldsymbol{\rho}_{odt}^k) \quad (2.72)$$

where vectors $\boldsymbol{\rho}_{odt}^k = (\rho_{od1Ft}^k, \dots, \rho_{odAMt}^k)$ are age-sex distributions for either the sending or receiving country, M is for male, F is for female, A is the oldest age group, and the subscript $+$ denotes summation over a given index. This multinomial expression is redefined as a Poisson model as:

$$z_{odast}^k \sim \text{Poisson}(v_{odast}^k) \quad (2.73)$$

where:

$$\rho_{odast}^k = \frac{v_{odast}^k}{v_{od+++}^k} \quad (2.74)$$

The existing inconsistencies in the available data are adjusted through a log-normal transformation and then a multivariate logit transformation is applied to model the true spatial flows on the logarithmic scale. The posterior distributions for the model parameters are estimated using MCMC simulation with Gibbs sampling, which results in an age-and-sex-specific bilateral migration flow database with measures of uncertainty.

The LC based dimension reduction methods are also proposed within Bayesian perspectives for age-specific migration modeling. Raymer *et al.* [93] examine the applicability of LC type models to forecast age-specific migration. They claim that the quality of migration data is relatively worse than mortality and fertility data, therefore, some smoothing should be performed before implementing a model on migration data. Later, following a Bayesian scheme, Wiśniowski *et al.* [17] formalized Raymer *et al.* [94]'s study by extending the LC model to cover age-specific fertility, mortality and

migration, hence a total population forecasting method. In this Bayesian LC approach, the counts of migrants, which are separated into two as counts of emigrants and immigrants, are assumed to have a Poisson distribution with a lognormally distributed age-and-time-specific mean. They models emigration rates as:

$$E_{x,t} \sim \text{Poisson}(\gamma_{x,t} R_{x,t}) \quad (2.75)$$

$$\ln(\gamma_{x,t}) = a_x^E + b_x^E k_t^E + \varepsilon_{x,t}^E \quad (2.76)$$

where $\gamma_{x,t}$ is the emigration rate for age group x at time period t , $R_{x,t}$ is the population at risk, and the superscript E represents emigration. For modeling immigration, due to the ambiguities resulting from determining the population at risk, counts are modeled instead of rates as:

$$I_{x,t} \sim \text{Poisson}(\varphi_{x,t}) \quad (2.77)$$

$$\ln(\varphi_{x,t}) = a_x^I + b_x^I k_t^I + \varepsilon_{x,t}^I \quad (2.78)$$

Here, $\varphi_{x,t}$ is the number of immigrants belonging to age group x at time period t , and the superscript I is used to denote immigration.

In estimating the time-specific parameters in Equ. (2.76) and Equ. (2.78), Wiśniowski *et al.* [17] consider univariate and bivariate autoregressive processes and use Bayesian inference. More recently, Raymer and Wiśniowski [62] modeled both emigration and immigration counts which they assume to follow Poisson distribution whose mean is lognormally distributed as in the case of Wiśniowski *et al.* [17]. They test this LC model through Bayesian perspectives for Sweden, South Korea and Australia and demonstrate the flexibility and applicability of LC model and Bayesian inference for migration forecasting.

2.4. COHORT COMPONENT METHOD

The cohort component method is one of the most utilized technique for estimating a population of a city, region, or a country through age-specific mortality, fertility, and migration values [95]. In this procedure, the population is split into age and sex groups or cohorts and births, deaths, and migration values take place to make sound population

estimates for a single or five year projection interval (t to $t+1$ or t to $t+5$) [96]. For the quinquennially aggregated case, there are usually sixteen or eighteen five-years-age groups starting with the age group less than 5 years old (0-4 years old) and ending with age group 75+ or 85+ based on the number of groups chosen [3]. The underlying mathematical formulations can be grouped in three; namely estimating the population at age five and over, estimating the population below age five, and estimating other demographics. The following sub-sections 2.4.1 to 2.4.3 are dedicated to mathematical formulations for estimating these three outcomes.

2.4.1. Estimating the Population at Age Five and Over

The procedure starts with the estimation of survival ratios which can be accomplished as:

$$SR(x,s) = T[ELB(s)] \quad (2.79)$$

where $x = 1, \dots, 18$ denote the five year age group, $s = 1, 2$ is the sex group (1 for male and 2 for female), $SR(a,s)$ is the survival ratio for age group x and sex group s over the interval, $ELB(s)$ is the life expectation at birth of sex group s for a specified projection interval; and T is the function that transforms $ELB(s)$ into $SR(x,s)$ based on a selected life table.

Once the survival ratios for each age group x and sex group s are found, the number of survivors belonging to a specific age and sex group by the termination of a quinquennial interval can be calculated excluding the migration values as follows:

$$P(x+1,s,t+5) = P(x,s,t) * SR(x,s) \quad \text{for } x = 1, \dots, 18, s = 1, 2 \quad (2.80)$$

where t is the first year of the projection, $P(x+1,s,t+5)$ is the number of survivors of age group $x+1$ and sex group s by the termination of the projection interval excluding migration, and $P(x,s,t)$ is the number of survivors of age group x and sex group s at the start of the projection interval.

Since above calculations do not include concepts associated with migration, population estimation for those that are aged 5 and over is necessary. First net migration rates should be determined for each age and sex group. That is;

$$MR(x,s,t+5) = TMR(s,t+5) * PMR(x,s,t+5) \text{ for } x=1,\dots,18, s=1,2 \quad (2.81)$$

where $MR(x,s,t+5)$ is the net migration rate for survivors of age group x and sex group s by the termination of the projection interval $(t+5)$, $TMR(s,t+5)$ is the total migration rate for survivors of sex group s by the termination of the projection interval, and $PMR(x,s,t+5)$ is the proportionate net migration rate for survivors of age group x and sex group s by the termination of the projection interval.

The calculation of net migration rates of each age and sex group combination makes it possible to estimate net change in population resulting from migration. This is achieved by:

$$NC(x,s,t+5) = P(x,s,t+5) * MR(x,s,t+5) \text{ for } x=2,\dots,18, s=1,2 \quad (2.82)$$

where $NC(x,s,t+5)$ is the net population change as a result of migration for the survivors of age group x and sex group s by the termination of the projection interval.

Following this, the population of those that are aged five and over by the termination of the projection interval, which is expressed as $Pop(x,s,t+5)$, can be enumerated for each age and sex group by combining Equ. (2.80) and Equ. (2.82). This can be shown as:

$$Pop(x,s,t+5) = P(x,s,t+5) + NC(x,s,t+5) \text{ for } x=2,\dots,18, s=1,2 \quad (2.83)$$

2.4.2. Estimating the Population Below Age Five

Projecting the population below age five first requires estimating age-specific fertility rates, number of births and counts of migration respectively. Age-specific fertility rates can be calculated as:

$$FR(x) = (TFR/5) * PFR(x) \text{ for } x=4,\dots,10 \quad (2.84)$$

where $FR(x)$ is the average annual fertility rate of age group x during the projection interval, TFR is the total fertility rate for the quinquennial projection interval, and $PFR(x)$ is the proportionate fertility rate of age group x for the corresponding projection interval. Here, $x=4,\dots,10$ reflects the age groups for childbearing span.

The computation of the number of births requires the calculation of the number of females at ages corresponding to childbearing span at the middle of the projection interval. This is done through taking the geometric mean of the number of females at the start and by the termination of time interval, which is stated as:

$$MP(x,2)=[P(x,2,t)*P(x,2,t+5)]^{1/2} \quad \text{for } x=4,\dots,10 \quad (2.85)$$

where $MP(x,2)$ is the mid-interval population of females of age group x . Together with the age-specific fertility rates, mid-interval population of females for age groups four to ten is used to compute the number of births for the time interval of interest, which can be formulated as:

$$Births = 5 * \left[\sum_{x=4}^{10} FR(x) * MP(x,2) \right] \quad (2.86)$$

To enumerate the number of children who survive by the termination of this time interval, first, the sex structures at birth should be computed with the help of sex ratios at birth. The number of births grouped by sex is given as:

$$B(s) = B * RBS(s) \quad \text{for } s = 1, 2 \quad (2.87)$$

where

$$RBS(s) = \begin{cases} SRB / (100 + SRB), & \text{for } s = 1 \\ 100 / (100 + SRB), & \text{for } s = 2 \end{cases} \quad (2.88)$$

and $B(s)$ is the number of births of sex group s that occur during the projection interval, $RBS(s)$ is the proportion of births of sex group s , and SRB is the sex ratio at birth.

Ignoring the migration counts, the population below age five is then computed as:

$$P(1,s,t+5) = B(s) * SR(1,s) \quad \text{for } s = 1, 2. \quad (2.89)$$

To complete this subsection, external migration amounts for the age groups of interest should be included in the calculations. The net population changes as a result of migration for survivors below age five is:

$$NC(1,s,t+5) = P(1,s,t+5) * MR(1,s,t+5) \text{ for } s = 1,2. \quad (2.90)$$

Then population below age 5 can be obtained by:

$$Pop(1,s,t+5) = P(1,s,t+5) + NC(1,s,t+5) \text{ for } s = 1,2. \quad (2.91)$$

2.4.3. Other Demographic Outcomes

The age and sex structures that are estimated through Equ (2.79) to Equ. (2.91) can be used to compute some other demographic indicators. To start with, population size can be computed via summation of all age and sex group combinations as:

$$Pop(t+5) = \sum_{x=1}^{18} \sum_{s=1}^2 Pop(x,s,t+5) \quad (2.92)$$

where $Pop(t+5)$ is the size of population by the termination of the projection interval. As well as this aggregation; population can be examined in several age groups, namely; young-age population, working-age population, old-age population, and school-age population. Young-age population, which is the sum of all survivors below age 15, can be estimated by:

$$YP(t+5) = \sum_{x=1}^3 \sum_{s=1}^2 Pop(x,s,t+5) \quad (2.93)$$

where $YP(t+5)$ is the young-age population by the termination of the projection interval. Similarly, working-age population within the age interval 15-64 is obtained as:

$$WP(t+5) = \sum_{x=4}^{13} \sum_{s=1}^2 Pop(x,s,t+5) \quad (2.94)$$

where $WP(t+5)$ is the working-age population by the termination of the projection interval. The old-age population corresponding to age groups of 65+ is:

$$OP(t+5) = \sum_{x=14}^{18} \sum_{s=1}^2 Pop(x,s,t+5) \quad (2.95)$$

where $OP(t+5)$ is the old-age population at the end of the projection interval. In a similar manner school-age population which is composed of population groups within the age interval 5-24 can be computed as:

$$SP(t+5) = \sum_{x=2}^5 \sum_{s=1}^2 Pop(x,s,t+5) \quad (2.96)$$

where $SP(t+5)$ is the school-age population by the termination of the projection interval.

The number of females belonging to childbearing span, which is the group of females of ages 15 to 49, can be estimated via:

$$CBS(t+5) = \sum_{x=4}^{10} Pop(x,2,t+5) \quad (2.97)$$

where $CBS(t+5)$ is the population of females that are in childbearing span by the termination of the time interval.

The mid-interval population size MP is measured by the geometric mean of the population sizes at the start and end termination the projection interval, which is stated as:

$$MP = [Pop(t) * Pop(t+5)]^{1/2} \quad (2.98)$$

Furthermore, the total number of person-years-lived, demonstrated as $NPYL$ is computed by the product of mid-interval population size and number of years in the projection interval. That is:

$$NPYL = MP * 5 \quad (2.99)$$

The population growth over the projection interval, illustrated as $PopGr$, equals to the difference between the population sizes at the termination and start of the time interval. The population growth can be mathematically expressed as:

$$PopGr = Pop(t+5) - Pop(t) \quad (2.100)$$

Changes due to migration are essential in calculating the number of deaths that take place during the projection interval. The net population change in the population due to migration during the interval t to $t+5$, NCM , can be expressed as:

$$NCM = \sum_{x=1}^{18} \sum_{s=1}^2 NC(x,s,t+5) / SRF(x,s) \quad (2.101)$$

where for each s :

$$SRF(x,s) = \begin{cases} 0.67 + 0.33 * SR(1,s), & \text{for } x=1 \\ (1 + SR(x,s)) / 2, & \text{otherwise} \end{cases} \quad (2.102)$$

is the survival ratio factor while $SR(x,s)$ is the survival ratio. Then, the number of deaths that occur during the projection interval, expressed as D , can be obtained via:

$$D = B - PopGr + NCM \quad (2.103)$$

The cohort component method also makes it possible to derive some estimates on rates of population change. Crude birth rate, crude death rate, rate of natural increase, rate of population growth, crude net migration rate are some of these indicators that can be obtained via cohort component technique. Crude birth rate, displayed as CBR , can be obtained by the proportion of the average annual number of births to the mid-interval population as:

$$CBR = [(B/5) / MP] * 1000 \quad (2.104)$$

Similarly crude death rate, CDR , is:

$$CDR = [(D/5) / MP] * 1000 \quad (2.105)$$

The average annual rate of natural increase, RNI , is determined by the change of the population size as a result of births and deaths, and it can be obtained as:

$$RNI = CBR - CDR \quad (2.106)$$

The rate of population growth, GR , is computed via utilizing natural logarithm as:

$$GR = [\ln(Pop(t+5) / Pop(t)) / 5] * 1000 \quad (2.107)$$

Finally, the average annual crude net migration rate, CMR , can be enumerated as the average annual net population change as a result of migration by the mid-interval population size and multiplied by 1000:

$$CMR = [NCM / 5] / MP * 1000 \quad (2.108)$$

2.4.4. Applications Areas

The cohort component method has been used in population projections by several significant organizations such as United Nations, World Bank, the US Census Bureau, Eurostat and etc. As well as these organizations, national statistical offices mainly make use of cohort component method in producing national level forecasts [97]. The use of cohort component technique is not limited to population forecasting, but it is also applied in medicine, education, economics, and so on. That is, the method has been utilized to forecast populations by level of their education [98], labor force forecasts [99], projection of future cancer incidence [100], predicting the number of surgeries [101], and so on.

Through cohort component method; number of births, deaths, and migration are treated separately [95]. In order to make use of the model a number of age-specific demographic inputs should be given to the model including expectation of life at birth, survival ratio transformation parameters, fertility rates, external migration levels and etc. Estimation of these inputs may be quite difficult for countries or regions in which healthy population statistic are not recorded [102]. For such cases there exist several strategies to come up with appropriate input values developed by Population Division of the Department of International Economic and Social Affairs of the United Nations Secretariat. Smith [95] asserts that although a recording system is available for population demographics, obtaining sound data on migration is extremely difficult.

With the developments in computer technologies, today there are several soft wares which can perform population projections based on cohort component method. In 2010, China Population and Development Research Center launched a software named PADIS-INT in cooperation with United Nations Population Division [103]. PADIS-INT is a web-based software for population projections making use of cohort component method with access to United Nations' life tables online [104]. There are also some other software for cohort component projections such as Spectrum. A module named DemProj in Spectrum software is developed for making population projections using cohort component method [105].

2.5. LESLIE MATRIX

In 1945, Leslie introduced the matrix representation of a population projection method based on assumed mortality (or survival) and fertility values [1]. The Leslie matrix model is based on matrix algebra in which a population is treated as a combination of discrete age cohorts with corresponding fertility and survival ratios, similar to cohort component method. The model can be written as:

$$\mathbf{n}(t+1) = \mathbf{X}\mathbf{n}(t) \quad (2.109)$$

where $\mathbf{n}(t)$ is a population vector with entries $n_i(t)$ representing the number of persons in each age class i at time t , $\mathbf{n}(t+1)$ is a population vector of the next time period, and \mathbf{X} is the $n \times n$ Leslie matrix, which is sometimes referred as projection matrix [69].

The two of the standard components of population projection methods, fertility and mortality are hidden in the projection matrix \mathbf{X} . For female population, the first row of the matrix \mathbf{X} is dedicated to fertility of an age group i , F_i ; whereas the sub-diagonal entries correspond to survival probabilities, P_i , and all the other entries are set to zero. In explicit form, Equ. (2.108) can be reorganized as:

$$\begin{pmatrix} n_1(t+1) \\ n_2(t+1) \\ n_3(t+1) \\ \vdots \\ n_3(t+1) \end{pmatrix} = \begin{pmatrix} F_1 & F_2 & F_3 & \dots & F_{w-1} & F_w \\ P_1 & & & & & \\ 0 & P_2 & & & & \\ \cdot & & P_3 & & & \\ \cdot & & & \ddots & & \\ 0 & \cdot & \cdot & \dots & P_{w-1} & 0 \end{pmatrix} \begin{pmatrix} n_1(t) \\ n_2(t) \\ n_3(t) \\ \vdots \\ n_3(t) \end{pmatrix} \quad (2.110)$$

For male population the entries in first row of projection matrix \mathbf{X} are also set to zero. The whole population is then calculated as the sum of male and female population. If the matrix \mathbf{X} is constant over time, then given the population at time t , the population after p projection intervals can be computed via:

$$\mathbf{n}(t+p) = \mathbf{X}^p \mathbf{n}(t) \quad (2.111)$$

Although Equ. (2.111) depends on a constant \mathbf{X} , in most of the cases the projection matrix can vary within time as well [15]. In this case, Equ. (2.111) can be modified as:

$$\mathbf{n}(t+p) = \mathbf{X}(t+p)\mathbf{X}(t+p-1)\dots\mathbf{X}(t)\mathbf{n}(t) \quad (2.112)$$

Leslie matrix model is the underlying principle model in many of the projection and forecasting methods. It is used together with Markov chains [1], stochastic estimation [57] and in many other population estimation techniques [106].



3. MOTIVATION FOR THE STUDY

In addition to the shortcomings of the existing demographic forecasting methods in terms of their strict statistical or subjective assumptions that may not always be met, the most problematic issue in demographic analysis is the high amount of uncertainty and vagueness in data. Although the quality of mortality and fertility data is better compared to that of migration for most of the developed countries, there are still several issues regarding the accuracy as a result of data recording and collection errors. The situation is worse in some of the developing and under developed regions, in which the age-decompositions of mortality or fertility are incomplete, thus, they are generated through some estimation methods.

The issue is even more complicated for migration modeling. In addition to the difficulties in generating realistic predictions, another issue in migration modeling is the term migration itself: there is no universally accepted definition of the term “migrant” [107]. Thus, even for a single country, different statistics bureaus may give different number of migrants based on their perception of migration. Methods using aggregated data from distinct datasets may result in inconsistencies and be misleading [108–110]. Moreover, the exact values of migrants or migration rates are rarely known due to errors in data collection and recording systems [111].

In general international migration data are shown as total stocks or bilateral flows, in which age or sex profiles of migrants are often neglected, even for the developed countries. However, forecasts regarding age and sex profiles of migrants are vital in public and private policy designs and long and short term socio-economic decisions [97]. Furthermore, numbers of emigrants and immigrants or emigration and immigration rates are not available in some datasets; and migration is represented through the concept of net migration which is the difference between number of immigrants and emigrants, but in reality the term is artificial since there exists no individual as a net migrant. Thus, the use of net migrants or net migration rates for modeling migration would yield vague results [112]. Moreover, net migration rates are seldom known, and often are estimates through the census data based on number of births and deaths in a time interval. However, forecasts based on these estimates are in fact estimates from estimated figures. This kind of *ex ante*

analysis may be misleading since the error bounds expands proportional to the existing errors in data used.

Despite some advocates of modeling net migration rates or counts, the current state of art is modeling rates of emigration relative to the population at risk and counts of immigration [113]. The immigration phenomenon is not represented by rates, since the population at risk for immigrants is not often known.

In general if there exist high uncertainty due to lack of data or knowledge, the utilization of probability distributions becomes questionable, which leads the researchers to non-probabilistic approaches such as fuzzy, evidence or interval theories [114]. In this study, considering the lack of coherent definitions of migration and the previously mentioned ambiguities in mortality, fertility and migration data, a novel fuzzy method for modeling age-and-sex-specific population is proposed. Here, the purpose is to model and forecast age-specific *mortality* and *fertility rates* and *emigration* and *immigration counts* for each sex. These demographic indicators are then integrated to generate fuzzy age-specific population forecasts for the following years. The reason to model emigration counts instead of emigration rates is to provide means for comparing emigration and immigration behaviors. All of the demographic indicators are expressed as triangular symmetric fuzzy numbers rather than the classical crisp notation, so that the uncertainty and vagueness in data are represented coherently.

3.1. CONTRIBUTIONS AND RESEARCH AIMS OF THE STUDY

The main contributions and research aims of this study can be listed as:

- to analyze the applicability of fuzzy set theory in demographic forecasting,
- to derive a coherent fuzzy representation for the observed crisp mortality and fertility rates and emigration and immigration counts,
- to enhance the fitting capability by introducing a bi-level structure representing both the country-specific and age-group-oriented behaviors in demographic components

- to fit models with small errors to the fuzzified observed data and forecast the future values with fuzzy intervals (the aim is to provide fuzzy intervals for future forecasts instead of precise predictions),
- to include subjective judgement on model parameters that shape the future levels of demographic components through Bayesian inference and generate informative forecasts within not-too-wide fuzzy intervals.

3.2. A SUMMARY OF THE PROPOSED METHOD

The proposed fuzzy method for modeling age-specific demographic indicators is denoted by FMM (Fuzzy Modeling Method) and is developed based on the existing fuzzy Lee-Carter mortality modeling technique [16]. Originally proposed for modeling human mortality, Lee-Carter (LC) method [15] is an extrapolation approach in which the natural logarithm of mortality rates for age group x at time t are expressed through a regression equation as:

$$\ln(\mathbf{m}_{x,t}) = \mathbf{a}_x + \mathbf{b}_x \mathbf{k}_t + \varepsilon_{x,t} \quad (3.1)$$

Here, the intercept value \mathbf{a}_x and the regression coefficient \mathbf{b}_x are the unknown age-specific parameters, whereas the time-specific independent variable \mathbf{k}_t is named as mortality index. Lee and Carter utilize singular value decomposition (SVD) technique to find the unknown regression parameters and the mortality indices. According to this technique the error terms $\varepsilon_{x,t}$ reflect the historical effects that are not covered by the model and are assumed to be normally distributed with mean 0 and a small constant variance. The extensions of LC model are discussed in Section 2.1.

This method is able to capture the decreasing mortality trend in most of the developed countries. The highlighted singular value-eigenvector structure in SVD allows the model to emphasize the fundamental characteristics in mortality rates, which follow similar patterns in all age groups throughout time. Thus, LC model can be extended to model fertility and migration rates as long as there are consistent similarities between the trends and patterns followed by these demographic rates in different age groups. Although fertility rates exhibit a slightly more variable trend [115], the last century witnessed a certain decline in

both mortality rates [15] and fertility rates [116] in the developed and most of the developing countries (in which data are available) by time. Considering the similarities in mortality and fertility trends for most of the developed countries, LC model is also implemented for modeling fertility rates [17,117]. Moreover, Wiśniowski *et al.* [17] apply this method for modeling age specific migration through a Bayesian approach. Furthermore, Garcia-Guerrero [118] uses this method to forecast the international age-and-sex-specific net migration rates of Mexico.

In general, the underlying SVD structure in LC model relies on the assumption that the rows of the data matrix Z which include the data to be decomposed should refer to a fixed effects domain such as space, time, genes, age groups, cohorts, and etc. In case of demographic modeling, these fixed effects are the age cohorts. This domain is expected to share similarities which can be reflected within the entries z_{ij} of data matrix Z in terms of smoothness or clustering as a function of the row domain [119]. Since the age cohorts exhibit alike patterns in terms of trends in mortality and fertility rates, SVD seems to be a good choice to be included in an age-specific mortality, fertility or migration model.

FMM proposed in this study first fits a fuzzy bi-level model to the fuzzified observed age-specific demographic indicators of mortality, fertility and migration, in which the first level is dedicated to general demographic characteristics due to country-specific factors and the second level mimics the behaviors of analogous age groups. In fact, a single leveled model is adequate to represent age-specific mortality and fertility; but a second level is included into the model to fit the migration values. Next, the method forecasts the future fuzzy migration values using the fuzzy model parameters and time series analysis through Bayesian approach. Finally, fuzzy forecasts for future mortality, fertility and migration levels are integrated within a fuzzy population model so that future population can be forecasted. To the best of our knowledge, there exists no study incorporating fuzziness in age-specific fertility and migration modeling and population estimation.

4. METHODOLOGY

The proposed FMM for modeling and forecasting demographic indicators is a bi-level fuzzy approach in which the general demographic characteristics of a country and the age group cluster impacts are sequentially processed in two phases. For mortality and fertility only the first level is used while the bi-level structure is necessary for migration modeling. Following the estimation of age and time variant fuzzy parameters, the future demographic indicators are forecasted using time series models through Bayesian approach. Finally, mortality, fertility and migration forecasts are aggregated within a fuzzy population model to obtain future population within fuzzy intervals.

4.1. PRELIMINARIES

Some fuzzy set theory basics and fuzzy terminology that are used throughout the study are given in the following. The singular value decomposition utilized in fuzzification of observed demographic data is also summarized at the end of this subsection.

4.1.1. Fuzzy Set Theory and Related Terminology

Definition 4.1 [120]. A fuzzy subset \tilde{A} over a universe set U is denoted by $\tilde{A} = \{x, \mu_{\tilde{A}}(x) \mid x \in U\}$ where $\mu_{\tilde{A}} : U \rightarrow [0,1]$ is called the membership function of \tilde{A} . If $U = \mathbb{R}$, where \mathbb{R} is the real line, the convex subset \tilde{A} is called a fuzzy number.

Definition 4.2 [120]. A triangular fuzzy number $\tilde{A} = (a, l_A, r_A)$ with center $a \in \mathbb{R}$, left and right spreads l_A and r_A is defined by the membership function

$$\mu_{\tilde{A}}(x) = \begin{cases} 1 - \frac{|a-x|}{l_A} & \text{if } a-l_A \leq x \leq a \\ 1 - \frac{|a-x|}{r_A} & \text{if } a \leq x \leq a+r_A \\ 0 & \text{otherwise} \end{cases} \quad (4.1)$$

A triangular fuzzy number \tilde{A} is symmetric if $l_A = r_A = l$. A symmetric triangular fuzzy number \tilde{A} with center a and spread l can be denoted as $\tilde{A} = (a, l)$.

Definition 4.3 The α -cuts of a triangular fuzzy number $\tilde{A} = (a, l_A, r_A)$ are $\tilde{A}_\alpha = [A_\alpha^1, A_\alpha^2]$ which equals to $[a - l_A(1 - \alpha), a + r_A(1 - \alpha)]$, $\forall \alpha \in [0, 1]$. Figure 4.1 displays a triangular fuzzy number and the α -cut notion.

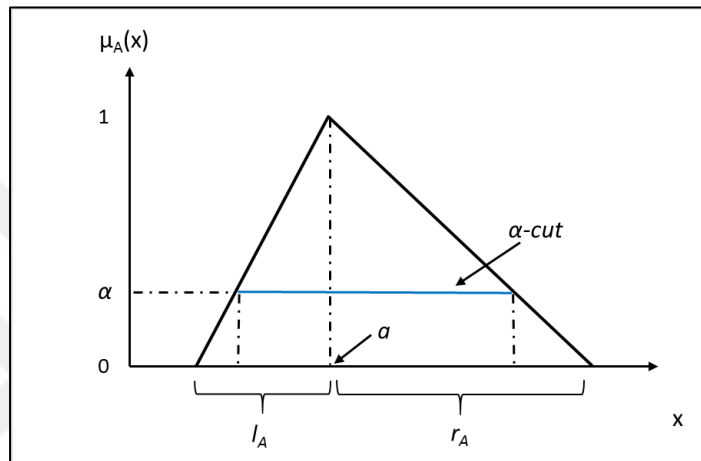


Figure 4.1. Triangular fuzzy number with α -cut

Definition 4.4 [120]. A fuzzy number $\tilde{A} = (a, l_A, r_A)$ with center a , left spread l_A , and right spread r_A is of LR -type if there exist nondecreasing continuous reference functions L (for left) and R (for right) to define its membership function as:

$$\mu_{\tilde{A}}(x) = \begin{cases} L\left(\frac{a-x}{l_A}\right) & \text{if } a-l_A \leq x \leq a \\ R\left(\frac{x-a}{r_A}\right) & \text{if } a \leq x \leq a+r_A \\ 0 & \text{otherwise} \end{cases} \quad (4.2)$$

Here, L and R are non-decreasing continuous functions mapping $[0, 1]$ onto $[0, 1]$.

Definition 4.5 [120]. A triangular norm (t -norm) T is a binary operation on $[0, 1]$ which is associative, commutative, non-decreasing and has the property $T(x, 1) = x$ for all $x \in [0, 1]$.

With the ordinary fuzzy arithmetic operations (fuzzy addition and multiplication) spreads enlarges as a result of Zadeh's extension principle [121]. The utilization of t -norm based operators prevents such accumulation of fuzziness by controlling the growth of uncertainty [122,123]. Furthermore, the extension principle also leads to deteriorations in the piecewise linear shapes of triangular fuzzy numbers for multiplication [124]. However, for computational simplicity, it is important for a fuzzy operator to preserve the shapes of fuzzy numbers [16]. The shape preserving property can be achieved through the use of weakest t -norm (T_w) based operators.

Definition 4.6 [120]. Weakest t -norm T_w is a binary operation on $[0,1]$ defined as:

$$T_w(x, y) = \begin{cases} \min(x, y) & \text{if } \max(x, y) = 1 \\ 0 & \text{otherwise} \end{cases} \quad (4.3)$$

Definition 4.7 [125]. For two symmetric triangular fuzzy numbers $\tilde{A} = (a, I_A)$ and $\tilde{B} = (b, I_B)$, weakest t -norm based addition (\oplus_{T_w}), subtraction (\ominus_{T_w}), and multiplication (\otimes_{T_w}) are defined as follows:

$$\tilde{A} \oplus_{T_w} \tilde{B} = (a + b, \max(I_A, I_B)) \quad (4.4)$$

$$\tilde{A} \ominus_{T_w} \tilde{B} = (a - b, \max(I_A, I_B)) \quad (4.5)$$

$$\tilde{A} \otimes_{T_w} \tilde{B} = (ab, \max(I_A | b |, I_B | a |)) \quad (4.6)$$

Definition 4.8 [126]. The Diamond distance D_{LR} between two symmetric triangular fuzzy numbers $\tilde{A} = (a, I_A)$ and $\tilde{B} = (b, I_B)$ is defined as:

$$D_{LR}(\tilde{A}, \tilde{B}) = (a - b)^2 + [(a - I_A) - (b - I_B)]^2 + [(a + I_A) - (b + I_B)]^2 \quad (4.7)$$

Definition 4.9 [127]. A fuzzy number \tilde{A} with membership function $\mu_{\tilde{A}}(x)$ can be defuzzified into the crisp number A as:

$$A = \frac{\int \mu_{\tilde{A}}(x)xdx}{\int \mu_{\tilde{A}}(x)dx} \quad (4.8)$$

This defuzzification approach is named as center of gravity defuzzification method.

4.1.2. Singular Value Decomposition

Definiton 10 [128]. An $m \times n$ rectangular matrix Z can be decomposed into product of three matrices as USV^T , where superscript T denotes the transpose of a matrix. Here, U is an $m \times m$ orthogonal matrix whose columns are orthonormal eigenvectors of ZZ^T , V is an $n \times n$ orthogonal matrix whose columns are orthonormal eigenvectors of $Z^T Z$, and S is an $m \times n$ diagonal matrix composed of the singular values (square roots of eigenvalues) from U or V in descending order. This decomposition technique is named as singular value decomposition (SVD).

4.2. FUZZY LEE-CARTER MODEL

LC model has become a popular method in mortality forecasting because of the fact that it is simple to be utilized for capturing the mortality trends in most of the developed countries. However, in some cases the application of LC model is limited. The outputs obtained from LC model may not reflect a reasonable trend in lack of relevant data for whole age and sex groups or in case of random fluctuations due to small sample size or exogenous effects [129]. Standard Lee-Carter Model uses SVD method and assumes that error terms are normally distributed with constant variance σ_{ε}^2 , which is a strict homoscedasticity assumption that is difficult to satisfy especially in cases where precise and enough historic data are not available. The magnitude of this variance is hoped to be small for sound forecasts but there is an obvious ambiguity in how small it should be [130]. These kinds of problems are also present in time-series and Bayesian based forecasting methods as a major weakness.

Considering the vagueness in how small the variances of error terms should be and problems related with assuming that the error terms are Gaussian, Koissi and Shapiro [16]

(2006) reformulate the Lee-Carter (LC) model by including fuzziness. The fuzzy formulation of the LC model is:

$$\tilde{Y}_{x,t} = \tilde{A}_x \oplus_{T_w} \tilde{B}_x \otimes_{T_w} \tilde{K}_t, \quad x = x_1, \dots, x_N, \quad t = t_1, t_1 + 1, \dots, t_1 + T - 1 \quad (4.9)$$

Here, $\tilde{Y}_{x,t}$ is the observed fuzzy \ln -mortality rate of age group x at time t , \tilde{A}_x and \tilde{B}_x are the unknown fuzzy age-specific parameters, and \tilde{K}_t is the unknown fuzzy time-variant mortality index. These quantities and parameters are expressed as triangular symmetric fuzzy numbers such that $\tilde{Y}_{x,t} = (y_{x,t}, e_{x,t})$, $\tilde{A}_x = (a_x, \alpha_x)$, $\tilde{B}_x = (b_x, \beta_x)$, and $\tilde{K}_t = (k_t, \delta_t)$ where $y_{x,t}$, a_x , b_x , and k_t are the centers and $e_{x,t}$, α_x , β_x , and δ_t are the spreads. The natural logarithmic transformation enables fitting a linear model to the observed rates and ensures positive estimates.

4.3. BI-LEVEL FUZZY AGE SPECIFIC DEMOGRAPHIC MODEL

The fuzzy formulation of LC model requires the fuzzification of crisp $Y_{x,t}$ values, which can be performed by adding a number $\pm\theta$ to each value, where θ is chosen to be small. The choice of θ may be arbitrary [131], or by utilizing random number generation. Koissi and Shapiro use fuzzy least squares regression based on minimum fuzziness criterion developed by Chang and Ayyub [131]. They try to find $\tilde{A}_0 = (c_{0x}, s_{0x})$, $\tilde{A}_1 = (c_{1x}, s_{1x})$, and $\tilde{Y}_{x,t} = (y_{x,t}, e_{x,t})$ with centers c_{0x} , c_{1x} , and $y_{x,t}$, and spreads s_{0x} , s_{1x} , and $e_{x,t}$, so that:

$$(y_{x,t}, e_{x,t}) = (c_{0x}, s_{0x}) + (c_{1x}, s_{1x}) \times t \quad (4.10)$$

where time t is treated as the independent variable. Although most of the mortality modeling methods rely on the fact that mortality rates can be viewed as time series, it may not be proper to directly use time as the only explanatory variable in the model. In fact, t , the independent variable in Equ. (4.10) is a monotonically increasing variable, hence the center and spread of \ln -mortality rate (dependent variables in Equ. (4.10)) take a linear form. In this study, in order to overcome this issue, a modified version of the fuzzification of crisp $Y_{x,t}$ values based on singular value decomposition (SVD) technique is proposed, so that, the fluctuations in \ln -demographic rates/counts can be included in the model. The

proposed novel method also aims to eliminate the homoscedasticity assumptions and assumptions related to the magnitude of error term variances. Moreover, it can be used in cases where there are concerns about the validity of data and when the number of data prohibits the usage of standard LC or other stochastic methods. The proposed method extends the existing fuzzy model to fertility and migration modeling as well. Thus, a complete fuzzy population modeling is possible with the proposed method.

The fuzzy model in Equ. (4.9) makes use of SVD in fuzzification of observed ln -mortality rates. SVD technique is an operative approach for modeling age-specific mortality and fertility rates because; mortality/fertility rates follow similar patterns for common time periods in all age groups, although magnitude differences might exist. That is; if mortality/fertility rate decreases (increases) in a time period for an age cohort then it decreases (increases) for all age groups in that period. For example during World War II years mortality rates decrease for all age groups. The existence of such similar fluctuations for specific time periods in all age groups allows SVD to give reasonable fits to the observed rates.

However, the nature of migration phenomenon does not necessarily exhibit similar behavior for distinct age groups. Therefore extending the existing fuzzy method for modeling age-specific migration may not result in appropriate fits. Age group is among the most dominant factors in migration behavior since there are strong dependencies between migration characteristics and age groups. For example; infants and toddlers display migration behavior similar to the young adults, whereas there is a tendency for old age groups not to migrate whatever the conditions at their origin are. Additionally, young adults are migrating more than other age groups [65].

Being aware of these behavioral differences for distinct age groups and the necessity for age-specific enhancements, the fuzzy method for modeling mortality rates can be modified to model human migration, mortality and fertility as follows.

Let $m_{x,t}$ denote the demographic indicator value (mortality/fertility rate or emigration/immigration count) of age group x at time period t for one of the sexes: females or males. The demographic indicator value is fitted via the proposed model that includes a bi-level structure as:

$$\tilde{Y}_{x,t} = [\tilde{A}_x \oplus_{T_w} \tilde{B}_x \otimes_{T_w} \tilde{K}_t] \oplus_{T_w} \tilde{C}_{i,x,t} \quad (4.11)$$

where $\tilde{Y}_{x,t}$ is the observed fuzzy \ln -demographic indicator value of age group x at time t , \tilde{A}_x and \tilde{B}_x are the unknown fuzzy age-specific parameters, and \tilde{K}_t is the unknown fuzzy time-variant demographic index. In Equ. (4.11), different than the fuzzy mortality model in Equ. (4.9), an additional term $\tilde{C}_{i,x,t}$ named as cluster factor is present. $[\tilde{A}_x \oplus_{T_w} \tilde{B}_x \otimes_{T_w} \tilde{K}_t]$ in Equ. (4.11) represents the general country profile in terms of demographic attitudes; and the cluster factor $\tilde{C}_{i,x,t}$ reflects the age group cluster impact, that is, the special demographic characteristics of an age group x at time t within a class i of analogous age groups. The country profile and age cluster factor are modeled sequentially through a fuzzy method with two levels: Level-I, modeling country profile, and Level-II, modeling the age group cluster factor.

This model is referred as fuzzy method for modeling age-specific demographic indicators (FMM).

4.3.1. Level-I: Modeling Country Profile

The country profile, expressed as $[\tilde{A}_x \oplus_{T_w} \tilde{B}_x \otimes_{T_w} \tilde{K}_t]$ in Equ. (4.11), refers to the effects of a country or a region on the overall migration behaviors of both emigrants and immigrants from and to the origin or destination respectively. This profile can be viewed as the impacts of the country's socio-economic and geographical structure on general migration characteristics of age groups related to that country.

4.3.1.1. Fuzzification Phase

The fuzzy formulation of in Equ. (4.11) requires the fuzzification of observed \ln -migration values. This fuzzification phase can be summarized via a regression model in which the task is to find a fuzzy intercept $\tilde{A}_0 = (c_{0x}, s_{0x})$ and regression coefficient $\tilde{A}_1 = (c_{1x}, s_{1x})$ so that:

$$(\mathcal{Y}_{x,t}, e_{x,t}) = (c_{0x}, s_{0x}) + (c_{1x}, s_{1x})f_t \quad (4.12)$$

The independent variable f_t in Equ. (4.12) is defined as the fuzzification index, which is capable of capturing the possible fluctuations in data. f_t can be expressed as $f_t = g_t(\vec{m}_{xt})$, where g_t is a function mapping \vec{m}_{xt} to fuzzification index f_t for each time t , and \vec{m}_{xt} is a vector composed of demographic indicator values (mortality/fertility rates or emigration/immigration counts) $m_{x_1t}, m_{x_2t}, \dots, m_{x_Nt}$ for each time t and age group $x_i = x_1, \dots, x_N$. t , the independent variable in Equ. (4.10) is a monotonically increasing variable, hence the center and spread of \ln -demographic indicator values (dependent variables in Equ. (4.10)) take a linear form. However, the proposed fuzzification index f_t , which is based on the aggregated age group demographic indicator values, does not necessarily show a linear trend. Consequently, Equ. (4.12) generates a better fitting model. The values of f_t are computed via SVD approach, in which the first singular value and its corresponding-eigenvectors allow the model to represent the fundamental characteristic of data [132].

The center values in fuzzification of \ln -migration values are based on:

$$\mathcal{Y}_{x,t} = c_{0x} + c_{1x} \times f_t \quad (4.13)$$

The application of SVD technique on Equ. (4.13) yields the following scheme: first, f_t s are assumed to be normalized to sum up to 0 and coefficients $c_{1,x}$ to sum up to 1 to ensure the model identifiability [133]. Then, in each age group x , $c_{0,x}$ is set to the average value of the observed $\ln(m_{x,t})$ for all time periods t . Next, a decomposition matrix Z with entries $z_{x,t}$ s as $\ln(m_{x,t}) - c_{0,x}$ is formed. SVD is applied on this decomposition matrix as:

$$z_{x,t} = \sum_{i=1}^{\min(x,T)} u_i(x) s_i v_i^T(t) \quad (4.14)$$

where s_i , $u_i(x)$, and $v_i(t)$ denote the i^{th} greatest singular value and its respective left and right eigenvectors. Taking the greatest singular value and its corresponding left and right eigenvectors the entry $z_{x,t}$ becomes:

$$z_{x,t} = u_1(x)s_1v_1^T(t) + \varepsilon_{x,t}^* \quad (4.15)$$

where $\varepsilon_{x,t}^*$ corresponds to the information hidden in the remaining singular values and eigenvectors, Ignoring $\varepsilon_{x,t}^*$, fuzzification index f_t is estimated as $s_1v_1^T(t)$ and $c_{1,x}$ is set to be $u_1(x)$, which completes the calculation of center values.

Calculation of the center values is followed by the computation of spread values. The spreads are obtained based on the minimum fuzziness criterion suggested by Tanaka, Ueijima and Asai [134] for fuzzy regression. This leads to linear programming models for each age group x as:

$$\text{minimize } Ts_{0x} + s_{1x} \sum_{t=t_0}^{t_0+T-1} |f_t| \quad (4.16)$$

Subject to

$$c_{0x} + c_{1x}f_t + (1-h)[s_{0x} + s_{1x}|f_t|] \geq \ln(m)_{x,t}, \quad \forall t = t_0, t_0+1, \dots, t_0+T-1 \quad (4.17)$$

$$c_{0x} + c_{1x}f_t - (1-h)[s_{0x} + s_{1x}|f_t|] \leq \ln(m_{x,t}), \quad \forall t = t_0, t_0+1, \dots, t_0+T-1 \quad (4.18)$$

$$s_{0x}, s_{1x} \geq 0 \quad (4.19)$$

The objective function given in Equ. (4.16) minimizes the total spread while constraints in Equ. (4.17) and Equ. (4.18) ensure that the observed \ln -demographic indicator value lie within the fuzzy interval defined by the corresponding center and spread values at a level h , which is a predetermined small parameter (generally preferred to be 0). h can be considered as α -cuts in fuzzy set theory, thus, the spreads increase as h . The last constraint, given in Equ. (4.19), guarantees the non-negativity.

4.3.1.2. Estimation Phase

Once the observed \ln -demographic indicator values are fuzzified, the next task becomes to estimate the fuzzy parameters in the country profile $[\tilde{A}_x \oplus_{T_w} \tilde{B}_x \otimes_{T_w} \tilde{K}_t]$. For this purpose, the total distance between the fuzzified \ln -demographic indicator values and the estimated

values is minimized. Here, Diamond distance (D_{LR}), a frequently used fuzzy distance metric in fuzzy regression methods, is employed and the corresponding optimization model is given as:

$$\text{Minimize } \sum_x \sum_t D_{LR}[\tilde{A}_x \oplus_{T_w} (\tilde{B}_x \otimes_{T_w} \tilde{K}_t), \tilde{Y}_{xt}]^2 \quad (4.20)$$

When the Diamond distance and T_w based addition and multiplication are utilized together, Equ. (4.20) becomes an unconstrained nonlinear optimization problem with the form:

$$D_{LR}[\tilde{A}_x \oplus_{T_w} (\tilde{B}_x \otimes_{T_w} \tilde{K}_t), \tilde{Y}_{xt}]^2 = (a_x + b_x k_t - y_{xt})^2 + [a_x + b_x k_t - \max\{\alpha_x, |b_x| \delta_t, \beta_x |k_t|\} - (y_{xt} - e_{xt})]^2 + [a_x + b_x k_t + \max\{\alpha_x, |b_x| \delta_t, \beta_x |k_t|\} - (y_{xt} + e_{xt})]^2.$$

This unconstrained nonlinear optimization problem is solved via Nelder-Mead (NM) simplex algorithm, which is a derivative free method. NM algorithm searches for the minimum solution of a discontinuous nonlinear function via a simplex, which adapts itself to the search space through reflection, expansion, outside/inside contraction and shrinkage [135]. A simplex in n dimensions can be defined as the convex hull of a set of $n+1$ noncoplanar points in a hyperplane of n dimension, E^n [136]. To illustrate how NM algorithm operates, assume a hyperplane E^2 of 2 dimensions. A simplex in this hyperplane corresponds to a triangle. Furthermore, let $f(x, y)$ be the function to be minimized. The algorithm starts with an initial simplex (in this case a triangle) having the vertices $B = (x_1, y_1)$, $G = (x_2, y_2)$, and $W = (x_3, y_3)$, where B corresponds to the best vertex, G is good vertex (the next best), and W is the worst vertex in terms of fitness values [137]. Furthermore, let M be the midpoint of the line segment joining vertices B and G , R is the point obtained using reflection operation, E is the point obtained using expansion operation, C_1 and C_2 are the points obtained through inside and outside contraction operations respectively, and S is the point obtained through shrinkage operation. If d represents the distance between the points W and M , then the four operations used in NM algorithm can be illustrated as in Figure 4.2. The logical decisions in each step of the NM algorithm are also provided in the following Algorithm 4.1 [138].

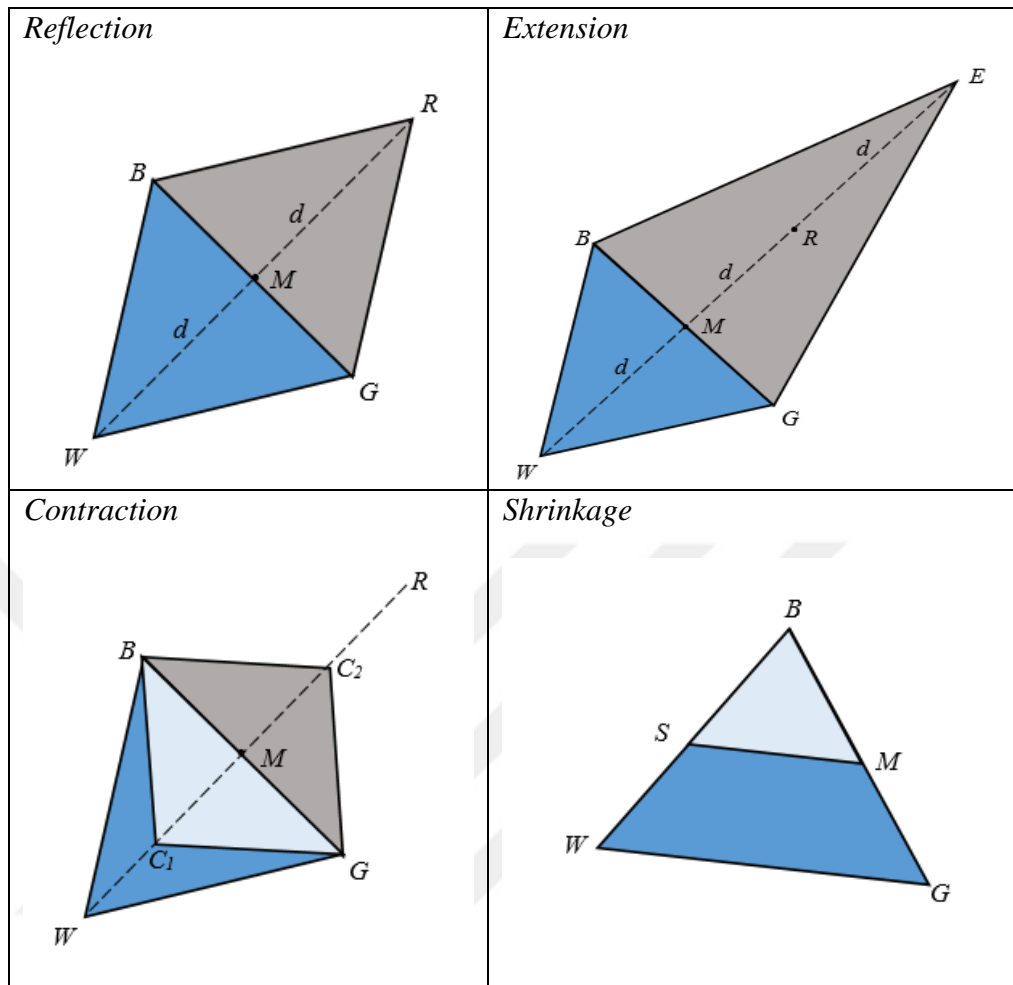


Figure 4.2. Reflection, extension, contraction and shrinkage operations of NM algorithm

Algorithm 4.1. Nelder-Mead simplex algorithm

If $f(R) < f(G)$, **then** apply reflection or extension operations

Begin

If $f(B) < f(R)$, **then** change W with R

Else calculate E and $f(E)$

If $f(E) < f(B)$, **then** change W with E

Else change W with R

Endif

Endif

End

Else apply contraction or shrinkage operations

Begin

If $f(R) < f(W)$, **then** change W with R

```

Else calculate  $E$  and  $f(E)$ 
  If  $f(E) < f(B)$ , then change  $W$  with  $E$ 
  Calculate either  $C = (W + M)/2$  or  $C = (M + R)/2$  and  $f(C)$ 
    If  $f(C) < f(W)$ , then change  $W$  with  $C$ 
  Else calculate  $S$  and  $f(S)$ 
  change  $W$  with  $S$ 
  change  $G$  with  $M$ 
  Endif
Endif
End

```

In literature, it is shown that the solutions found via NM simplex algorithm strongly depend on the initial solution and the dimensionality [139]. Here, the parameters obtained during the fuzzification of observed data is used as an initial solution, hence enhances the computation capacity of the algorithm. After the estimation of fuzzy parameters in Level-I are completed, the estimated fuzzy country profile are defuzzified via center of gravity.

For modeling mortality and fertility, Level-I is adequate due to the relatively simple regularities followed by the age groups. However, a second level of modeling is required to fit migration trends.

4.3.2. Level-II: Modeling Age-Cluster Factor

Level-I is succeeded by computing the difference between the observed ln -demographic indicator values and the defuzzified country profile which is named as the cluster factor. In fact, cluster factor $\tilde{C}_{i,x,t}$ represents the demographic behaviors that cannot be captured by the general country profile and is assumed to be a consequence of differences in age group attitudes. In Level-II, the demographic indicator of interest is emigration or immigration counts, since mortality or fertility modeling does not require a second level of modeling effort.

Here, the age groups are clustered such that neighbor age groups follow similar patterns while distinct clusters possess diverse migration behaviors. This clustering operation allows a method based on SVD technique analogous to the method used in Level-I to be utilized in level-II as well. The clustering operation, which can be viewed as a hierarchical clustering approach, is as follows:

- **Step 1:** For each age group x_i and x_j , $x_i \neq x_j$, and $x_i, x_j = x_1, \dots, x_N$, calculate slope similarity index S_{ij} . Call maximum S_{ij} value as $\max(S_{ij})$.
- **Step 2:** For each age group x_i , select the age group x_j , $x_i \neq x_j$, such that S_{ij} is the smallest and connect age group x_i to age group x_j . Now, age group x_i is labeled as a candidate member of class C_i which includes age group x_j as a member.
- **Step 3:** If for all $x_k \in C_i$, $S_{ik} \leq p * \max(S_{ij})$; then age group x_i is re-labeled as a member of C_i . Else, connect age group x_i to the most similar age group x_k and form a new class $C_n = \{x_i, x_k\}$, where $x_k = x_{i-1}$ or $x_k = x_{i+1}$. Here, p is the dissimilarity proportion indicating the maximum dissimilarity ratio allowed, $0 \leq p \leq 1$. For instance, if p is chosen as 0.1, the dissimilarity within a class cannot be greater than 10 percent of $\max(S_{ij})$.

As mentioned in the previous steps, the age groups are clustered into classes based on a similarity measure called slope similarity index. Li *et al.* [140,141] define a slope similarity metric via piecewise linear approximations on a time series which corresponds to v piecewise linear subsequences expressed as $y = b + mx$. If the approximation is denoted by *PLA*, then $PLA = (b_1, m_1; b_2, m_2, \dots, b_w, m_w)$, where b_i and m_i , $i = 1, \dots, w$, are the intercept and the slope of the i^{th} piecewise linear subsequence. Li *et al.* [140] show that a slope based distance between two linear subsequences as:

$$d(m_1, m_2) = \frac{|m_1 - m_2|}{|m_1 m_2|} \quad (4.21)$$

The slope based distance in Equ. (4.21) satisfies positivity, symmetry, constancy, and triangular inequality, so that, it is a metric. For clustering the age groups based on their migration behaviors, the error $\varepsilon_{x,t}$ between the observed ln -demographic indicator value and the defuzzified estimates $a_x + b_x k_t$ obtained at the end of Level-I modeling are calculated. Next, for each age group x , a piecewise linear segment is formed between all adjacent errors $\varepsilon_{x,t}$ and $\varepsilon_{x,t+1}$, making $T-1$ segments for each age group x . Then, the slopes of each linear segment are computed. Finally, the slope similarity index between age groups x_i and x_j is calculated via:

$$S_{ij} = \sum_{l=1}^{T-1} d(m_{il}, m_{jl}) \quad (4.22)$$

where, l is the label of piecewise linear segment $l = 1, \dots, T-1$, and $d(m_{il}, m_{jl})$ is the slope based distance between the l^{th} linear segments of age groups x_i and x_j .

After clustering the age groups into appropriate classes, the previously discussed fuzzy method (Level I of FMM) is applied on each class C_i separately. That is, for all $x \in C_i$ and $\forall t = t_0, t_0 + 1, \dots, t_0 + T - 1$, the error terms $\varepsilon_{x,t}$ s obtained after Level-I modeling are assumed to be consequences of age group cluster characteristics, and modeled as:

$$\tilde{C}_{i,x,t} = \tilde{D}_x \oplus_{T_W} \tilde{G}_x \otimes_{T_W} \tilde{R}_{i,t} \quad (4.23)$$

where $\tilde{C}_{i,x,t}$ is the fuzzy cluster factor for age group x and class C_i at time t , \tilde{D}_x and \tilde{G}_x are the fuzzy age-specific parameters, and $\tilde{R}_{i,t}$ is the time-variant fuzzy cluster index with $c_{i,x,t}$, d_x , g_x , and $r_{i,t}$ as center and $\psi_{i,x,t}$, λ_x , γ_x , and $\tau_{i,t}$ as spread values, respectively. Here, the fuzzy numbers are symmetric and triangular. After estimating the fuzzy parameters in Equ. (4.23) via the method used to fit Level-I model, age-specific migration modeling is completed with the addition of country profile outputs and cluster impact estimates as in Equ. (4.11).

4.3.3. Forecasting Future Migration Values

To forecast future demographic indicator values, the time-variant fuzzy parameters $\tilde{K}_t = (k_t, \delta_t)$ in Equ. (4.11) and $\tilde{R}_{i,t} = (r_{i,t}, \tau_{i,t})$ in Equ. (4.23) are predicted through time series models based on Bayesian approach. Bayesian models integrate subjective prior beliefs with the observed historic data. In addition, these models are efficiently used in case of short data series. Bijak and Wiśniowski [113] state that the application of Bayesian approach in forecasting demographic values generates similar *ex post* errors to the classical approach; yet, it yields more realistic predictive intervals. Here, six models are specified to predict the time-variant parameter y_t , where y_t is one of the parameters k_t , δ_t , $r_{i,t}$, or

$\tau_{i,t}$; $\forall t = t_0, t_0 + 1, \dots, t_0 + T - 1, \dots, t_0 + T + H - 1$ and for all classes i , where H denotes the length of the forecast horizon. Each model is denoted by M_j , $j = 1, 2, \dots, 6$ and defined as:

$$M_1: y_t = c_{1,1} + c_{1,2}t + \varepsilon_1(t) \quad (4.24)$$

$$M_2: y_t = y_{t-1} + \varepsilon_2(t) \quad (4.25)$$

$$M_3: y_t = c_3 + y_{t-1} + \varepsilon_3(t) \quad (4.26)$$

$$M_4: y_t = c_4 + \varphi_4 y_{t-1} + \varepsilon_4(t); \varphi_4 \neq 0, \varphi_4 \neq 1 \quad (4.27)$$

$$M_5: y_t = c_5 + \varepsilon_5(t) - \theta_5 \varepsilon_5(t-1); \theta_5 \neq 0 \quad (4.28)$$

$$M_6: y_t = c_6 + \varphi_6 y_{t-1} + \varepsilon_6(t) - \theta_6 \varepsilon_6(t-1); \varphi_6 \neq 0, \varphi_6 \neq 1, \theta_6 \neq 0 \quad (4.29)$$

The models displayed in Equ. (4.24) to Equ. (4.29) are namely linear trend model, random walk model, random walk model with drift, autoregressive process – AR(1), moving average process – MA(1), and autoregressive moving average process – ARMA(1,1), with respectively. Except the linear trend model M_1 given in Equ. (4.24), the remaining models M_2 to M_6 are treated as Bayesian models. The reason why these six models are to be used is that the orders of the ARIMA models in demographic forecasting do not go beyond (1,1,1) [142]. In this study, integrating fuzzy modeling into Bayesian forecasting allows representing the future forecasts within fuzzy prediction intervals.

For the models specified in Equ. (4.24) to Equ. (4.29), $\varepsilon_j(t)$ denotes the Gaussian white noise, $\varepsilon_j(t) \sim N(0, \sigma_j^2)$. For mortality/fertility rates and emigration/immigration counts, these models are fitted using MCMC simulation with Gibbs sampling. To accomplish this task, the prior distributions for the model parameters are determined based on the data and some prior beliefs. The Gibbs sampling leads to convergence in most cases, however the simulation may start at a distinct point from the stable distribution. The impacts of the prior values are mitigated by discarding some initial portion of the simulation, named as the *burn-in* iterations. The posterior distributions of the model parameters are determined based on the remaining iterations in the simulation.

The model to be utilized in forecasting demographic indicator values is selected according to posterior probabilities of each model (referred as *posterior odds criterion*). Here, posterior probability of model M_j given the marginal distribution of data is computed through the Bayes rule [143] as:

$$p(M_j | x) = \frac{p(x | M_j)p(M_j)}{p(x)} \quad (4.30)$$

For forecasting, the model with the highest $p(M_j | x)$ is selected. This selection criterion requires defining the prior probabilities $p(M_j)$ for each model. The prior probabilities for the models are determined based on the famous *Occam's razor* principle, which indicates that in model selection problems, the selection criterion should support the simpler explanations of the phenomena under study. Here, as suggested by Bijak [144], the prior probabilities can be set in such a way that $p(M_j)$ is proportional to 2^{-n_j} , where n_j is the number of parameters in model M_j . This prior probability setting assumes that the measure of complexity of a model can be represented by the number of parameters in that model. MCMC simulation refines the prior probabilities based on the estimation capability of the model and provides posterior distributions for the models given the data.

4.4. MODELING AND FORECASTING THE POPULATION

After all of the fuzzy ln -demographic indicators, ln -mortality, ln -fertility, ln -immigration, and ln -immigration for males and females are estimated, it is possible to construct a fuzzy population model. The first step in this phase is converting the fuzzy ln -demographic values to fuzzy demographic values by taking the exponential of their center and spread values.

The next step is to convert fuzzy mortality rates to fuzzy survival ratios. Here, for each fuzzy mortality rate, the spread value is added to and subtracted from the center value to form the left and right tails of the fuzzy number respectively. Let $\tilde{M}_{x,t}^s$ be the fuzzy mortality rate for age group x at time t for sex group s with center $(m_{x,t}^s)_C$ and spread $e_{x,t}^s$

where s equals to 1 for females and 2 for males. Then, the left and right tales of $\tilde{M}_{x,t}^s$ are obtained by

$$(m_{x,t}^s)_L = c_{x,t}^s - e_{x,t}^s \quad (4.31)$$

$$(m_{x,t}^s)_R = c_{x,t}^s + e_{x,t}^s \quad (4.32)$$

where $(m_{x,t}^s)_L$ is the left tail and $(m_{x,t}^s)_R$ is the right tail of the fuzzy mortality rate. Next, the center, and the left and right tails of the fuzzy survival ratio are obtained by;

$$(sr_{x,t}^s)_i = \begin{cases} \frac{2 - (m_{1,t}^s)_i}{2 + (m_{1,t}^s)_i}, & \text{for ages 0-1} \\ \exp[-4(m_{1,t}^s)_i - (4)^3(0.008)((m_{1,t}^s)_i)^2], & \text{for ages 1-4} \\ \exp[-5(m_{x,t}^s)_i - (5)^3(0.008)((m_{x,t}^s)_i)^2], & \text{otherwise} \end{cases} \quad (4.33)$$

where subscript i denotes the center and left and right tails of the fuzzy quantity. The fuzzy triangular survival ratio $\tilde{S}_{x,t}^s$ can then be identified as $\tilde{S}_{x,t}^s = ((sr_{x,t}^s)_L, (sr_{x,t}^s)_C - (sr_{x,t}^s)_L)$ or $\tilde{S}_{x,t}^s = ((sr_{x,t}^s)_C, (sr_{x,t}^s)_R - (sr_{x,t}^s)_C)$ where $(sr_{x,t}^s)_C - (sr_{x,t}^s)_L$ or $(sr_{x,t}^s)_R - (sr_{x,t}^s)_C$ corresponds to the spread value.

Once the above operations are performed and given the population at time t , the total population at time $t+1$ can be forecasted by;

$$\tilde{N}_{t+1} = \tilde{N}_{t+1}^1 \oplus_{T_w} \tilde{N}_{t+1}^2 \quad (4.34)$$

where \tilde{N}_t , \tilde{N}_t^1 and \tilde{N}_t^2 stand for the total fuzzy population, fuzzy female population and fuzzy male population at time t respectively. The fuzzy female and male population at time $t+1$ can be computed via:

$$\tilde{N}_{t+1}^1 = \sum_x^{x_{N-1}} \tilde{S}_{x,t}^1 \otimes_{T_w} \tilde{N}_{x,t}^1 \oplus \sum_x SRB_t^1 \times \tilde{F}_{x,t}^1 \otimes_{T_w} \tilde{N}_{x,t}^1 \oplus \sum_x^{x_{N-1}} \tilde{S}_{x,t}^1 \otimes_{T_w} \tilde{I}_{x,t}^1 \oplus \sum_x^{x_{N-1}} \tilde{E}_{x,t}^1 \quad (4.35)$$

$$\tilde{N}_{t+1}^2 = \sum_x^{x_{N-1}} \tilde{S}_{x,t}^2 \otimes_{T_w} \tilde{N}_{x,t}^2 \oplus \sum_x \text{SRB}_t^2 \times \tilde{F}_{x,t}^2 \otimes_{T_w} \tilde{N}_{x,t}^2 \oplus \sum_x^{x_{N-1}} \tilde{S}_{x,t}^2 \otimes_{T_w} \tilde{I}_{x,t}^2 \ominus \sum_x^{x_{N-1}} \tilde{E}_{x,t}^2 \quad (4.36)$$

where; $\tilde{S}_{x,t}^s$, $\tilde{F}_{x,t}^s$, $\tilde{E}_{x,t}^s$, and $\tilde{I}_{x,t}^s$ are fuzzy survival and fertility rates, and emigration and immigration counts for age group x and sex group s at time t to $t+1$ respectively, $\tilde{N}_{x,t}^s$ is the fuzzy number of persons of age group x and sex group s at time t , and SRB_t^s is the sex ratio at birth for sex group s at time t . The first summation refers to the individuals surviving the age group x and reaching to age group $x+1$ from time t to $t+1$. The second summation deals with the newborns; whereas the last two summations refer to the number of surviving individuals that immigrate and emigrate from time t to $t+1$. If crisp values, rather than fuzzy ones for the number of persons of age group x and sex group s at time t which is denoted by $N_{x,t}^s$, are used Equ. (4.35) and Equ. (4.36) can be modified as:

$$\tilde{N}_{t+1}^1 = \sum_x^{x_{N-1}} \tilde{S}_{x,t}^1 \times N_{x,t}^1 \oplus \sum_x \text{SRB}_t^1 \times \tilde{F}_{x,t}^1 \times N_{x,t}^1 \oplus \sum_x^{x_{N-1}} \tilde{S}_{x,t}^1 \otimes_{T_w} \tilde{I}_{x,t}^1 \ominus \sum_x^{x_{N-1}} \tilde{E}_{x,t}^1 \quad (4.37)$$

$$\tilde{N}_{t+1}^2 = \sum_x^{x_{N-1}} \tilde{S}_{x,t}^2 \times N_{x,t}^2 \oplus \sum_x \text{SRB}_t^2 \times \tilde{F}_{x,t}^2 \times N_{x,t}^2 \oplus \sum_x^{x_{N-1}} \tilde{S}_{x,t}^2 \otimes_{T_w} \tilde{I}_{x,t}^2 \ominus \sum_x^{x_{N-1}} \tilde{E}_{x,t}^2 \quad (4.38)$$

where $N_{x,t}^s$ denotes the crisp number of persons of age group x and sex group s at time t .

5. NUMERICAL FINDINGS

The proposed FMM is applied to the age-specific mortality and fertility rates and emigration and immigration counts of Finland for each sex (female and male) separately (For fertility only female dataset is used since fertility is referred to females). Finland is located in Northern Europe between Norway, Sweden and Russian Federation and Baltic Sea. The country is a member of United Nations, OECD, and European Union, and ranked as fifteenth in the world according to human development index (HDI for 2017 is 0.920, which is which is categorized as very high based on [145]).

There are several reasons why Finland data are selected for application. First of all, mortality and fertility rates in Finland for age groups are available for males and females separately in official statistics, which are believed to be of high quality. The emigration and immigration values are available as counts in official population statistics in age groups for the two genders as well. The country displays a stable population profile by time with several fluctuations observed in fertility rates, and almost linear declining trends of mortality in diverse age groups by time. The trends in emigration and immigration values display several fluctuations for years around the collapse of Soviet Union and expansion of the European Union (EU), but the country did not witness mass emigration or immigration due to global financial crisis of 2008 when compared to some other EU countries. Beside the accessibility and quality of age-specific demographic data of the country, another reason for selecting Finland as the application region is that the existing fuzzy method of Koissi and Shapiro [16] has also been applied on Finland data.

The total male and female populations of Finland for all age groups are displayed in Table 5.1 for selected years between 1940 and 2015. As observed from Table 5.1, the total population in 2015 is 47.97 percent greater than the population in 1940; due to natural growth of population and net migration. The number of females are greater than the number of males in all displayed years, although the percentage of females in total population in 1940 decreases from 51.21 percent to 50.80 percent in 2015. The population statistics reveal a monotonic growth for Finland changing in between 0.97 percent and 6.77 percent. The country witnessed a significant population growth right after the World War

II, but the growth percentage decreased to 2.25 percent in 2015 with several fluctuations in years.

Table 5.1. Summary of total population statistics of Finland

Year	Female	Male	Total	Growth Percentage
1940	1893736	1804098	3697834	
1945	1955020	1778959	3733979	0.98
1950	2083150	1903480	3986630	6.77
1955	2193006	2018698	4211704	5.65
1960	2288868	2124788	4413656	4.8
1965	2357881	2200716	4558597	3.28
1970	2384336	2230286	4614622	1.23
1975	2428607	2273819	4702426	1.9
1980	2464449	2306777	4771226	1.46
1985	2524507	2369234	4893741	2.57
1990	2561750	2412798	4974548	1.65
1995	2617095	2481685	5098780	2.5
2000	2648125	2523032	5171157	1.42
2005	2674268	2562053	5236321	1.26
2010	2725859	2624963	5350822	2.19
2015	2779251	2691760	5471011	2.25

The age-specific population of Finland for 2015 is given in Table 5.2. The last column in Table 5.2 provides the percentage of each age group population within the total population for 2015. The distribution of the population among age groups indicate that 16.39 percent of the total population are younger than 15 years old, 63.69 percent of the population is in between ages 15 and 65, and 19.93 percent of the population is older than 65 years old. Thus, the ratio of children within the total population is less than the ratio of old people, which is common in most of the developed countries in Europe.

Considering the fluctuations in population growth percentages and the necessity of age-group decomposition of the population in further analysis, the proposed FMM is applied on mortality, fertility and migration data of Finland. The content and sources of data used and

the modeling and forecasting results for each demographic indicator are provided in sub-sections 5.1 to 5.3, and the aggregated population forecasts are given in sub-section 5.4. To display the modeling and forecasting outputs for each of the demographic indicators age group [20,25) is selected for exemplary purposes. In fact, this age group corresponds to young adults, in which a tendency of high mobility and fertility is observed.

Table 5.2. Age-specific distribution of Finland in year 2015

Age Group	Female	Male	Total	Percentage of the age group population in total population
[0,5)	146650	153486	300136	5.49
[5,10)	148856	155317	304173	5.56
[10,15)	142702	149597	292299	5.34
[15,20)	150090	156492	306582	5.6
[20,25)	167324	174762	342086	6.25
[25,30)	165545	174020	339565	6.21
[30,35)	172264	183123	355387	6.5
[35,40)	167323	177106	344429	6.3
[40,45)	154103	160576	314679	5.75
[45,50)	177605	181712	359317	6.57
[50,55)	187142	188443	375585	6.87
[55,60)	187031	183866	370897	6.78
[60,65)	191909	183321	375230	6.86
[65,70)	195527	181087	376614	6.88
[70,75]	128836	110037	238873	4.37
[75,80]	113191	85233	198424	3.63
[80,85)	88410	55027	143437	2.62
[85,90)	62245	28807	91052	1.66
[90,95)	27051	8469	35520	0.65
95+	5447	1279	6726	0.12

Furthermore, Bayesian migration modeling and forecasting method of Wiśniowski *et al.* [17] (denoted as BMM, henceforth) is also implemented on the same data for comparison purposes. BMM is also based on Lee-Carter model as discussed in Section 2.3 and it forecasts age-specific demographic indicator values using analogous parameters to FMM.

The main difference between the two is that BMM uses a Bayesian approach whereas FMM utilizes fuzzy set theory in model fitting.

The linear programming models for spread optimization as part of fuzzification of actual demographic values are solved using GAMS 24.4 software, while the fuzzy parameter estimation is accomplished using optimization toolbox of MATLAB R2014a software. In forecasting phase, OpenBUGS 3.2.3 software is used. GAMS code for spread optimization in Level I of FMM is given in Appendix A, while MATLAB function used as an input to NM simplex algorithm is displayed in Appendix B. OpenBUGS code for demographic forecasting is provided in Appendix C.

5.1. MORTALITY RESULTS

5.1.1. Mortality Data

Finnish mortality dataset for each sex (females and males) considered in this study consists of 21 age groups including $[0,1)$, $[1,5)$, $[5,10)$, ..., $[95,100)$ for 15 quinquenal (five-year) time periods of 1940-1944, 1945-1949, ..., 2010-2014. The datasets are retrieved from “Human Mortality Database” at www.mortality.org. The main reasons to aggregate data within five-year age groups and time periods are to reduce dimensionality for computational purposes and to obtain smoother data as suggested by Rogers *et al.* [79].

Figure 5.1 and Figure 5.2 display the mortality profiles of Finland throughout time for females and males respectively. The year axes in these figures illustrate the first year in each five-year time period, that is, year 1940 corresponds to time period 1940-1944 actually. Similarly, in age group axes, the starting age of a quinquenal group is provided. As displayed in Figure 5.1 and Figure 5.2, mortality rates are relatively high among infants, then, reach their minimum in childhood. The rates exhibit almost stable trends up to pre-retirement ages and start to increase afterwards.

The fluctuations in mortality rates among young adult males in Figure 5.2 in period 1940-1944 are due to World War II, however, females display a more non-fluctuating mortality profile for the same period. Furthermore, it is observed that mortality rates for both sexes are decreasing by time and the rates are lower for females when compared to males. The

regular patterns followed by age groups throughout time enable the proposed FMM to be applied in Finnish mortality data.

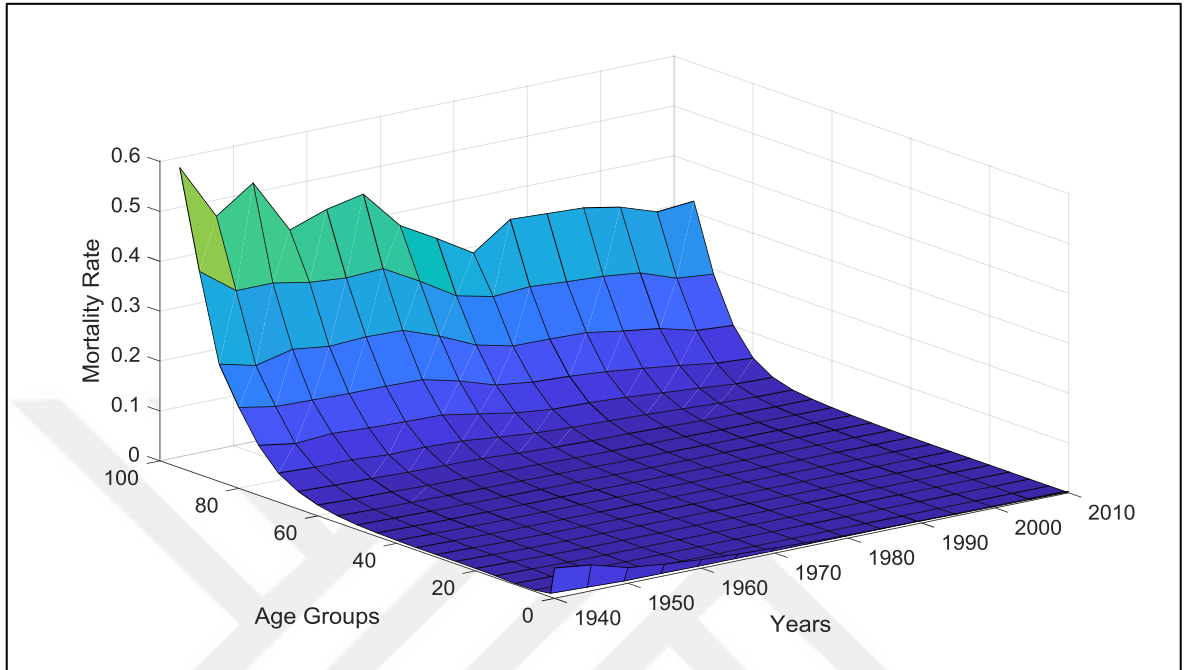


Figure 5.1. Observed mortality rates, females

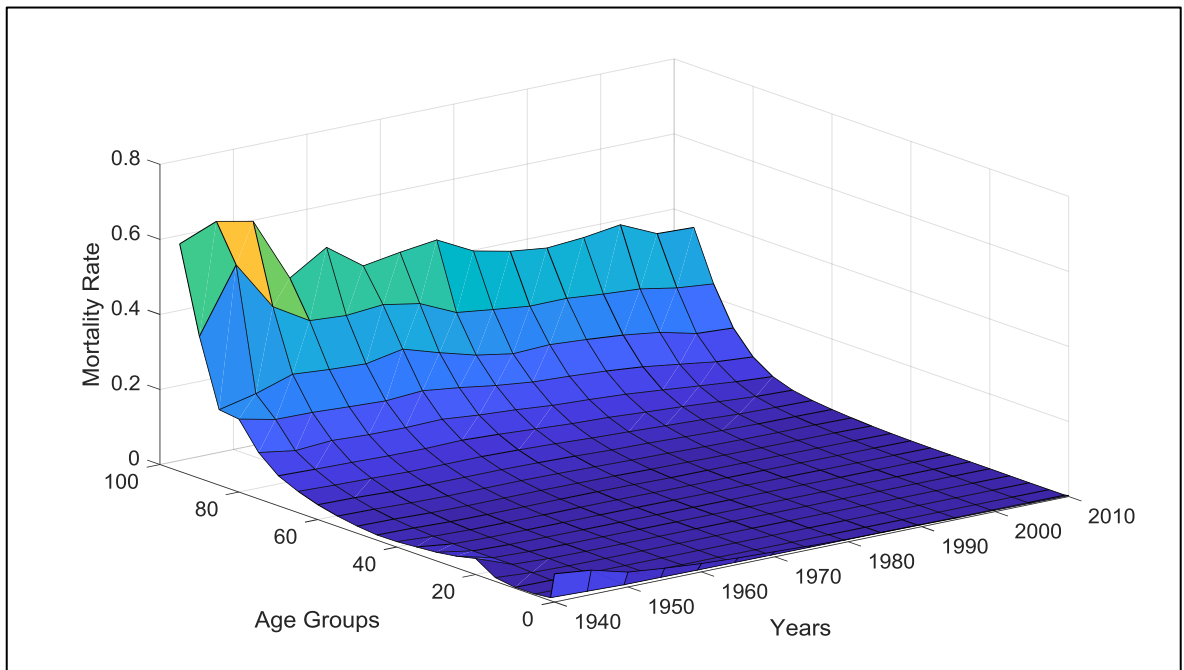


Figure 5.2. Observed mortality rates, males

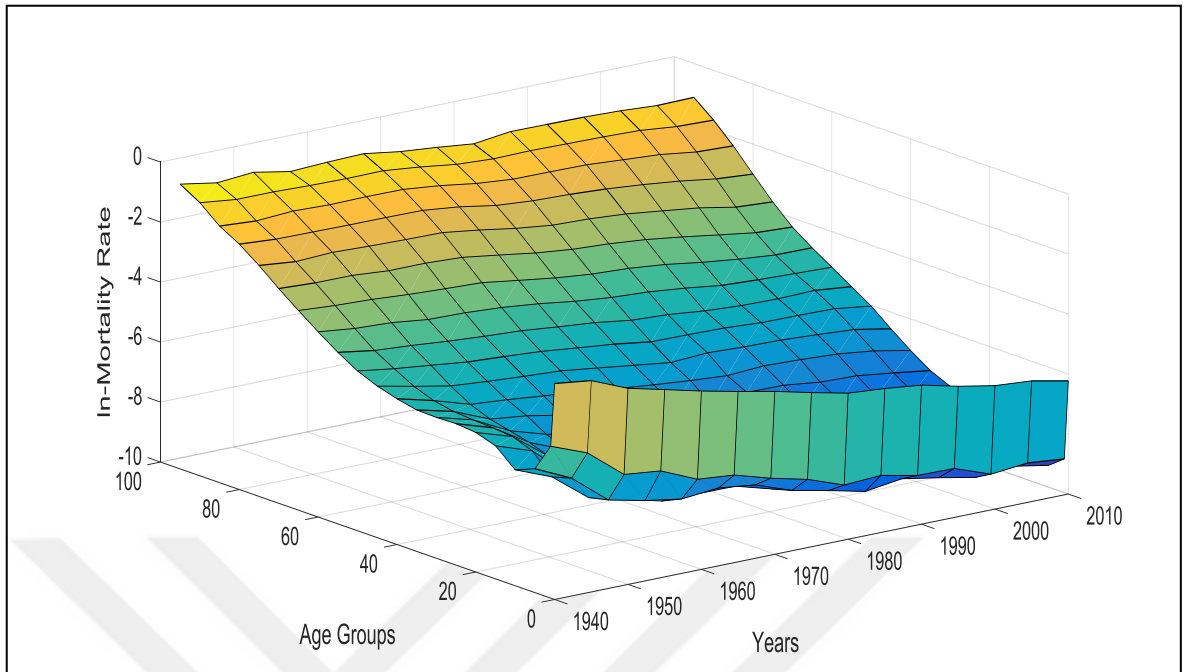


Figure 5.3. Observed In-mortality rates, females

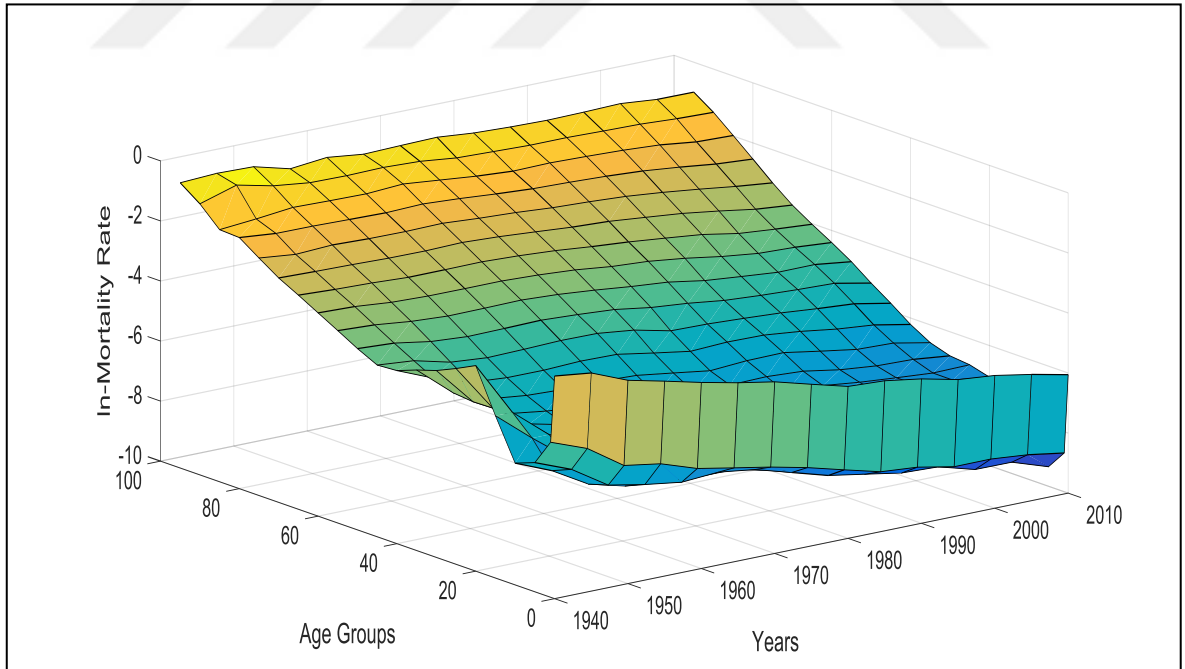


Figure 5.4 Observed In-mortality rates, males

The natural logarithms of observed mortality rates (*ln*-mortality rates) for females and males are illustrated in Figure 5.3 and Figure 5.4 respectively. As it can be seen from these

figures, natural logarithmic transformation smooths the observed mortality rates and results in almost linear trends for most of the age groups although some amount of fluctuations are still observed. Thus, natural logarithmic transformation of demographic rates/values makes it possible to obtain accurate fits via singular value decomposition based methods such as FMM.

The proposed FMM is applied on mortality data of Finland for 1940-1999 time periods, that is, the data used for modeling consists of 12 quinquenal time periods and 21 age groups for each sex. Using the model outputs, future mortality rates are forecasted for 2000-2004, 2005-2009, ..., 2020-2024 periods. This enables to measure the forecasting performance of FMM by *ex-post* analysis for 2000-2004, 2005-2009, 2010-2014 periods. The modeling and forecasting performances of the proposed FMM are also compared with Koissi and Shapiro's fuzzy mortality modeling method (KSM) and the Wiśniowski *et al.*'s BMM in the following sub-sections.

5.1.2. Validity of FMM Modeling Results

The validity of FMM in generating realistic fuzzy estimates for datasets covering 1940-1999 mortality rates is analyzed via fuzzy paired *t*-tests. Here, the equality of fuzzy estimates obtained via only the level-I of the proposed method and the fuzzified actual mortality rates is tested through paired fuzzy sample differences tests. Based on Liu and Kao [146]; Tsai and Chen [147] suggests using fuzzy sample differences test for testing the equality of paired fuzzy data; in which the null hypothesis H_0 states that the difference between two fuzzy sets is zero (or in other words, the two data sets are equal). A lower and an upper test statistics t_L and t_U for all α -cuts of the mean fuzzy differences are computed; and if both t_L and t_U lay within the *t*-value for $n-1$ degrees of freedom at a specified significance level, where n is the number of observations, the null hypothesis H_0 cannot be rejected. In this case, the test results indicate that there is no sufficient evidence to say that the two datasets are different from each other, therefore, it is concluded that they are the same. Otherwise, H_0 is rejected in favor of the alternative hypothesis H_1 , which states that the two samples are different from each other.

Here, the null and the alternative hypothesis are constructed as:

H_0 : The fuzzified actual mortality rates and the fuzzy estimates obtained via Level-I of FMM are equal.

H_1 : The fuzzified and estimated values be considered as the same.

For each sex, the null hypothesis is tested at a significance level of 0.05 for all α -cuts of the mean fuzzy differences. The results are displayed in Table 5.3, in which t_L and t_U values of only five different α -cuts are given due to space limitations. For two samples to be considered as equal, t_L and t_U values should be in the interval $[-1.969, 1.969]$, specified by the corresponding t values for 0.05 significance level and 251 degrees of freedom. The test results indicate that using only general country profiles (refers to level-I) in the method provide equality of the estimates and the actual fuzzy values in modeling mortality rates. Thus, it is decided to use only one level in FMM for mortality modeling and forecasting.

Table 5.3. Results of paired fuzzy sample differences tests for the equality of actual mortality values and FMM estimates

Demographic Indicator	Sex	Model	t	α						Decision
				$\alpha=0$	$\alpha=0.2$	$\alpha=0.4$	$\alpha=0.6$	$\alpha=0.8$	$\alpha=1$	
Mortality	Female	Level I	t_L	-0.063	-0.058	-0.051	-0.036	0.008	0.632	Cannot Reject H_0
			t_U	0.098	0.103	0.110	0.125	0.170	0.632	
	Male	Level I	t_L	-0.341	-0.296	-0.221	-0.069	0.388	1.353	Cannot Reject H_0
			t_U	0.695	0.738	0.809	0.950	1.088	1.353	

5.1.3. Comparison of FMM and KSM

The modeling performance of the proposed FMM is first compared with that of Koissi and Shapiro's fuzzy Lee-Carter method (KSM). This comparison examines the enhancements of FMM in fuzzification and estimation phases of fitting observed rates for 12 quinquennial time periods between 1940-1999 period and for the 21 age groups mentioned previously, making 252 observations for each sex.

The modeling outputs obtained via FMM and KSM for the example age group [20,25) are given in Figure 5.5 and Figure 5.6 for females and males respectively. In these figures, the

horizontal axis displays the beginning year of each quinquennial time period while the vertical axis corresponds to the mortality rates. Both figures display the actual mortality rates in addition to the center and the $\alpha=0.05$ -cut fuzzy intervals obtained through KSM and FMM.

From Figure 5.5 and Figure 5.6, it is seen that the center values generated via FMM are more congruent to the actual values when compared to the center values obtained via KSM in this age group for both females and males. This is mainly due to the modifications in fuzzification phase of FMM, in which the mortality rates are fitted based on singular value decomposition technique rather than the ordinary least squares regression with the time as the regressor embedded in KSM. Furthermore, FMM generates smaller spreads, that is, the uncertainty in fitted mortality rates, which is assumed to be due to fuzziness, is less for FMM outputs. It is worth mentioning that even though FMM gives narrower fuzzy intervals, it is still able to cover all of the fluctuations in observed mortality rates.

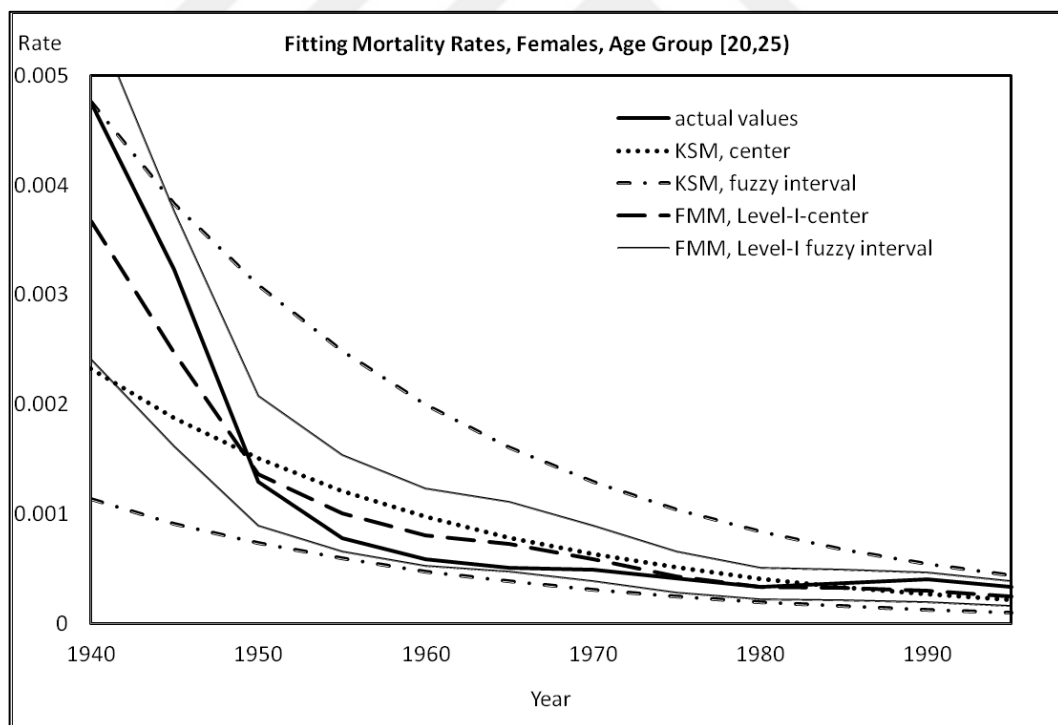


Figure 5.5. Fitting mortality rates for age group [20,25), females: FMM versus KSM

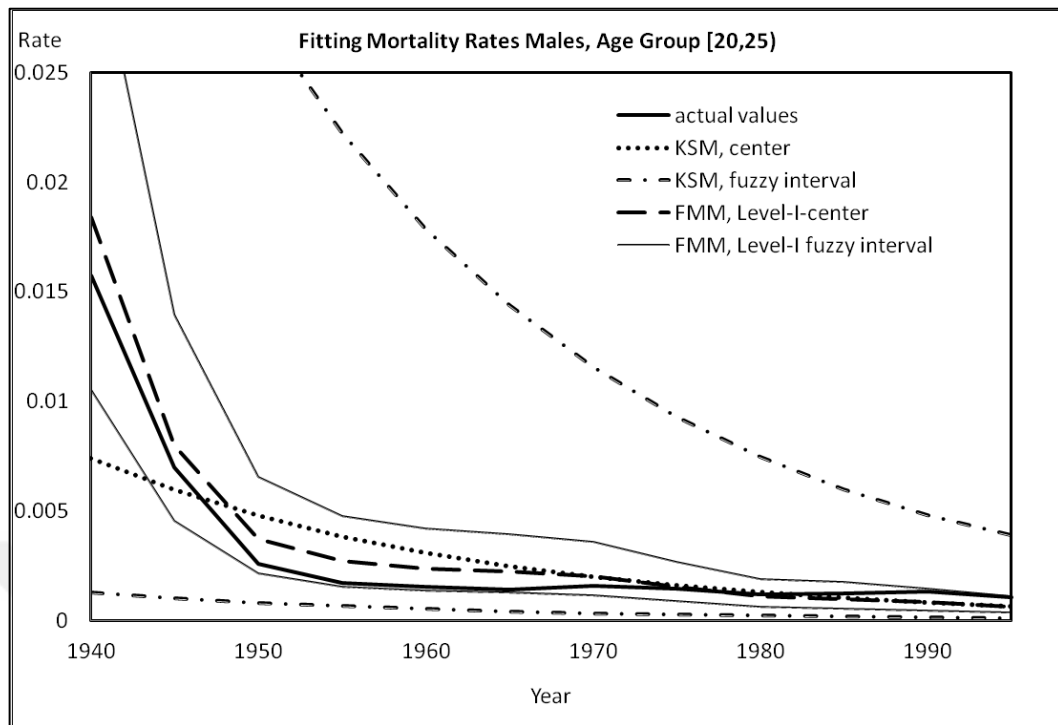


Figure 5.6. Fitting mortality rates for age group [20,25), males: FMM versus KSM

The performance of FMM and KSM are also compared in terms of fitting and the results are provided in Table 5.4. In this table, mean absolute percentage error (MAPE) between the actual and the center values obtained via KSM and FMM are given for each sex. When all age groups are considered, it is seen that fitting errors in FMM are relatively smaller compared to that of KSM. The enhancements in modeling capabilities achieved via FMM can be figured out as the MAPE decreases from approximately 15 percent to 10 percent and 13 percent for females and males respectively. Thus, it can be concluded that FMM provides superior results in terms of modeling accuracy compared to the existing KSM.

Table 5.4. MAPE between actual and fitted mortality values for 1940-1999 period obtained via KSM and FMM

Demographic Indicator	Sex	MAPE (%) between actual and fitted values		
		KSM		FMM
Mortality	Female	14.82		10.61
	Male	15.31		12.94

5.1.4. Mortality Modeling Results of FMM and BMM

The modeling performance of the proposed FMM is also compared with that of BMM for 1940-1999 period. The results for the example age group [20,25) for females and males are displayed in Figure 5.7 and Figure 5.8 respectively together with the actual values. In these figures FMM results are obtained using only a single level of modeling as it is shown in Section 5.1.2 that the Level-I model is adequate to represent the actual mortality rates. In Figure 5.7 and Figure 5.8, the center values and $\alpha=0.05$ -cut fuzzy intervals generated via FMM are depicted in addition to the median fits and the 95 percent Bayesian prediction interval obtained via BMM.

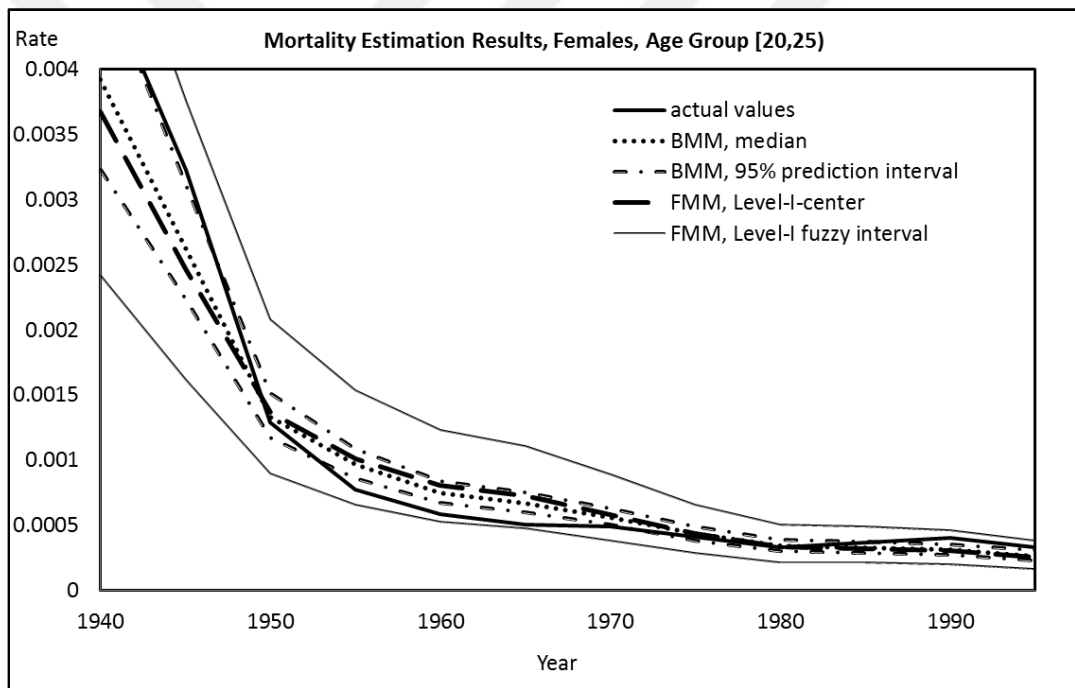


Figure 5.7. Mortality modeling estimates for age group [20,25), females, using 1940-1999 data: FMM versus BMM

In Figure 5.7 and Figure 5.8 the center values obtained via FMM and the median fits generated via BMM both seem to represent the actual mortality rates for each sex for age group [20,25). The actual mortality rates are covered within the $\alpha=0.05$ -cut fuzzy intervals and 95 percent Bayesian prediction intervals, however, the Bayesian prediction intervals of BMM are too narrow when compared to fuzzy intervals of FMM for this age group in each sex. Furthermore, in both figures, it is observed that the Bayesian and fuzzy intervals are

narrowing by time. This is due to exponential transformation of natural logarithms of the fitted mortality rates.

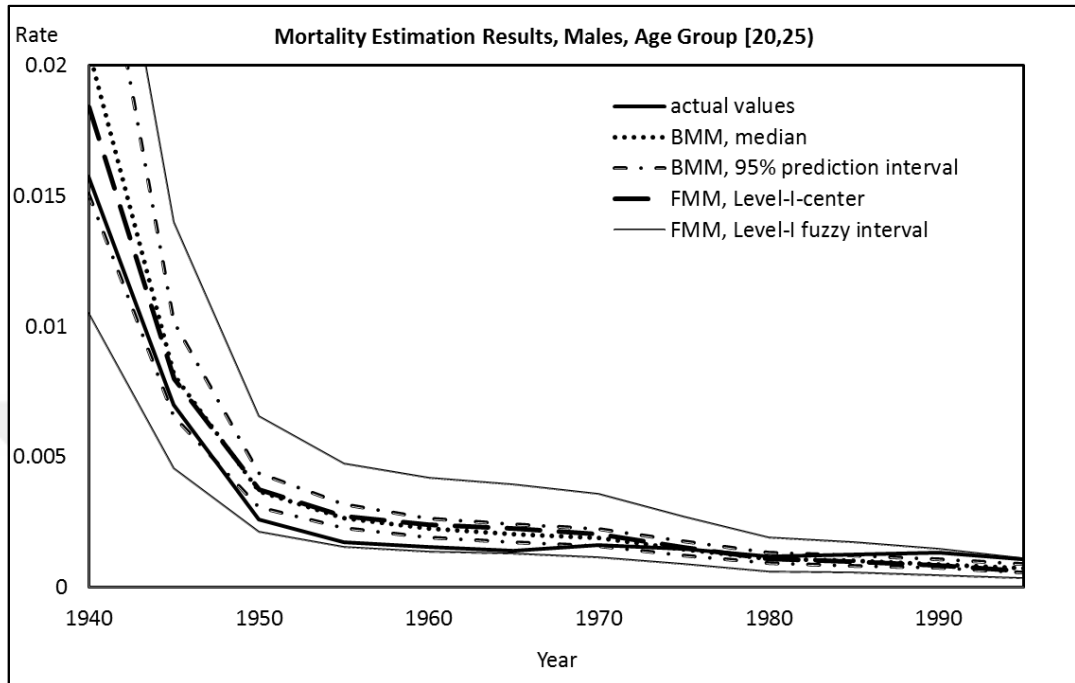


Figure 5.8. Mortality modeling estimates for age group [20,25), males, using 1940-1999 data: FMM versus BMM

Table 5.5. MAPE between actual and fitted mortality values for 1940-1999 period obtained via BMM and FMM

Demographic Indicator	Sex	MAPE (%) between actual and fitted values	
		BMM	FMM
Mortality	Female	10.28	10.61
	Male	13.24	12.94

The mortality modeling performance of FMM and BMM are also compared for 1940-1999 period. The MAPE between actual mortality rates and median fits obtained via BMM as well as the MAPE between actual mortality rates and center values obtained via FMM are given in Table 5.5. Here, all age groups in the datasets are considered. The comparison results indicate that BMM and FMM generating almost the same amount of fitting errors

which are in between approximately 10 percent and 13 percent. Thus, it can be asserted that the two methods perform similarly in modeling historic age-specific mortality rates.

5.1.5. Mortality Forecasting Results of FMM and BMM

After the modeling part is over, the future mortality rates are forecasted using the age-specific fuzzy parameters \tilde{A}_x and \tilde{B}_x , and the future values of the time-specific fuzzy parameter \tilde{K}_t for FMM. This requires forecasting the future values of $\tilde{K}_t = (k_t, \delta_t)$, which is accomplished through fitting the six Bayesian time series models discussed in Section 4.3 and choosing the one with the highest posterior probability. The prior distributions of the model parameters are based on a data-driven approach. The constants c_j are assumed to follow a normal prior distribution $N(0, 100^2)$, which display non-informative characteristics. The prior distributions for the autoregressive parameters ϕ_j and the moving average parameters θ_j are also normal, but more informative, following $N(0.5, 1^2)$. Similar to Wiśniowski *et al.* [17], the precision parameters $1/\sigma_j^2$ are assumed to follow a Gamma distribution with scale parameter 0.5 and shape parameter 0.5, reflecting a low precision of estimation.

The ultimate models selected to forecast female mortality rates are ARMA (1,1) model for future k_t values and random walk without drift model for future δ_t values. For male mortality rates, similarly, random walk without drift model is selected to forecast future δ_t , but random walk with drift model is chosen for estimating future k_t values. Using these models and the age-specific parameters computed in modeling part, future mortality rates for females and males are forecasted for 2000-2004, 2005-2009, ..., 2020-2024 periods. Similarly BMM is also applied on the same datasets for comparison purposes.

As observed in Figure 5.9, the actual female mortality rates for 2000-2004, 2005-2009 and 2010-2014 are almost at the edge of the right tail of $\alpha=0.05$ -cut fuzzy interval while the 95 percent Bayesian interval fails to cover the actual mortality rates. However, the forecast intervals of both FMM and BMM capture the actual male mortality rates for the three quinquenal time periods between 2000 and 2014 as illustrated in Figure 5.10.

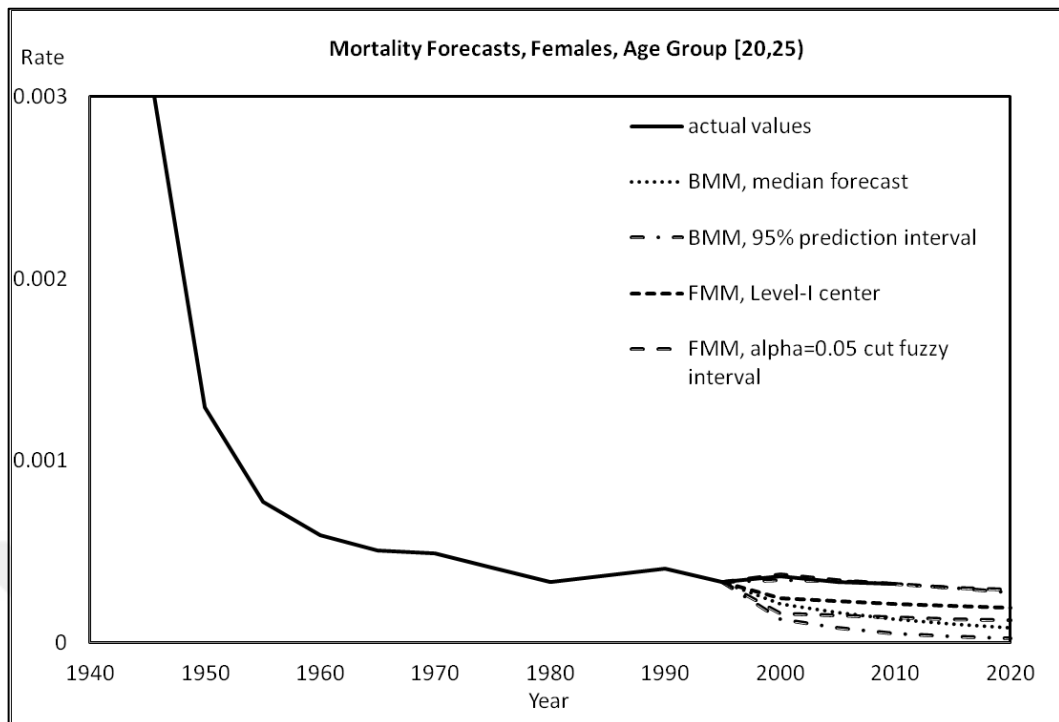


Figure 5.9. Mortality forecasts for age group [20,25), females

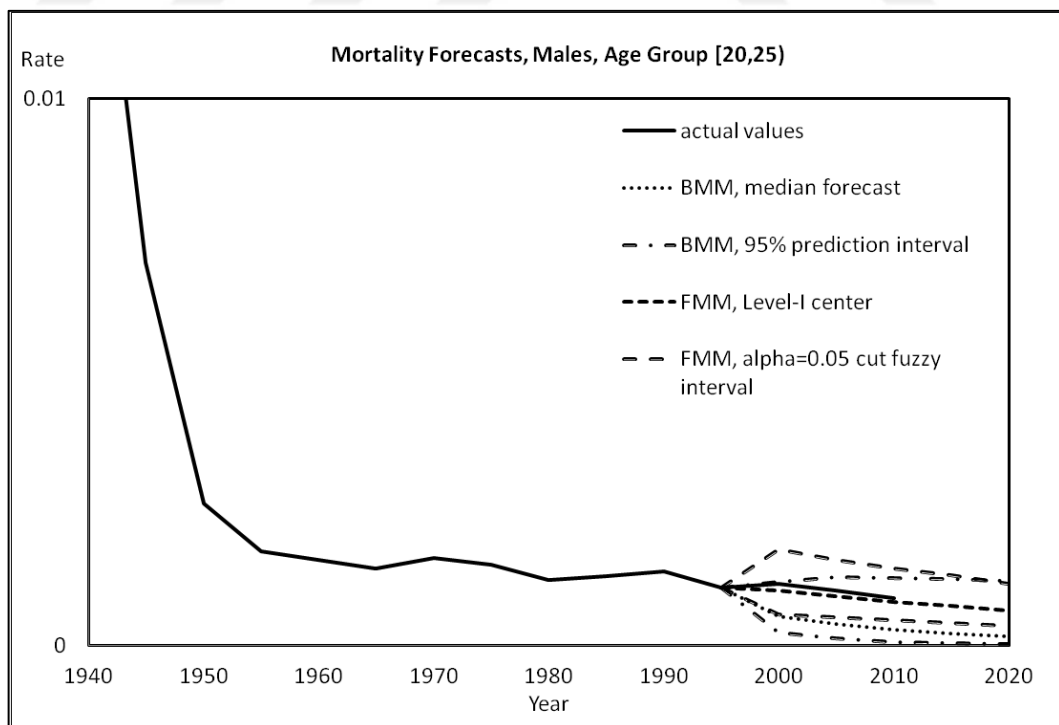


Figure 5.10. Mortality forecasts for age group [20,25), males

Table 5.6. Forecast analysis of actual and forecasted mortality values for 2000-2014 period

Demographic Indicator	Sex	MAPE between actual values and forecasts		Percentage of actual values covered within the forecast intervals	
		BMM	FMM	95% Bayesian prediction interval	$\alpha=0.05$ -cut fuzzy interval
Mortality	Female	21.08	14.15	90.47	93.65
	Male	24.85	14.91	90.47	93.65

When all of the twenty one age groups are considered, the *ex-post* analyses of comparisons between actual and forecast values for 2000-2014 period are in favor of FMM method for both females and males as depicted in Table 5.6. In Table 5.6, MAPE between actual mortality rates and median forecasts and center values obtained via BMM and FMM are provided in addition to the percentage of actual mortality rates covered within the $\alpha=0.05$ -cut fuzzy intervals and the 95 percent Bayesian intervals. The MAPE between actual mortality rates and median forecasts of BMM are approximately 21 percent for females and 25 percent for males while the MAPE between actual mortality rates and center values of FMM are approximately 14 percent for females and 15 percent for males. That is to say, FMM is more accurate in generating point forecasts compared to BMM.

Table 5.7. Mortality forecast interval comparisons for the BMM and the FMM

Demographic Indicator	Sex	Average prediction interval width (in rates)		BMM 95% prediction interval vs FMM $\alpha=0.05$ cut fuzzy interval
		BMM	FMM	
Mortality	Female	0.018	0.013	BMM interval is 41.58% wider
	Male	0.031	0.022	BMM interval is 41.67% wider

Another important information given in Table 5.6 is that the percentage of actual mortality rates covered within the $\alpha=0.05$ -cut fuzzy intervals are almost 94 percent for both sexes while approximately 90 percent of the observed mortality rates for 2000-2014 period are covered within the 95 percent Bayesian prediction interval. Table 5.7 provides deeper insight to comparison of forecast intervals obtained via FMM and BMM in which it is seen that the Bayesian prediction intervals are approximately 42 percent wider than the fuzzy

forecast intervals for both sexes. That is to say, it can be concluded that the proposed FMM cover more amount of actual mortality rates within significantly narrower forecast intervals. Thus, the proposed FMM is superior to the existing BMM in forecasting age-specific mortality rates in terms of both point forecasts and forecast interval comparisons.

5.2. FERTILITY RESULTS

5.2.1. Fertility Data

Finnish fertility data to be used in this study are retrieved from “Human Fertility Database” at www.humanfertility.org. The dataset consists of fertility rates for 15 quinquennial time periods of 1940-1944 to 2010-2014 for nine age groups of below 15, [15-20), [20, 25), ..., [50, 55) making a total of 135 data points. The corresponding dataset is for females as they are accepted as the fertile gender in human demography. Similar to the datasets used in mortality modeling, fertility rates are also aggregated into time and age groups to provide dimensionality reduction and smoothness.

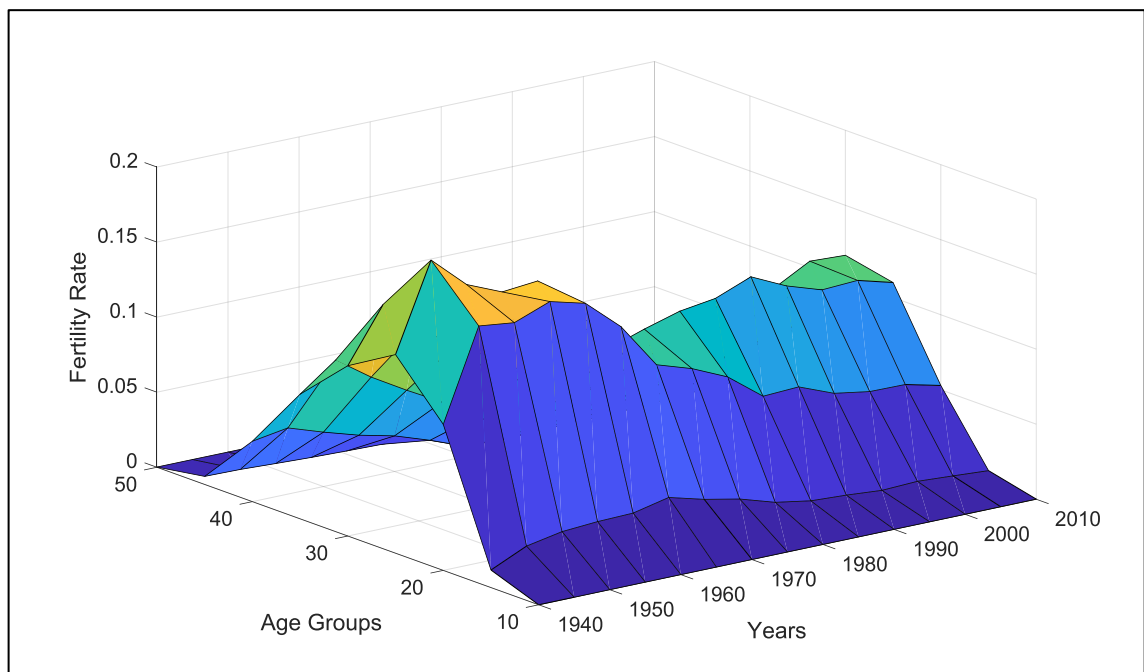


Figure 5.11. Observed fertility rates

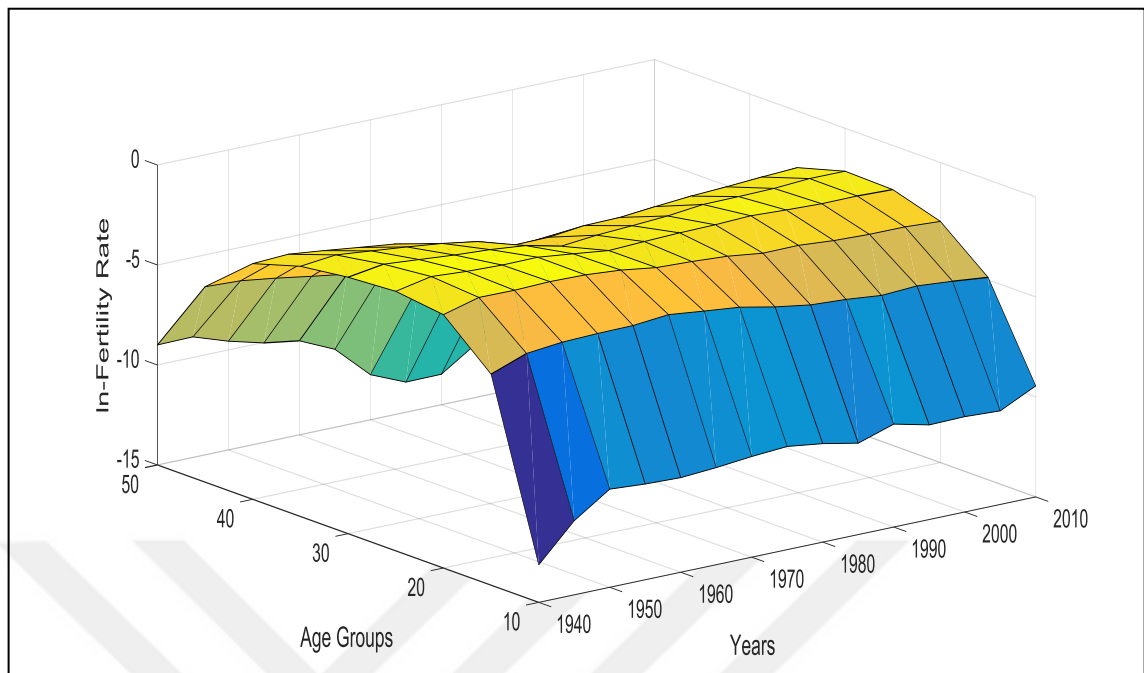


Figure 5.12. Observed \ln -fertility rates

The fertility profiles of Finland throughout time are displayed in Figure 5.11. The year axis in Figure 5.11 corresponds to the first year in each five-year time period, and likewise, in age group axis, the starting age of a quinquenal group is provided.

As displayed in Figure 5.11 fertility rates are almost zero below the age 15, then increase significantly and reach their maximum at age groups [20,25) and [25,30) and decrease to zero again by the age 55. The fertility rates are relatively high at the starting time period 1940-1944 and diminish until 1970s. Starting by 1970s, fertility rates slightly increase and after 1990s display a more stable profile.

Although the shape of the fertility age profile is completely different than that of mortality, the unimodal structure in the shape of fertility profiles is preserved throughout time, enabling the proposed FMM to be applied in Finnish fertility data. The natural logarithms of observed fertility rates (\ln -fertility rates) are depicted in Figure 5.12. Similar to the natural logarithmic transformation of mortality rates, natural logarithmic transformation of fertility rates smoothes the observed values, making it possible to obtain accurate fits via singular value decomposition based methods such as FMM.

The proposed FMM is applied on fertility data of Finland for 1940-1999 time periods, that is, the data used for modeling consists of 12 quinquenal time periods and nine groups. Using the model outputs, future mortality rates are forecasted for 2000-2004, 2005-2009, ..., 2020-2024 periods and the forecasting performance of FMM on fertility dataset is examined by *ex-post* analysis for 2000-2004, 2005-2009, 2010-2014 periods. The modeling and forecasting performances of the proposed FMM are also compared with the Wiśniowski *et al.*'s BMM. Here, different than mortality modeling, the proposed FMM is not compared with Koissi and Shapiro's fuzzy method KSM, since KSM is only applicable for mortality modeling in which the rates follow almost linear trends.

5.2.2. Fertility Modeling Results

The observed fertility rates for the nine age groups of below 15, [15-20), [20, 25), ..., [50, 55) for 12 quinquenal time-periods of 1940-1944 to 1995-1999, making a total of 108 observations, are fitted via FMM. The validity of FMM in generating realistic fuzzy estimates is analyzed via fuzzy paired *t*-tests as discussed in Section 5.1.1. Here, the equality of fuzzy estimates obtained via only the level-I of the proposed method and the fuzzified actual fertility rates is tested through paired fuzzy sample differences tests, in which the null and the alternative hypothesis are constructed as:

H_0 : The fuzzified actual fertility rates and the fuzzy estimates obtained via Level-I of FMM are equal.

H_1 : The fuzzified and estimated values be considered as the same.

The null hypothesis is tested at a significance level of 0.05 for all α -cuts of the mean fuzzy differences. The results are displayed in Table 5.8, in which t_L and t_U values of only five different α -cuts are given due to space limitations. For two samples to be considered as equal, t_L and t_U values should be in the interval [-1.982, 1.982], specified by the corresponding *t* values for 0.05 significance level and 107 degrees of freedom. The test results indicate that using only general country profiles (refers to level-I) in the method provide equality of the estimates and the actual fuzzy values in modeling fertility rates. Thus, it is decided to use only one level in FMM for fertility modeling and forecasting similar to the mortality case.

Table 5.8. Results of paired fuzzy sample differences tests for the equality of actual fertility values and FMM estimates

Demographic Indicator	Sex	t	α					Decision	
			$\alpha=0$	$\alpha=0.2$	$\alpha=0.4$	$\alpha=0.6$	$\alpha=0.8$		$\alpha=1$
Fertility	Female	t_L	$1.8*10^{-6}$	$1.8*10^{-6}$	$1.9*10^{-6}$	$1.9*10^{-6}$	$2*10^{-6}$	0.260	Cannot
		t_U	$-1.7*10^{-6}$	$-1.7*10^{-6}$	$-1.7*10^{-6}$	$-1.6*10^{-6}$	$-1.5*10^{-6}$	0.260	Reject H_0

The fertility modeling performance of the proposed FMM is also compared with that of BMM for the 12 quinquennial time periods of 1940-1944 to 1995-1999. The results for the example age group [20,25) are displayed in Figure 5.13 as well the actual values. Figure 5.13 provides the FMM results for only Level-I model as it is statistically found to represent the actual fertility rates. Therefore, in Figure 5.13, the center values and $\alpha=0.05$ -cut fuzzy intervals generated via FMM with Level-I model are depicted in addition to the median fits and the 95 percent Bayesian prediction interval obtained via BMM.

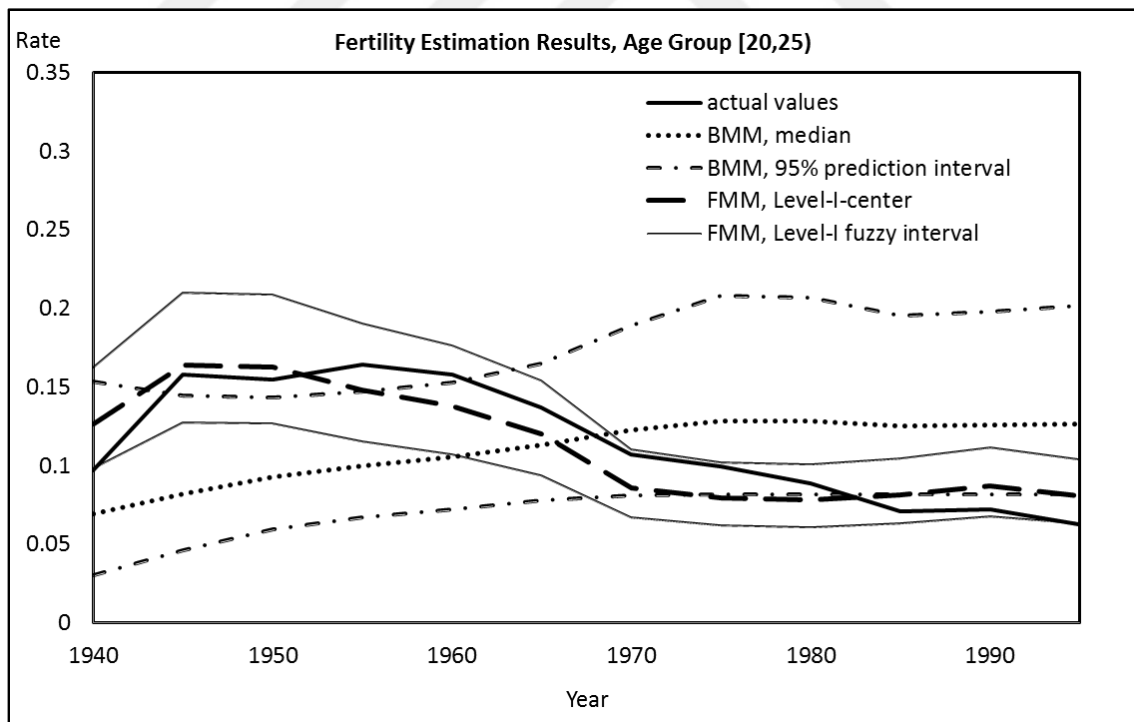


Figure 5.13. Fertility modeling estimates for age group [20,25), using 1940-1999 data:
FMM versus BMM

As observed in Figure 5.13, BMM seems to fail in generating accurate fits to the actual fertility rates for [20,25) age group since the actual rates are not covered within the generated 95% Bayesian prediction interval. However, the center values obtained via FMM are consistent with the actual fertility rates for age group [20,25). Furthermore, $\alpha=0.05$ -cut fuzzy intervals cover all actual fertility rates. The age group [20,25) corresponds to young adults in which the fertility rates reach their peak level. Thus, it can be claimed that FMM is capable of capturing the unimodal shape of the fertility age profiles while BMM fails to accomplish this task for Finland fertility dataset.

Table 5.9. MAPE between actual and fitted fertility values for 1940-1999 period obtained via BMM and FMM

Demographic Indicator	Sex	MAPE (%) between actual and fitted values	
		BMM	FMM
Fertility	Female	32.25	20.67

The fertility modeling performance of the two methods in generating accurate point fits to the observed rates are also compared in Table 5.9. In Table 5.9, the MAPE between the actual fertility rates and median fits obtained via BMM and the MAPE between actual fertility rates and the centers values computed via FMM are provided considering all of the nine age groups. Compared to mortality modeling, both BMM and FMM seem to generate more fitting errors in fertility modeling, but FMM performs still better than BMM.

5.2.3. Fertility Forecasting Results

After computing the age-specific fuzzy parameters \tilde{A}_x and \tilde{B}_x and the time-specific fuzzy parameter \tilde{K}_t via FMM with Level-I model, the future values of $\tilde{K}_t = (k_t, \delta_t)$ are forecasted so that the future fertility rates can be predicted. The six Bayesian time series models discussed in Section 4.3 are fitted separately on parameters k_t and δ_t computed in modeling part, and the model with the highest posterior probability is selected for each parameter. The prior distributions of the model parameters are based on a data-driven approach as in mortality forecasting. The constants c_j are assumed to follow a normal

prior distribution $N(0, 100^2)$, which display non-informative characteristics. The prior distributions for the autoregressive parameters ϕ_j and the moving average parameters θ_j are also normal, but more informative, following $N(0.5, 1^2)$. Similar to Wiśniowski *et al.* [17], the precision parameters $1/\sigma_j^2$ are assumed to follow a Gamma distribution with scale parameter 0.5 and shape parameter 0.5, reflecting a low precision of estimation.

The ultimate models selected to forecast fertility rates are ARMA (1,1) model for future k_t values and random walk without drift model for future δ_t values which are also the models used for female mortality forecasting. Using these models and the age-specific parameters computed in modeling part, future fertility rates for females and males are forecasted for 2000-2004, 2005-2009, ..., 2020-2024 periods. Similarly BMM is also applied on the same datasets for comparison purposes.

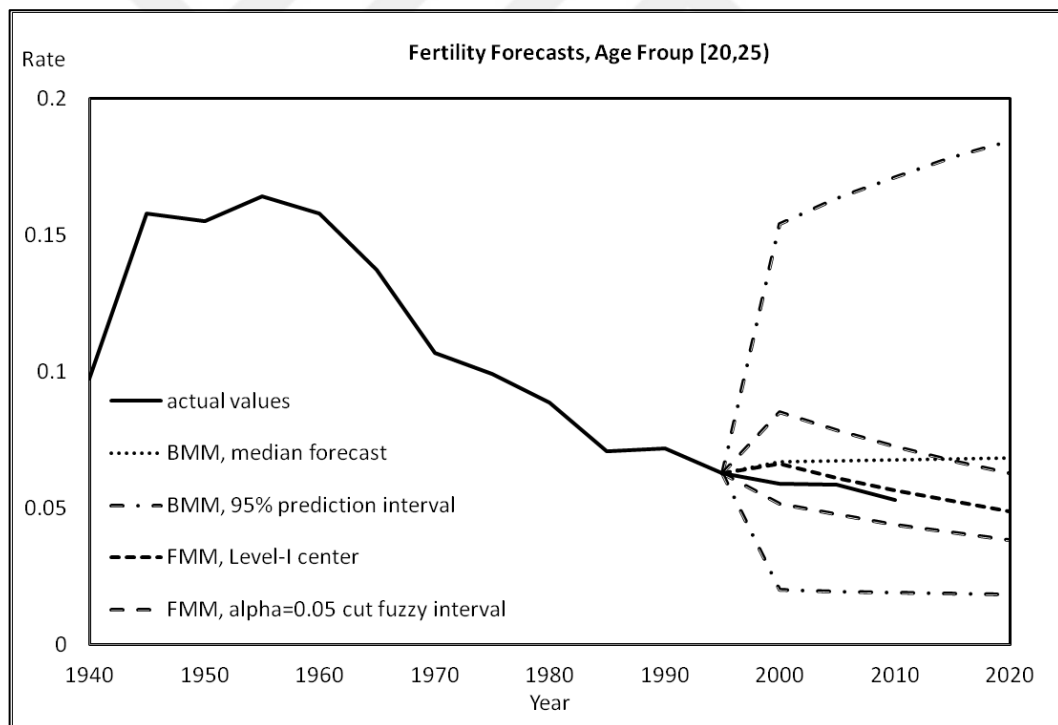


Figure 5.14. Fertility forecasts for age group [20,25)

The fertility forecasts obtained via FMM and BMM for the five quinquenal time periods of 2000-2004 to 2020-2024 are illustrated for the example age group [20,25) in Figure 5.14. The forecasts obtained via FMM are displayed through the center values and $\alpha=0.05$ -cut fuzzy intervals while the forecasts generated via BMM are represented through median

forecasts and 95 percent Bayesian prediction intervals. In Figure 5.14, median fits of BMM display an almost constant trend within the forecast horizon, while the center values of FMM forecasts are decreasing in a similar fashion to the actual fertility rates for age group [20,25). Although the forecast intervals of the two methods cover the actual fertility rates, 95 percent Bayesian prediction interval of BMM is significantly wider than $\alpha=0.05$ -cut fuzzy interval.

When all of the nine age groups are considered, the *ex-post* analyses of comparisons between actual and forecasted fertility rates for 2000-2014 period given in Table 5.10 and Table 5.11. In Table 5.10, MAPE between actual fertility rates and median forecasts of BMM and MAPE between actual fertility rates center forecasts of FMM are provided in addition to the percentage of actual fertility rates covered within the $\alpha=0.05$ -cut fuzzy intervals and the 95 percent Bayesian intervals. The MAPE between actual fertility rates and median forecasts of BMM are approximately 28 percent, while the MAPE between actual fertility rates and center values of FMM are approximately 26 percent. That is to say, FMM is slightly more accurate in generating point forecasts compared to BMM.

Table 5.10. Forecast analysis of actual and forecasted fertility values for 2000-2014 period

Demographic Indicator	Sex	MAPE between actual values and forecasts		Percentage of actual values covered within the forecast intervals	
		BMM	FMM	95% Bayesian prediction interval	$\alpha=0.05$ -cut fuzzy interval
Fertility	Female	27.81	25.57	96.29	88.89

Table 5.11. Fertility forecast interval comparisons for the BMM and the FMM

Demographic Indicator	Sex	Average prediction interval width (in rates)		BMM 95% prediction interval vs FMM $\alpha=0.05$ cut fuzzy interval
		BMM	FMM	
Fertility	Female	0.062	0.021	BMM interval is 192.3% wider

When all of the nine age groups are considered, the *ex-post* analyses of comparisons between actual and forecasted fertility rates for 2000-2014 period given in Table 5.10 and Table 5.11. In Table 5.10, MAPE between actual fertility rates and median forecasts of BMM and MAPE between actual fertility rates center forecasts of FMM are provided in addition to the percentage of actual fertility rates covered within the $\alpha=0.05$ -cut fuzzy intervals and the 95 percent Bayesian intervals. The MAPE between actual fertility rates and median forecasts of BMM are approximately 28 percent, while the MAPE between actual fertility rates and center values of FMM are approximately 26 percent. That is to say, FMM is slightly more accurate in generating point forecasts compared to BMM.

As displayed in Table 5.10, the percentage of actual fertility rates for 2000-2014 period covered within the $\alpha=0.05$ -cut fuzzy intervals are almost 89 percent while approximately 96 percent of the observed mortality rates are covered within the 95 percent Bayesian prediction interval. Although BMM covers more actual data within its forecast intervals, the widths of the 95 percent Bayesian prediction intervals are significantly larger than that of the $\alpha=0.05$ -cut fuzzy intervals, which can be observed in Table 5.11. The forecast interval of BMM is 192.3 percent wider than the forecast interval of FMM, which displays a tradeoff between the amount of the covered observed data and widths of the forecast intervals.

5.3. MIGRATION RESULTS

5.3.1. Migration Data

The proposed FMM is applied to the age-specific emigration and immigration counts of Finland for each sex separately. Although Finland displays stable migration profile for some specific periods, the migration patterns also fluctuates in certain time intervals such as in years around the collapse of Soviet Union and expansion of the European Union (EU); but the country did not witness mass emigration or immigration due to global financial crisis of 2008 when compared to some other EU countries. Finland migration data are accessible from the Official Statistics of Finland. Finnish population statistics are based on the Population Information System maintained by the Population Register Centre and includes immigration and emigration counts in total and for each sex separately. The

annual data are available as quinquenal (five-year) age groups from 1990 to 2016 (at the time of accession). In addition, both population and migration data of Finland are among the most reliable ones due to its high developed registration and data recording systems.

The observed emigration counts are displayed in Figure 5.15 and Figure 5.16 for females and males respectively. Moreover, the observed immigration counts for females and males are illustrated in Figure 5.17 and Figure 5.18 respectively. The datasets of annual age-specific immigration and emigration counts for females and males are composed of 16 quinquenal age groups including ages [0,5), [5,10), ..., [70,75] and 75 and over, making 432 data points in each set. The number of emigrants from Finland is smaller than the number of immigrants to the country in each year for 1990-2016 period, and it is observed that age groups between [20,35) constitute the main migrants. Number of migrants are also relatively high for age groups [0,5), [5,10), and [35,40) when compared to the remaining age groups.

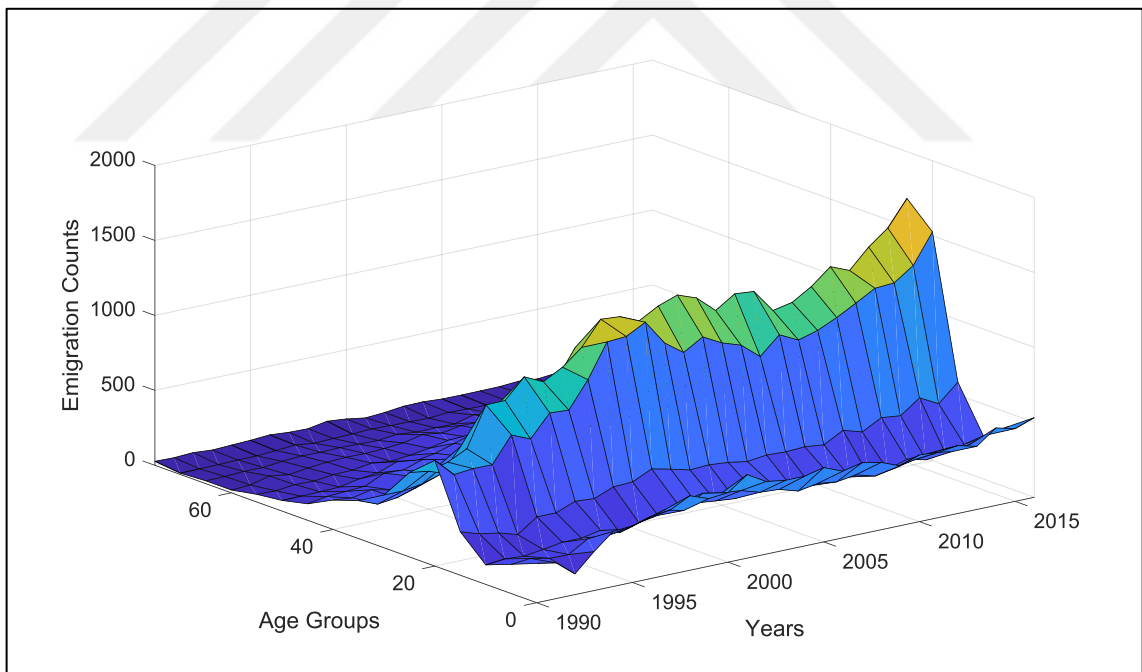


Figure 5.15. Observed emigration counts, females

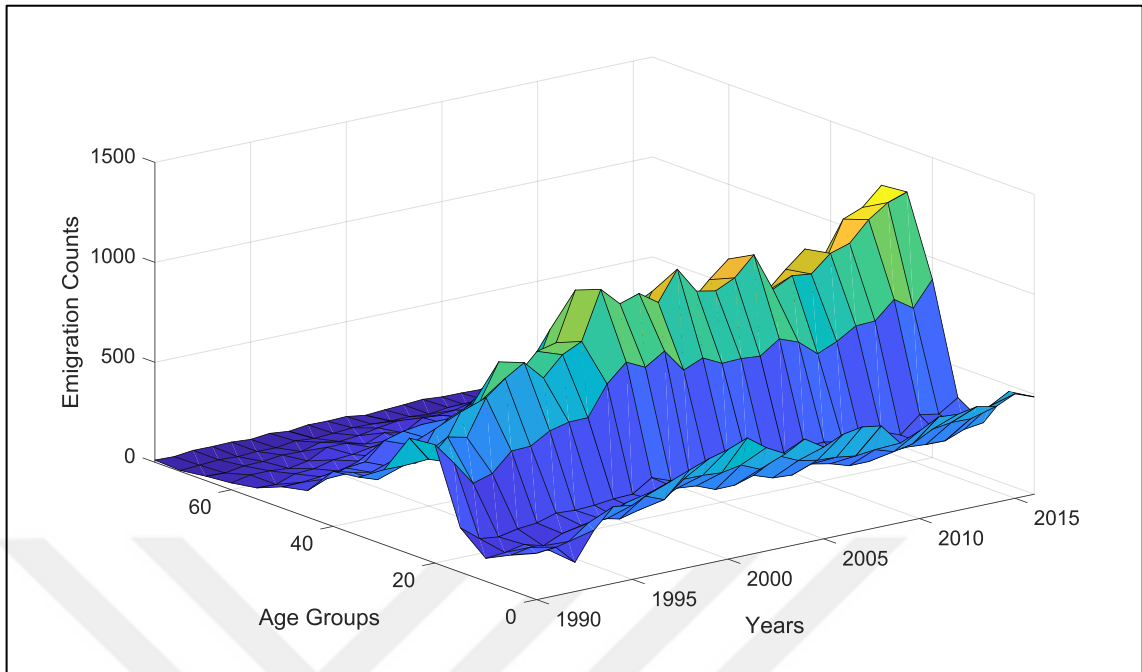


Figure 5.16. Observed emigration counts, males

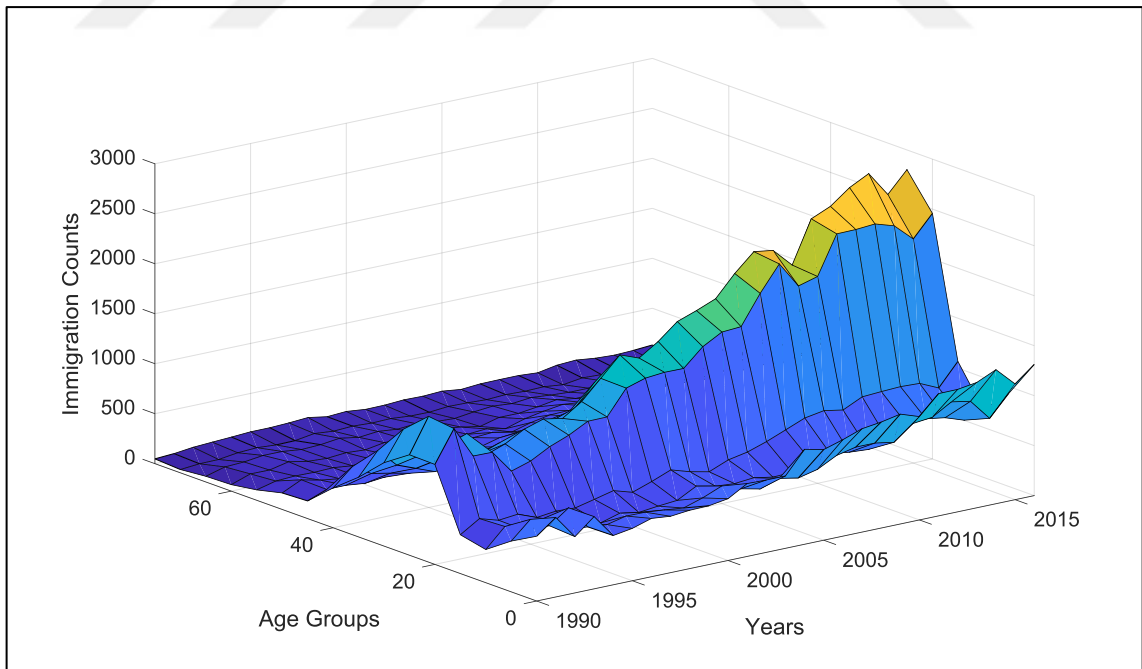


Figure 5.17. Observed immigration counts, females

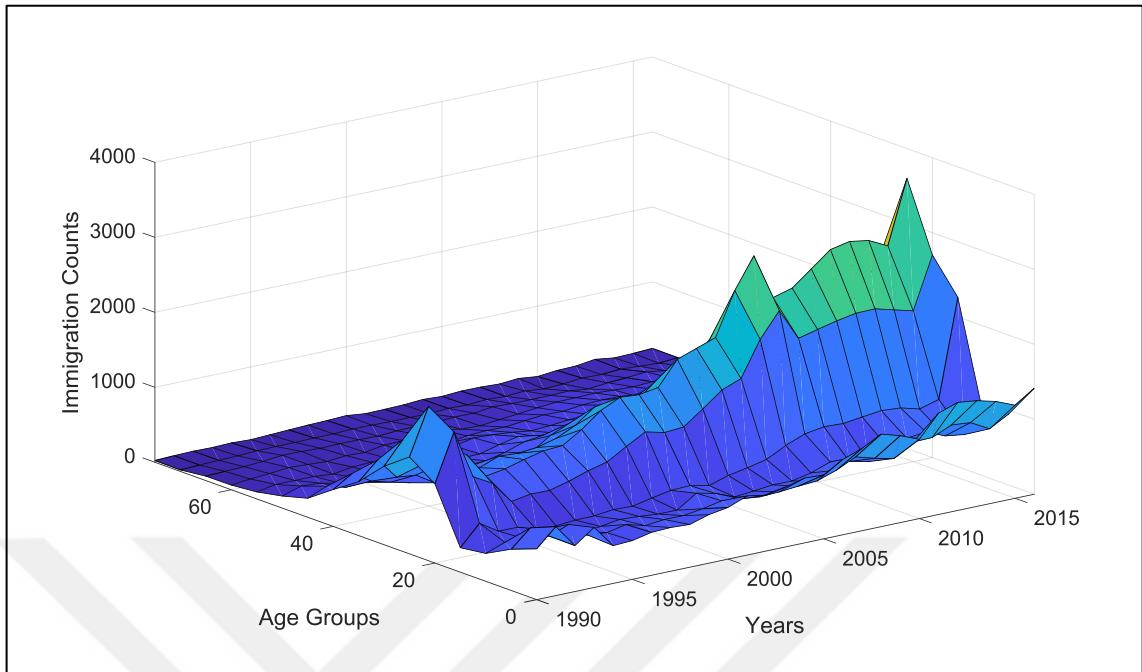


Figure 5.18. Observed immigration counts, males

Unlike mortality and fertility curves, immigration and emigration curves have bimodal structures with two peak levels young children and young adults. This bimodal shape is preserved throughout time with an increase in the level of both immigration and emigration as observed in Figure 5.15 to Figure 5.18.

The observed data are smoothed via natural logarithmic transformation to enable the application of proposed FMM on migration modeling and forecasting. The natural logarithms of emigration counts (\ln -emigration count) for females and males are displayed in Figure 5.19 and Figure 5.20; while the natural logarithms of immigration counts (\ln -immigration count) for females and males are illustrated in Figure 5.21 and Figure 5.22. Despite the observed regular structure of emigration and immigration counts in Figure 5.19 to Figure 5.22, the proposed FMM with a single level model may not be adequate to represent the bimodal shape of the migration curves, thus, the proposed method is enhanced via addition of a bi-level structure for migration modeling and forecasting.

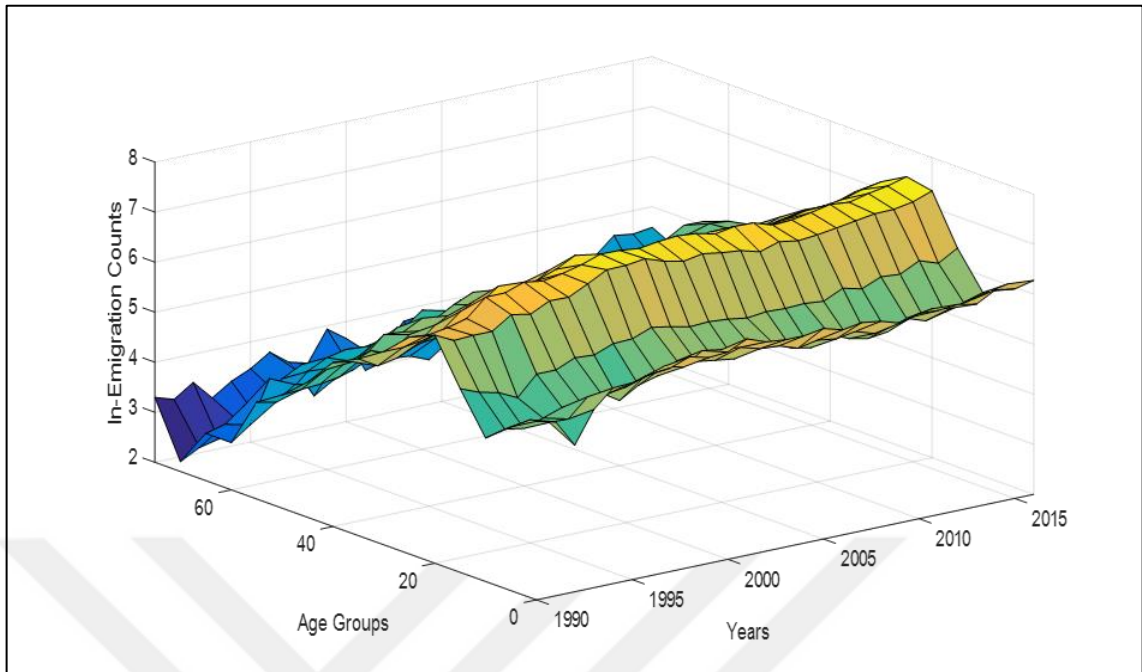


Figure 5.19. Observed In-emigration counts, females

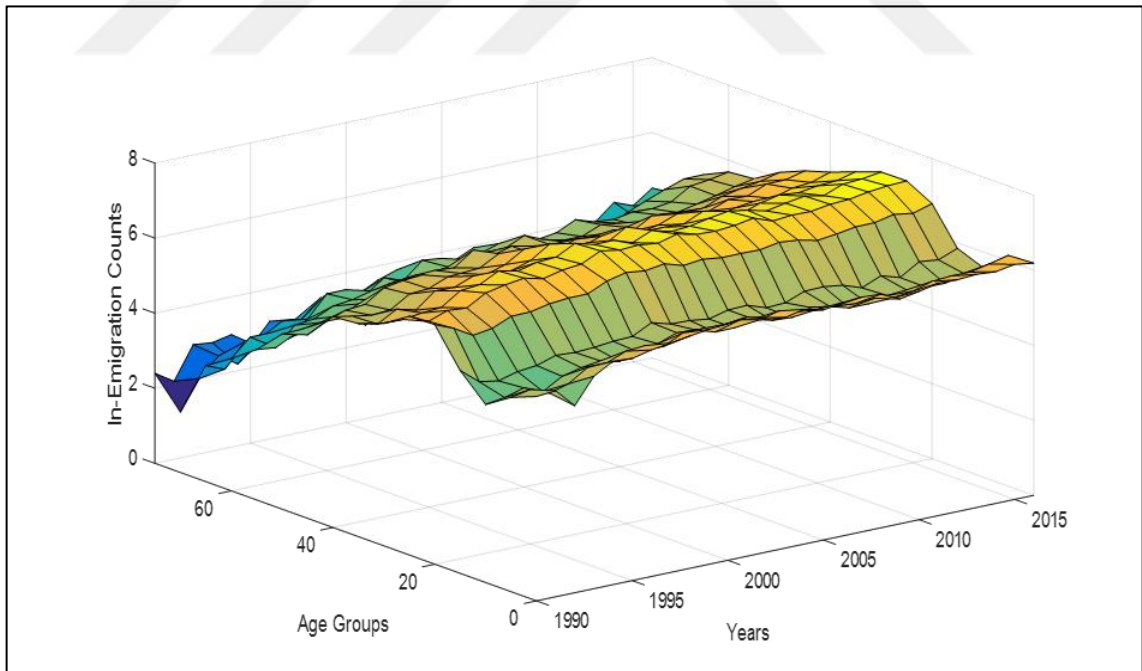


Figure 5.20. Observed In-emigration counts, males

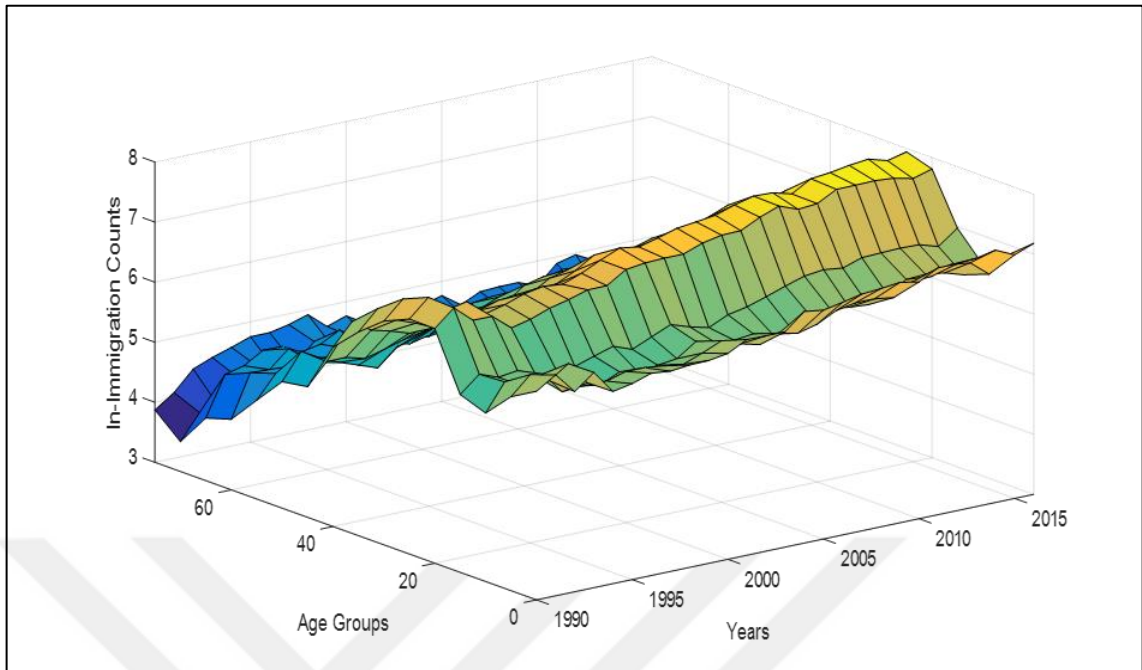


Figure 5.21. Observed In-immigration counts, females

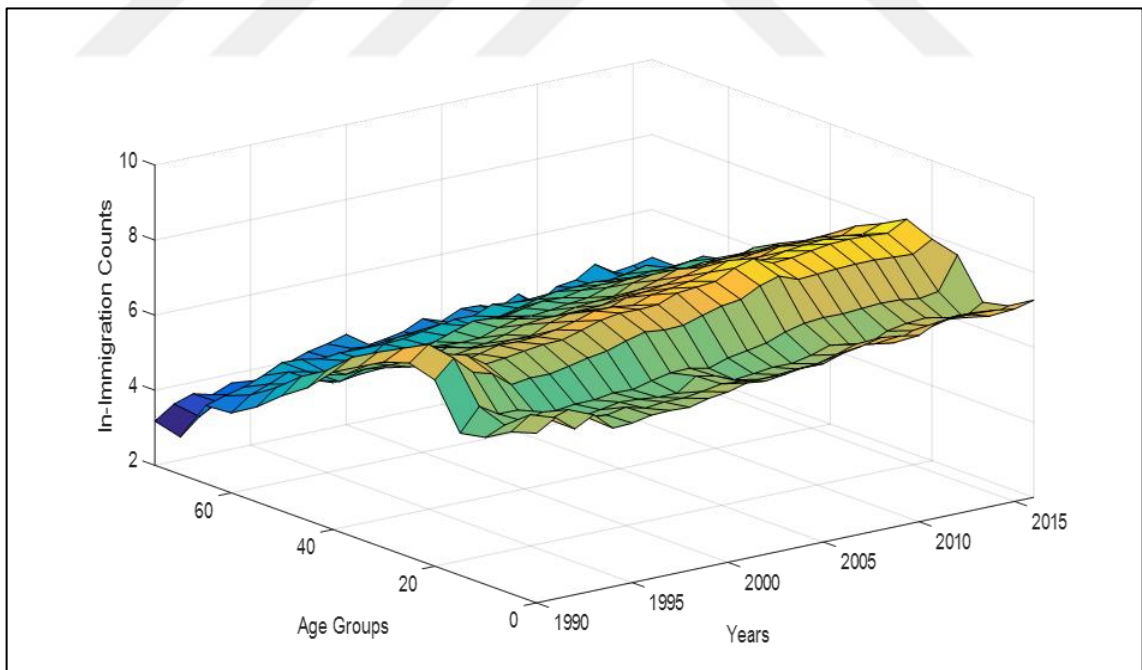


Figure 5.22. Observed In-immigration counts, males

Although the data sets are considered to be of high quality, there are still some problems regarding the completeness of migration data due to unregistered/illegal migration. Such

kind of under-registrations result in the fact that the exact values of migration can be rarely known; therefore, emigration and immigration counts are expressed as fuzzy numbers rather than their classical crisp representation.

The proposed FMM is applied on emigration and immigration counts for two sexes separately for 1990-2010 data (336 data points for each set). The fuzzy model estimates obtained by FMM are used in Bayesian time series analysis to forecast 2011-2025 migration values. Furthermore, Bayesian migration modeling and forecasting method of Wiśniowski et al. (2015) is also implemented on the same data for comparison purposes.

5.3.2. Migration Modeling Results

The two levels of FMM, level-I (general country factor) and level-II (age group cluster factor) are compared in terms of the mean absolute percentage errors (MAPE) between the observed migration values and the center values of the fuzzy estimates for 1990-2010 period. The MAPE values obtained in modeling emigration and immigration for females and males through the two levels of FMM are displayed in Table 5.12, in which results of different dissimilarity proportions (p) for Level-II are given.

Table 5.12. MAPE between actual and fitted migration values for 1990-2010 period obtained via different dissimilarity proportions (p) in Level II of FMM method

Migration Type	Sex	MAPE (%) between actual and fitted values for 1990-2010 period									
		$p=0.1$	$p=0.2$	$p=0.3$	$p=0.4$	$p=0.5$	$p=0.6$	$p=0.7$	$p=0.8$	$p=0.9$	$p=1$
Emigration	Female	5.59	5.59	5.79	6.31	6.32	6.56	6.56	7.39	7.39	8.57
	Male	6.21	6.21	6.38	7.18	7.83	8.02	8.02	8.02	8.02	9.16
Immigration	Female	3.97	3.97	4.21	4.42	4.92	4.95	4.72	4.72	5.60	8.81
	Male	4.19	4.19	4.50	4.61	5.82	6.48	6.48	6.48	6.48	10.45

The results in Table 5.12 indicate that FMM generates minimum absolute errors when the dissimilarity proportion p is set to be 0.1 or 0.2; and the amount of fitting errors increase as p increases. Further analyses reveal that the first time when MAPE starts to increase is observed if dissimilarity proportion exceeds 0.2157 for male emigration data set. Thus, the optimum dissimilarity proportion p^* is set to be 0.2157; meaning that error becomes

minimum if the dissimilarity between age groups within a cluster does not exceed 21.57 percent.

The validity of FMM in generating realistic fuzzy estimates are analyzed via fuzzy paired t -tests. Here, two paired fuzzy sample differences tests are performed for each data set. The first test is conducted to check the equality of fuzzy estimates in level-I of FMM and the fuzzified actual migration values; and the second test is performed to analyze the equality of fuzzy estimates of bi-level FMM (level-I plus level-II) and the fuzzified actual migration values. The null and the alternative hypothesis are constructed as:

H_0 : The fuzzified actual migration counts and the fuzzy estimates obtained via FMM are equal.

H_1 : The fuzzified and estimated values cannot be considered as the same.

Table 5.13. Results of paired fuzzy sample differences tests for the equality of actual migration values and FMM estimates

Migration Type	Sex	Model	t	α						Decision
				$\alpha=0$	$\alpha=0.2$	$\alpha=0.4$	$\alpha=0.6$	$\alpha=0.8$	$\alpha=1$	
Emigration	Female	Level I	t_L	-1.804	-2.082	-2.531	-3.368	-5.371	-10.05	Reject H_0
			t_U	-0.582	-0.890	-1.401	-2.403	-5.018	-10.05	
		Level I+II ($p=0.21$)	t_L	-0.039	-0.032	-0.024	-0.016	-0.008	0	Cannot
			t_U	0.039	0.031	0.024	0.016	0.008	0	Reject H_0
	Male	Level I	t_L	-2.299	-2.577	-3.030	-3.898	-6.168	-14.66	Reject H_0
			t_U	-0.038	-0.341	-0.848	-1.863	-4.800	-14.66	
		Level I+II ($p=0.21$)	t_L	-0.744	-0.603	-0.457	-0.307	-0.154	0	Cannot
			t_U	0.735	0.597	0.454	0.305	0.153	0	Reject H_0
Immigration	Female	Level I	t_L	-0.712	-0.741	-0.790	-0.880	-1.091	-1.297	Cannot
			t_U	0.452	0.417	0.360	0.246	-0.076	-1.297	Reject H_0
		Level I+II ($p=0.21$)	t_L	-0.033	-0.027	-0.020	-0.013	-0.006	0	Cannot
			t_U	0.033	0.027	0.020	0.013	0.006	0	Reject H_0
	Male	Level I	t_L	-0.029	-0.030	-0.031	-0.032	-0.037	-1.627	Cannot
			t_U	0.026	0.025	0.024	0.022	0.017	-1.627	Reject H_0
		Level I+II ($p=0.21$)	t_L	0.126	0.101	0.076	0.051	0.025	0	Cannot
			t_U	-0.127	-0.102	-0.076	-0.051	-0.026	0	Reject H_0

For each migration type and sex, the null hypothesis is tested at a significance level of 0.05 for eleven selected α -cuts (0, 0.1, 0.2, ..., 1) of the mean fuzzy differences. However, only six are demonstrated in Table 5.13 due to space limitations. In Table 5.13, results for Level II refer to outcomes obtained by using dissimilarity proportion $p^*=0.2157$. For two samples to be considered as equal, t_L and t_U values should be in the interval $[-1.967, 1.967]$, specified by the corresponding t values for 0.05 significance level and 335 degrees of freedom. The test results indicate that using general country factors only (refers to level-I) is not sufficient to accept the equality of the estimates and the actual values. However, with addition of age group cluster factors (level-II) into the FMM, H_0 cannot be rejected in both emigration and immigration modeling, which means that the estimates and actual values can be accepted as same.

Table 5.14. MAPE between actual and fitted migration values for 1990-2010 period obtained via BMM and FMM

Migration Type	Sex	MAPE (%) between actual and fitted values		
		BMM Method	FMM Method	
			Level I	Level I+II
Emigration	Female	8.92	8.90	5.59
	Male	9.91	9.80	6.21
Immigration	Female	8.98	9.38	3.97
	Male	11.21	10.97	4.19

Table 5.14 depicts the comparison of BMM and FMM in terms of fitting capabilities for 1990-2010 migration data. The MAPE between the actual values and the centers of the estimated fuzzy migration values obtained via level-I and bi-level FMM (dissimilarity proportion $p^* = 0.2157$ is taken for Level II estimates) are displayed separately to illustrate the enhancements achieved by adding cluster factor to the general country factor. Except for the female emigration data set, Level I produces slightly smaller fitting errors than BMM. However, the addition of a second level, the age group cluster factor, into FMM improves the fitting capability of the proposed method between 37.19 percent (MAPE reduces from 8.90 percent to 5.59 percent in modeling female emigration counts) and 61.80 percent (MAPE reduces from 10.97 percent to 4.19 percent in modeling male immigration counts). When BMM and the bi-level FMM are compared, the decrease in

MAPE is in between 37.33 percent (from 8.92 percent to 5.59 percent for female emigration counts) and 62.62 percent (from 11.21 percent to 4.19 percent for male immigration counts). Considering the results of paired fuzzy sample differences tests in Table 5.13 and errors illustrated in Table 5.14, it can be asserted that the inclusion of age group cluster factor into the model enhances the performance of FMM in capturing the actual data.

To provide a better insight, emigration modeling outputs for age group [20,25) of females are selected for illustration purposes. This age group corresponds to young adults that display high mobility characteristics; and the enhancements achieved through bi-level FMM are minimum at emigration modeling for females. These constitute the main reasons for analyzing the emigration modeling outputs for females of age group [20,25). Figure 5.23 and Figure 5.24 display the center values and $\alpha=0.05$ -cut fuzzy intervals obtained through Level I and the bi-level FMM. In both figures, the median estimates and 95 percent prediction interval of BMM as well as the actual emigration counts are also depicted.

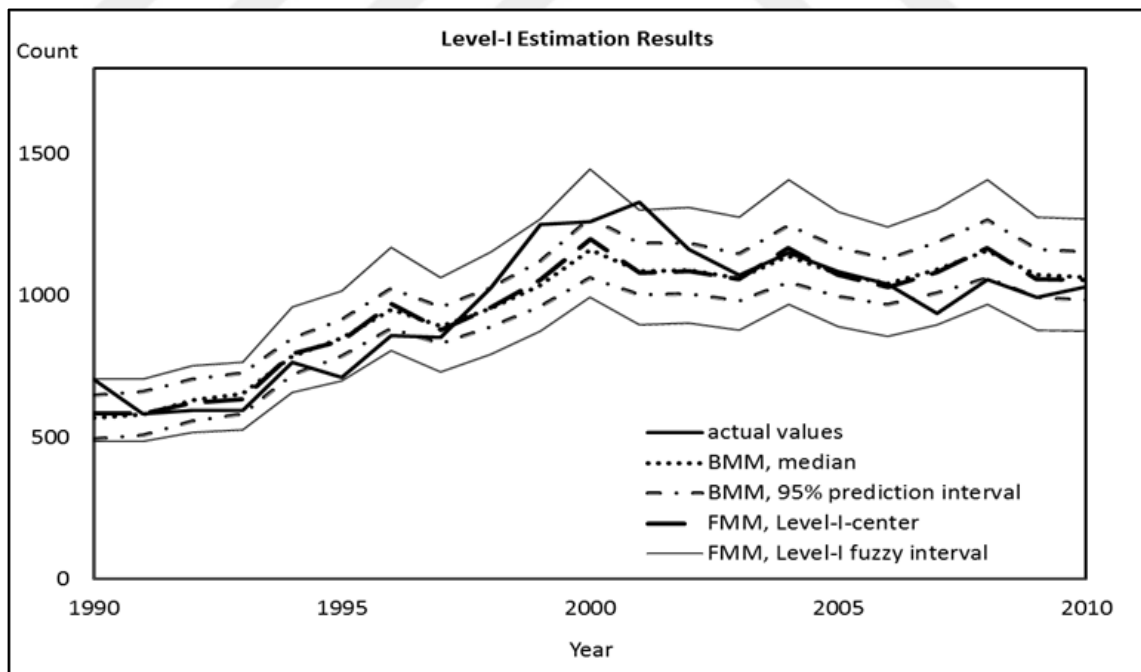


Figure 5.23. Emigration modeling estimates for age group [20,25), females, using 1990-2010 data: FMM with Level I versus BMM

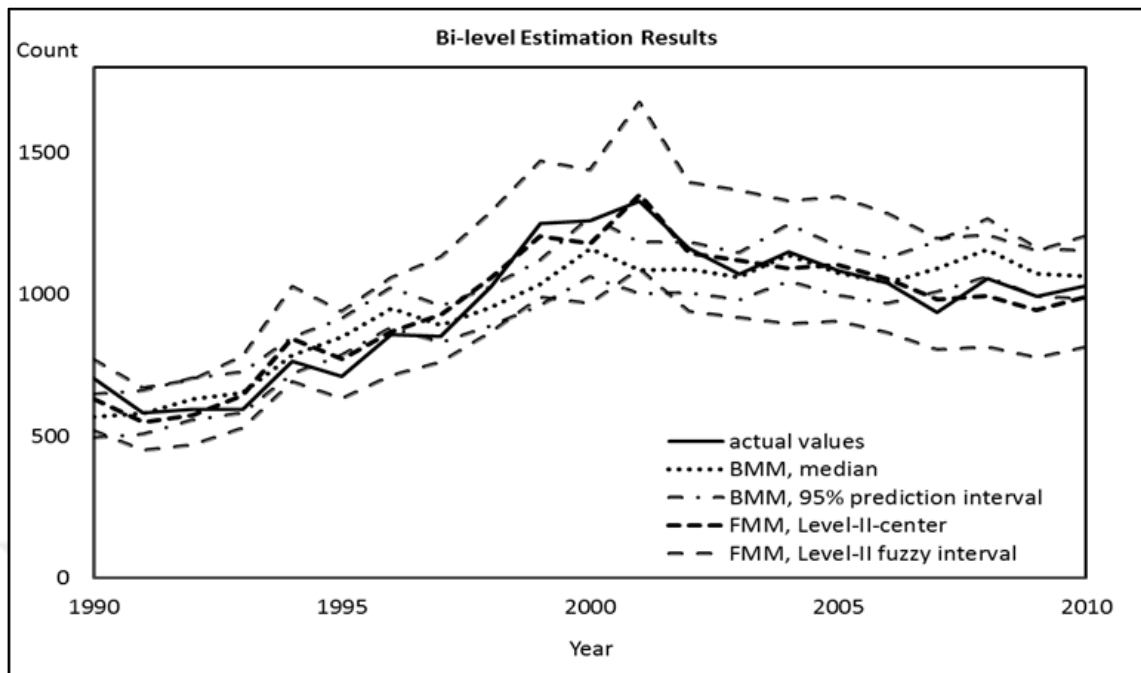


Figure 5.24. Emigration modeling estimates for age group [20,25), females, using 1990-2010 data: bi-level FMM versus BMM

As it is clear from these two figures, the center values obtained from the bi-level FMM generates better fits to the actual values when compared to BMM and Level-I of the FMM. This observation illustrates the enhancement in fitting capabilities achieved by the addition of Level-II outputs to the Level-I outputs. That is, the consideration of age group cluster factors in addition to the general country factors yields estimates that can mimic the nonlinear and fluctuating migration patterns. The emigration modeling outputs for males and immigration modeling outputs for both sexes for the example age group [20,25) are provided in Appendix D.

For this age group, for some observations, 95 percent prediction intervals of the BMM are unable to cover 1/3 of the actual migration values, which is a major drawback for the Bayesian approach in estimating the past data. In overall, 95 percent prediction intervals of the BMM do not cover 34.92 percent of the actual emigration and immigration counts for 1990-2010 period. In contrast, 99.27 percent of actual migration values are included within $\alpha=0.05$ -cut fuzzy intervals for both level-I and bi-level FMM for the same period. Therefore, the bi-level FMM is superior to BMM in generating better fits covering the actual migration values within the obtained fuzzy intervals. The inclusion of age group

cluster factors enlarges the fuzzy interval in small amounts thanks to the T_w based addition embedded in FMM.

5.3.3. Migration Forecasting Results

Using the fuzzy parameters obtained by applying FMM on 1990-2010 data, the future migration values for 2011-2025 period are forecasted using the Bayesian time series models discussed in Section 4.3.3. The six models, M_1, \dots, M_6 , given in Equ. (4.24) to Equ. (4.29) are applied on the estimates of time-variant parameters k_t and δ_t in general country factor. The six models are also applied for age group cluster factors on parameter $r_{i,t}$ of class C_i $i=1, \dots, 8$. Here, no operation is performed to forecast future $\tau_{i,t}$ values because all $\tau_{i,t}$ values for 1990-2010 period are estimated as zero according to MATLAB outputs.

The prior distributions of the model parameters are based on a data-driven approach and they are conforming to the existing literature. The constants c_j are assumed to follow a normal prior distribution $N(0, 100^2)$, which display non-informative characteristics. The prior distributions for the autoregressive parameters ϕ_j and the moving average parameters θ_j are also normal, but more informative, following $N(0.5, 1^2)$. Similar to Wiśniowski *et al.* [17], the precision parameters $1/\sigma_j^2$ are assumed to follow a Gamma distribution with scale parameter 0.5 and shape parameter 0.5, reflecting a low precision of estimation. The ultimate models to represent the future values are selected based on the posterior probabilities. The selected models are displayed in Table 5.15.

Table 5.15. The models used in forecasting future k_t , δ_t , and $r_{i,t}$ values.

Migration Type	Sex	Level I		Level II ($r_{i,t}$)							
		k_t	δ_t	C_1	C_2	C_3	C_4	C_5	C_6	C_7	C_8
Emigration	Female	M_1	M_2	M_6	M_2	M_2	M_5	M_5	M_2	M_4	M_5
	Male	M_1	M_2	M_6	M_5	M_5	M_5	M_5	M_5	M_5	M_4
Immigration	Female	M_1	M_2	M_4	M_2	M_4	M_4	M_5	M_5	M_5	M_4
	Male	M_1	M_2	M_6	M_5	M_4	M_4	M_2	M_2	M_4	M_4

C_i in Table 5.15 refers to the i^{th} class obtained in Level-II of the FMM for dissimilarity proportion $p^* = 0.2157$, $i = 1, \dots, 8$. As illustrated in Table 5.15, linear trend models (M_1) are fitted to k_t and random walk models (M_2) are utilized for δ_t based on posterior odds criterion. Forecasting class-and-time variant parameter $r_{i,t}$ requires more complex models like AR(1) (M_4), MA(1) (M_5), and ARMA(1,1) (M_6) as well as the simple random walk model.

Forecasts obtained from the bi-level FMM are compared to the forecasts obtained via BMM, and the results for female emigrants of age group [20,25) are displayed for exemplary purposes in Figure 5.25. This figure depicts the actual migration values for 2000-2016 period, median forecasts of BMM together with their 95 percent prediction interval; and center forecasts of the bi-level FMM with associated $\alpha=0.05$ -cut fuzzy prediction intervals. The fuzzy prediction intervals are computed based on median forecasts for the spread values, and because $\alpha=0.05$ -cuts are employed, they are comparable with the 95 percent Bayesian prediction intervals of the BMM. The emigration forecasting outputs for males and immigration forecasting outputs for both sexes for the example age group [20,25) are provided in Appendix D.

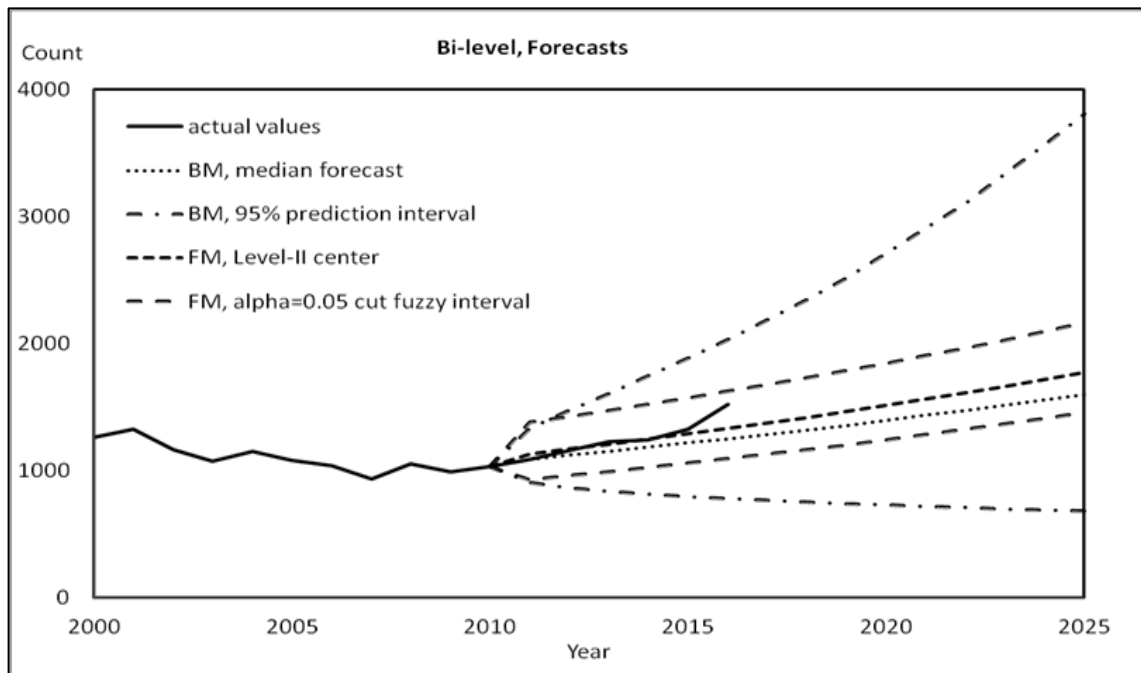


Figure 5.25. Emigration forecasts for age group [20,25), females

For age group [20,25), $\alpha=0.05$ -cut fuzzy prediction interval of the bi-level FMM is 42.21 percent narrower than 95 percent prediction interval for the BMM forecasts on average, but it still includes the actual migration values for 2011-2016 period. The Bayesian prediction interval expands significantly by time, even resulting in over-predictions for emigration counts larger than 4000 for 2025. Such kinds of expansions are witnessed as the forecast horizon enlarges, thus, only fifteen years ahead forecasts are provided within this study.

The available migration data for 2011-2016 period make forecast analysis possible to be performed. These analyses are summarized in Table 5.16, in which MAPE between actual and forecasted emigration and immigration values are given for BMM and FMM. The performances of the BMM and the bi-level FMM do not display significant differences in terms of the fitting error magnitudes. Both methods generate slightly smaller fitting errors in forecasting immigration counts when compared to emigration counts. The results of two methods are also compared in terms of percentage of actual values covered within the forecast intervals. When all observations are considered, 95 percent prediction intervals of the BMM cover approximately 89 percent to 94 percent of the actual data. Similarly, $\alpha=0.05$ -cut fuzzy intervals of the FMM include approximately 88 percent to 91 percent of the actual emigration and immigration counts for 2011-2016 period. This reveals the fact that both methods yield almost similar forecasts in general.

Table 5.16. Forecast analysis between actual and forecasted migration values for 2011-2016 period

Migration Type	Sex	MAPE between actual values and forecasts		Percentage of actual values covered within the forecast intervals	
		BMM	Bi-level FMM	95% Bayesian prediction interval	$\alpha=0.05$ -cut fuzzy interval
Emigration	Female	15.56	15.71	89.58	89.58
	Male	14.29	14.45	92.70	87.50
Immigration	Female	12.40	11.90	92.71	88.54
	Male	12.36	13.03	93.75	90.63

Table 5.17. Prediction and fuzzy interval comparisons for the BMM and the FMM

Migration Type	Sex	Average prediction interval width (in counts)		BMM 95% prediction interval vs FMM $\alpha=0.05$ cut fuzzy interval
		BMM	Bi-level FMM	
Emigration	Female	390.92	275.97	BMM interval is 41.65% wider
	Male	437.41	224.31	BMM interval is 95.00% wider
Immigration	Female	772.58	491.24	BMM interval is 57.27% wider
	Male	872.78	645.88	BMM interval is 35.13% wider

The two methods are also compared in terms of their forecast interval widths, which can represent the forecast information value. The comparisons are given in Table 5.17. The findings state that 95 percent prediction intervals generated via BMM are wider than $\alpha=0.05$ -cut fuzzy prediction intervals of FMM in both emigration and immigration forecasting. When the numerical outputs displayed in Table 5.16 are also taken into account, it is observed that the two methods cover almost the same amount of actual values for 2011-2016 period within their prediction intervals, yet FMM generates narrower prediction intervals. This observation forms the main advantage of the proposed bi-level fuzzy method over the existing Bayesian method since it is known that if the range is large, the forecast becomes uninformative [148].

5.3.4. Sensitivity Analysis

These results are obtained when the prior distributions of model parameters in the BMM are taken to be the same as in Wiśniowski *et al.* [17]. However, Wiśniowski *et al.* apply their Bayesian method on LC model using the migration data for United Kingdom (UK); which displays different migration characteristics than Finland. Therefore, the assumption that prior distributions of model parameters for forecasting the UK migration values also hold for Finland may be misleading. The assigned variances for the model parameters are capable of representing migration values in the UK, which are reported to be great in numbers. Thus, using the same variances may lead to wide Bayesian prediction intervals for Finland.

To check whether the variance magnitudes used in the UK case also holds for Finland, sensitivity analyses are performed on variance quantities in prior distributions of the LC model parameters embedded in BMM. For this task, a design of experiment consisting of

three different values for the related variances in prior distributions of the LC model parameters (a_x , b_x , and k_t) and the drift term c_j in Equ. (4.26) to Equ. (4.29) is conducted on each data set for Finland (making 81 experiments in total).

Table 5.18. Summary of sensitivity analyses conducted on variance magnitudes of prior distributions used in the BMM

Migration Type	Sex	The narrowest 95% Bayesian prediction interval obtained			The widest 95% Bayesian prediction interval obtained		
		% of actual values covered	Average prediction interval width (in counts)	Comparison with FMM $\alpha=0.05$ cut fuzzy interval	% of actual values covered	Average prediction interval width	Comparison with FMM $\alpha=0.05$ cut fuzzy interval
Emigration	Female	89.21	385.91	BMM interval is 39.83% wider	92.70	418.89	BMM interval is 51.78% wider
	Male	86.45	429.92	BMM interval is 91.66% wider	93.75	487.30	BMM interval is 117.25% wider
Immigration	Female	90.63	771.01	BMM interval is 56.95% wider	95.83	997.93	BMM interval is 103.14% wider
	Male	88.54	870.91	BMM interval is 34.84% wider	95.83	1141.17	BMM interval is 77.09% wider

The results indicate that 95 percent prediction intervals generated through BMM widens with the increase in variances for the migration index k_t and the drift factor c_j . Furthermore, the prediction interval width seems to be rather insensitive to variance magnitude changes for the age specific parameters a_x and b_x .

A summary of performed sensitivity analyses is displayed in Table 5.18. In this table, the percentage of actual values for 2011-2016 period covered within the narrowest and the widest 95 percent prediction intervals are provided. As it is seen from Table 5.18, FMM still performs better than the BMM with different prior model parameter variances in covering approximately same amount of actual migration values for 2011-2016 period within significantly narrower prediction intervals. Thus, altering the prior variance magnitudes does not lead to any significant performance changes in BMM for modeling Finland migration data. Sensitivity analyses are performed only on the variance terms of prior distributions because they are the main factor leading to the expansion of prediction intervals.

5.4. POPULATION FORECASTS

Once age-and-sex-specific mortality and fertility rates as well as emigration and immigration counts are modeled and forecasted, the population of Finland is estimated for years 1995, 2000, to 2025. Here, in each estimation year, 21 age groups of $[0,5)$, $[5,10)$, ..., $[90, \dots)$ are used. The estimation years and the age groups given are taken based on the common age groups and time periods used in modeling demographic indicators, and migration values for ages above 80 are assumed to be zero. The two methods, the proposed FMM and the existing BMM are compared in terms of their point forecast accuracy and interval widths.

The population estimates are illustrated through population trees, in which the populations of each group are also available. Population estimates for 1995, 2010, and 2025 are selected as example years due to space limitations and they are displayed in Figure 5.26 to Figure 5.28 respectively. The first population tree in each figure displays the observed male and female population disaggregated by age groups as shaded rectangles, and the fuzzy forecast interval obtained via FMM as borders without shading. Similarly, the second population tree in each figure displays the observed male and female age-specific population as shaded rectangles, and the fuzzy forecast interval obtained via FMM as borders without shading. For Figure 5.28, since there are no observed values yet, the shaded regions denote the point forecasts.

The dramatic changes in observed levels of age-specific population can easily be seen from Figure 5.26 to 5.27 in which the number of old people and adults are increasing from 1995 to 2010, while the number of children are decreasing. This reveals the fact that Finland is an ageing country, in which the percentage of young people follows a decreasing trend as in the rest of most of the developed countries. The difference between forecast intervals generated via FMM and BMM is mainly observed in age group [0,5) in 1995 and 2010, while the forecast intervals do not seem to differ much for the remaining age groups. This might be due to the large Bayesian prediction intervals of BMM computed for fertility forecasts. Furthermore, although the Bayesian prediction intervals of BMM are significantly wider than fuzzy forecast intervals of FMM in migration forecasting; they do not result in large intervals in population forecasts of especially young adult age groups since migration levels are low relative to the population levels.

The point forecasts for 2025 generated via FMM maintain the ongoing ageing population trend with increase in fuzziness in all age groups especially for the young ages as observed from the fuzzy intervals displayed in Figure 5.28. The uncertainty associated with BMM forecasts are even larger than FMM forecasts as displayed through the 95 percent Bayesian prediction intervals in the left population tree of Figure 5.28.

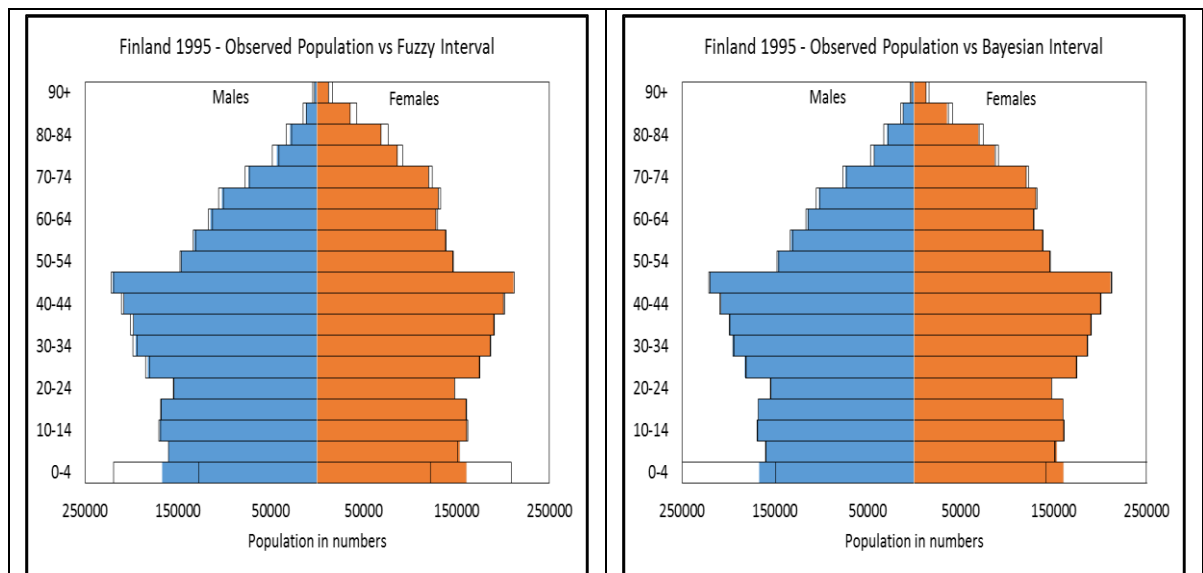


Figure 5.26. Observed versus forecasted population for Finland, 1995



Figure 5.27. Observed versus forecasted population for Finland, 2010

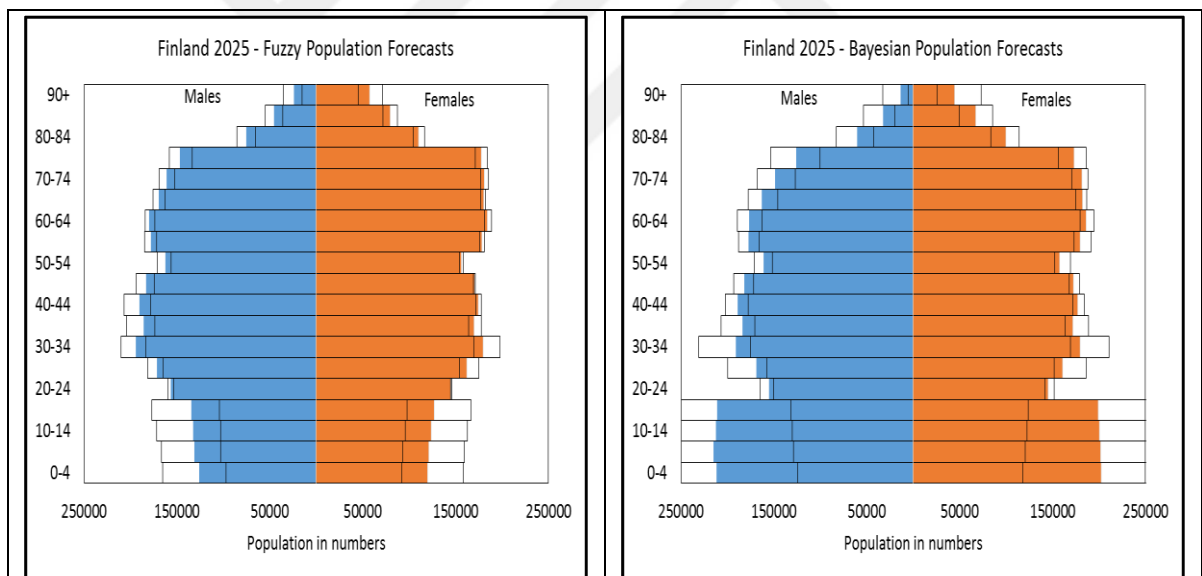


Figure 5.28. Forecasted population for Finland, 2025

5.4.1. Error Comparisons

The MAPE between observed and forecasted population, average forecast widths and percentage of observed population values covered within the forecast intervals are given for BMM and FMM outputs in Table 5.19 and Table 5.20 respectively. For both methods, it is observed that average forecast width is larger for males. This may be the reason for the

percentage of observed population levels covered within the forecast intervals to be higher for males, which can be seen at the fourth and the last columns of Table 5.19 and 5.20.

Table 5.19. Expost analysis for BMM population forecasts

Year	Female			Male		
	MAPE between actual & forecasted Population	Average forecast interval width (in counts)	% of actual values covered within the forecast interval	MAPE between actual & forecasted Population	Average forecast interval width (in counts)	% of actual values covered within the forecast interval
1995	3.84	12012.7	36.84	3.80	13071.0	89.47
2000	3.48	11837.6	68.42	3.50	12998.4	68.42
2005	3.29	13331.8	57.89	3.45	14762.4	84.21
2010	2.57	15110.3	84.21	3.10	17076.4	100.00
2015	4.79	31700.9	89.47	6.19	35889.7	100.00

Table 5.20. Expost analysis for FMM population forecasts

Year	Female			Male		
	MAPE between actual & forecasted Population	Average forecast interval width (in counts)	% of actual values covered within the forecast interval	MAPE between actual & forecasted Population	Average forecast interval width (in counts)	% of actual values covered within the forecast interval
1995	2.15	6700.2	78.95	1.94	7852.0	94.73
2000	1.76	5978.2	63.15	1.60	7155.7	100.00
2005	2.54	5502.8	52.63	2.42	7050	94.73
2010	2.33	5739.9	68.42	2.29	9694.4	89.47
2015	4.51	11188.6	63.15	4.13	14.954.7	100.00

Furthermore, for the two methods, the forecast interval widths for 2015 are larger than those of the other given years, which can be explained as the increase in uncertainty throughout the forecast horizon. Such increase in uncertainty is also observed in mortality, fertility, and migration forecasts as discussed in previous sections. Moreover, when Table

5.19 and Table 5.20 are compared, it is observed that FMM generates more accurate point forecasts than BMM. The fuzzy forecast intervals are narrower than Bayesian prediction intervals, yet they cover almost the same amount of actual population values for females and even more amount of actual values for males. This can be seen as a superiority of FMM over BMM.

The observed total population and forecasted levels via BMM and FMM are provided in Table 5.21 together with their forecast intervals. The age structure of Finland population is not given in Table 5.21, but the provided information is still valuable since the change in the two method outputs and the actual population levels can be directly observed. Based on the observed population levels, Finland population increases slightly from 1995 to 2015 reaching from 5.08 million to 5.47 million. This trend is closely captured by the point forecasts - the center forecast values – of FMM which increases from 5.11 million to 5.41 million from 1995 to 2015. FMM point forecasts indicate a slight increase for 2020, in which the population will be forecasted to be 5.48 million. Next, the Finnish population is forecasted to be 5.54 million based on FMM center estimates. The point forecasts generated via BMM seem to overestimate the observed population, which indicate that the population will increase from 5.23 million in 1995 to 6.06 million in 2025. If the forecast intervals are compared, it is seen that the Bayesian prediction intervals are a lot wider than the fuzzy forecast intervals.

Table 5.21. Population forecasts via BMM and FMM

Year	Actual Total Population	BMM		FMM	
		Point Forecast	Bayesian prediction interval	Point Forecast	Fuzzy forecast interval
1995	5098780	5235751	[5047829, 5524420]	5119687	[4995167, 5271658]
2000	5171157	5311489	[5126861, 5598747]	5175003	[5062092, 5311639]
2005	5236321	5360157	[5158718, 5692512]	5245599	[5137647, 5376152]
2010	5350822	5443239	[5214515, 5826063]	5330637	[5214913, 5470165]
2015	5471011	5646492	[5178231, 6462455]	5407940	[5185607, 5682331]
2020	-	5854417	[5126565, 7188935]	5479298	[5152390, 5890614]
2025	-	6062829	[5055876, 8033273]	5547305	[5112895, 6104774]

5.4.2. Age Distributions

Another important demographic output obtained from a population forecast is the distribution of population within young-age-population (ages 14 and below), working-age-population (between ages 15 and 64), and old-age-population (age 65 and over). The percentage distributions of the total population in these three age groups are summarized in Figure 5.29 for the example years 1995, 2010, and 2025. The first column in Figure 5.29 depicts the percentage distribution of age groups for the observed population, whereas FMM and BMM outputs are illustrated in the second and third columns respectively based on the point forecasts.

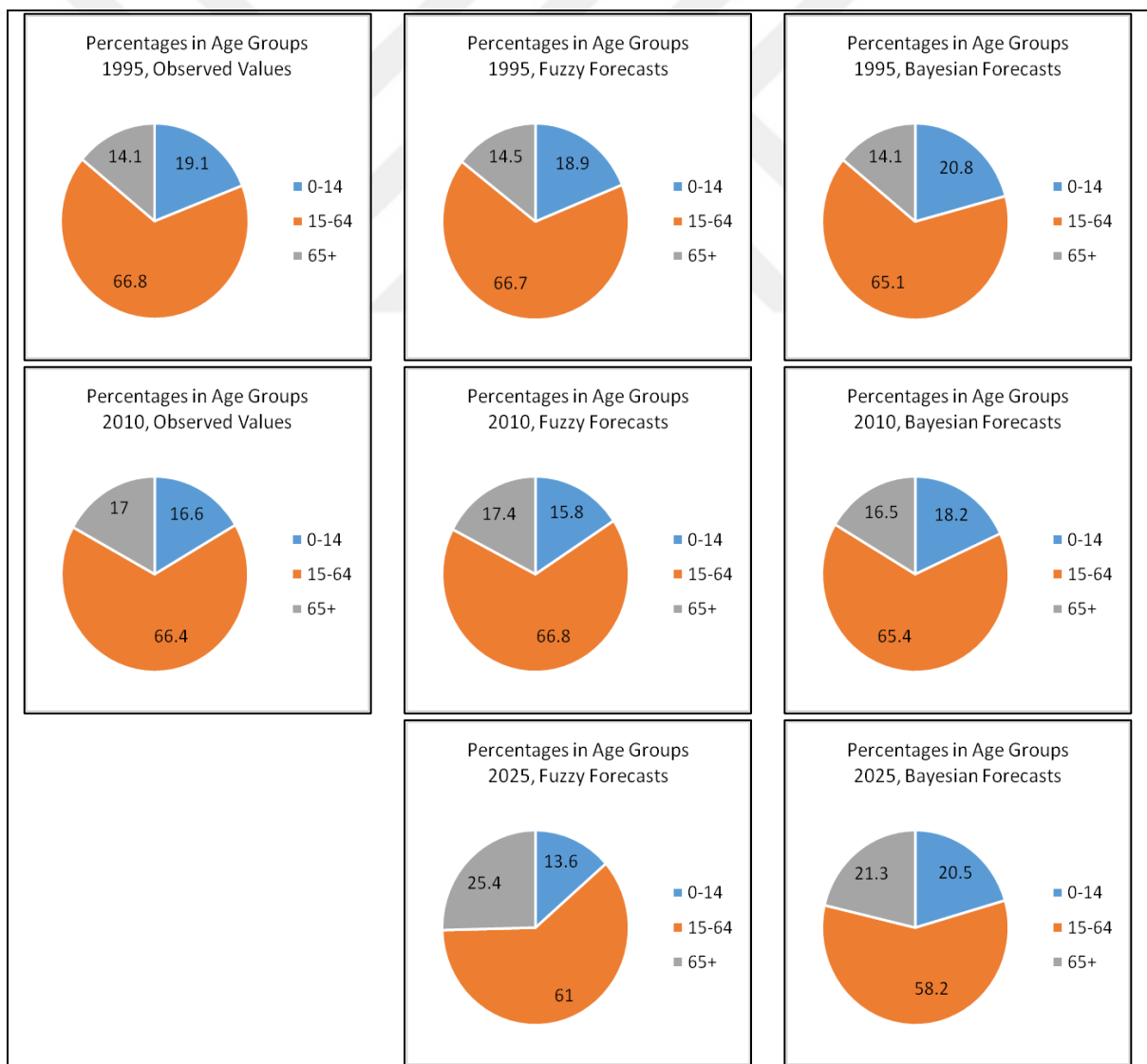


Figure 5.29. Distributions of the age group populations

The observed population levels indicate an increase in percentage of old-age-population and a decrease for the young-age-population within the total population, which supports the assertion that Finnish population is an ageing society. This ongoing trend is also observed within the FMM and BMM outputs. The FMM outputs suggest that the percentage of old-age-population within the total population will reach 25.6 percent in 2025, while this value is forecasted to be 21.3 percent for BMM outputs. However, BMM outputs forecast a more stable percentage for the young-age-population surprisingly, which contradicts the observed values and FMM forecasts.

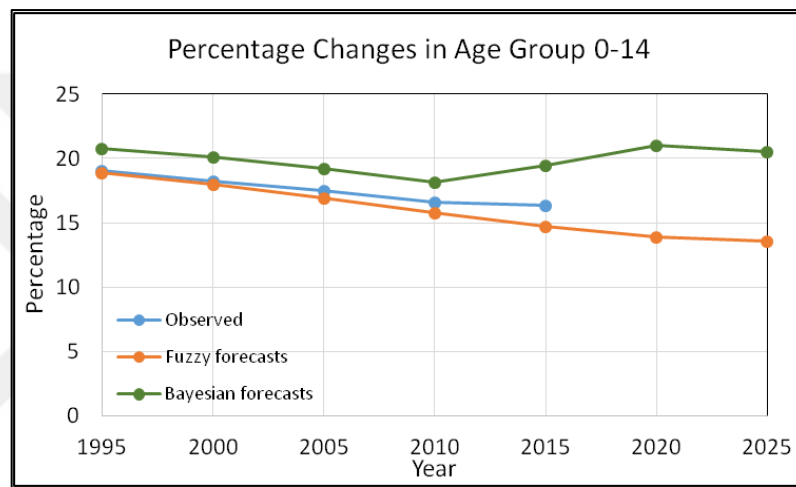


Figure 5.30. Percentage changes in distribution of young-age-population

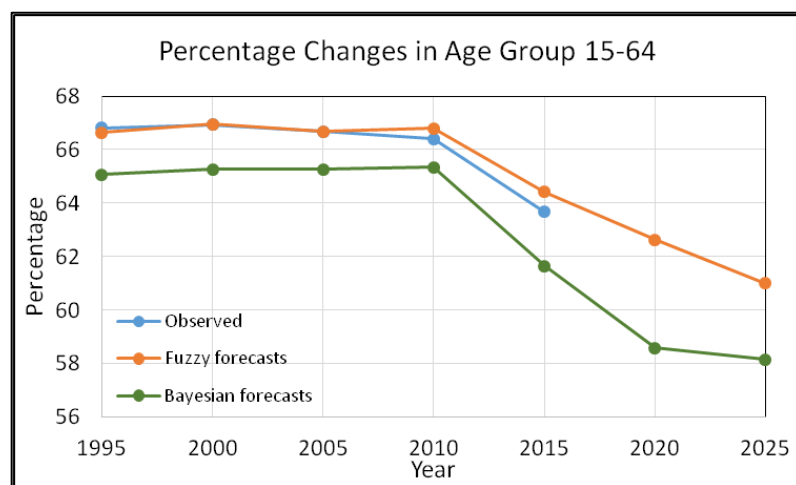


Figure 5.31. Percentage changes in distribution of working-age-population

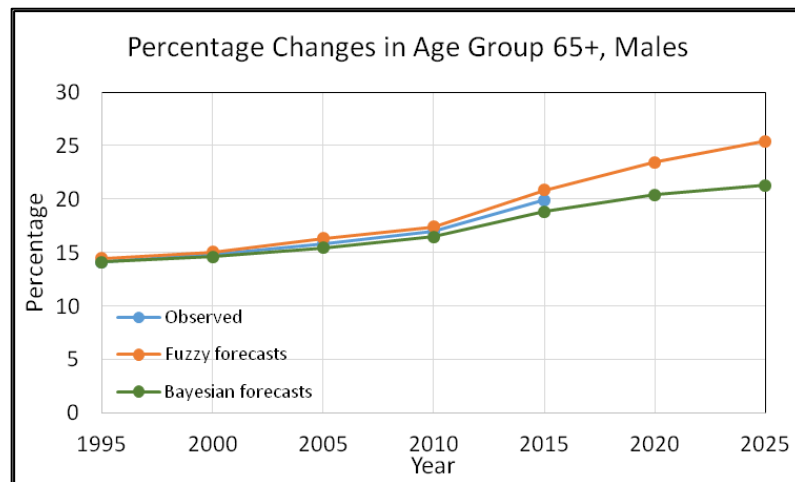


Figure 5.32. Percentage changes in distribution of old-age-population

The changes in percentage distributions of age groups throughout the forecast horizon are also graphically illustrated. For this purpose, the changes in percentage of young-age population, working-age-population, and old-age-population are given in Figure 5.30, Figure 5.31 and Figure 5.32 respectively. From these three figures, it is seen that the percentage distribution of age groups within total population obtained via FMM are consistent with the observed values, whilst there are some over/under-estimations for the BMM outputs as discussed previously.

6. DISCUSSION AND FUTURE PERSPECTIVES

The numerical findings state that the proposed FMM performs better than BMM in modeling and forecasting the future demographic indicators of age-specific mortality, fertility, and migration and results in more accurate future population forecasts that are consistent with the observed population levels values accurately. The application outputs of the proposed FMM method on demographic indicators and future population are discussed in the following sub-sections as well as the further implications of the method for future research.

6.1. ON RESULTS FOR DEMOGRAPHIC COMPONENTS

The proposed FMM method is generating more accurate fits to the observed mortality rates than the existing fuzzy method KSM for both males and females. The main reason for this is the fact that KSM utilizes time t as the independent variable of the regression equation for the fuzzification of the observed mortality rates. However, this results in linearly increasing or decreasing center values and left and right tails for the fuzzified mortality rates. Instead, the proposed FMM makes use of an artificial independent variable named as fuzzification index, whose value is computed via SVD technique. The numerical finding in Section 5.1.2 displays that the assumption on capability of this fuzzification index to capture the fluctuations in mortality data turns out to be true.

The bi-level structure embedded in FMM is assumed to enable the generation of realistic fits to the age-specific demographic indicators, and this assertion is supported through the numerical findings for migration modeling. For mortality and fertility modeling, the utilization of only Level-I, which corresponds to general country profile, turned out to be adequate as the outputs of paired fuzzy sample differences tests suggest. However, in both emigration and immigration modeling the addition of Level-II, which is the age cluster factor, improves the fitting capability of the proposed FMM method as it is illustrated via numerical findings in Section 5.3.

As claimed in Raymer *et al.* [93], cohort patterns are missing in for migration unlike mortality and fertility. That is, the population born in a specific time period exhibit alike

behavior in terms of mortality and fertility patterns throughout time. However, such behavior is unlikely to be observed for the migration case, which may be one of the reasons why a single level model is inadequate to generate accurate fits for immigration and emigration. In fact, the underlying mathematical reason why a single level is adequate for mortality and fertility modeling while a bi-level structure is required for migration modeling can be explained through the ratio of the largest eigenvalues to the sum of all eigenvalues that are extracted in SVD for each demographic indicator. Table 6.1 displays the value of the largest eigenvalue, which is the square of the singular value used in the fuzzification of observed data in Level-I modeling phase and the ratio of this eigenvalue to the sum of all eigenvalues extracted for the data matrix for each demographic indicator. Actually, the ratio given in the last column corresponds to the ratio of variance in data explained via the largest eigenvalue, thus it displays to what extent using a single level captures the variations in data.

Table 6.1. Summary of eigenvalues extracted via SVD in Level-I modeling phase

Demographic indicator	Sex	Largest eigenvalue	Ratio of the largest eigenvalue to the sum of all eigenvalues
Mortality rates	Female	90.09	0.958
	Male	78.91	0.913
Fertility rates	Female	60.63	0.903
Emigration counts	Female	4331907.75	0.831
	Male	3626535.70	0.824
Immigration counts	Female	13189792.94	0.867
	Male	21408472.75	0.870

Actually, based on the paired fuzzy sample differences test results, Level-I is accepted as capable of modeling the observed mortality and fertility rates and immigration counts, whereas a bi-level structure is necessary for modeling emigration counts. The last column in Table 6.1 indicate that the percentages of variance in data explained through the largest

eigenvalue – or the largest singular value which is the square root of the largest eigenvalue – are over 86.7 percent for mortality, fertility and immigration datasets. However, this amount turns out to be relatively small for emigration count data (83.1% for females and 82.4 percent for males). If 90 percent is selected as threshold value, then, it becomes clear why a bi-level structure is necessary for migration modeling. It is also worth mentioning that even for the emigration datasets, the variance explained via the largest eigenvalue can be considered as high, implying that the datasets have regular patterns for the age groups throughout time.

As it is seen in the former section, the inclusion of age group cluster factor in addition to the general country profile enhances the modeling capabilities of the fuzzy method. However, this inclusion may result in expansions in fuzzy intervals as depicted in Figure 5.23 and Figure 5.24, even though the utilization of T_w based addition and multiplication prevents the uniform accumulation of fuzziness. When the natural logarithms of migration values are transformed back into their usual values by taking their exponentials, the above mentioned issue may lead to over-predictions in the upper bounds of the fuzzy intervals.

When compared to the existing BMM, the success of both FMM in modeling and forecasting the demographic indicators for Finland can be clearly seen in Section 5.1 to Section 5.3. This is mainly due to minimum fuzziness criterion embedded in FMM which aims to cover the observed data within the possible smallest fuzzy interval. The numerical findings demonstrate that the Bayesian prediction intervals are significantly wider than the fuzzy forecast intervals, yet they cover less actual data.

The superiority of FMM over BMM in both modeling and forecasting may be the consequence of integrating fuzzy modeling with Bayesian inference. The hybridization of fuzzy and Bayesian concepts enable the explanation of uncertainty through fuzziness and randomness, which seems to perform better than relating the uncertainty to only randomness as BMM does.

6.2. ON POPULATION FORECASTS

The population forecasts obtained via aggregating the fuzzy mortality, fertility and migration estimates of FMM indicate a slight increase in the current population levels of

Finland for the year 2025 which is consistent with the trend followed by the historic data. The existing BMM also results in an increase in the 2025 population levels; however, it seems to overforecast the possible values. This is mainly due to the more accurate point forecasts and narrower forecast intervals obtained via FMM for the demographic indicators. Thus, the population forecasts of FMM can be viewed as more informative compared to that of BMM. Furthermore, deterministic projections for 2025 points out a population of approximately 5.6 million for Finland [149]. This projection result supports the efficient performance of FMM, which generates a point forecast of approximately 5.5 million for the year 2025 with a fuzzy interval ranging in between 5.1 million and 6.1 million.

The main uncertainties in the population forecasts are concentrated in the [0,5) age group for the year 1995 as observed in FMM outputs in Figure 5.26. However, as illustrated in Figure 5.28, the fuzzy intervals for the age groups [0,5) to [20,25) widens significantly. This can be explained as the relatively high fuzziness for the fertility rate forecasts, which results in uncertainties in the number of births. From 1995 to 2025, more uncertainty is added in number of newborns and these uncertainties are transferred to the next age groups in each five-year time interval.

Another important insight that can be obtained from the population forecasts is that the Finnish population continues to get older. This may result in socioeconomic problems as more old-age-population implies more dependency on working-age-population. As well as this, the decrease in the percentage of young-age-population will lead to negative natural growth of population, that is, the population of Finland may not increase or be maintained in its current level without a significant amount of immigration to the country in the upcoming years. However, the numerical findings reveal that although number of immigrants exceeds the number of emigrants for Finland, the net migration levels are still low compared to other European countries. If this trend maintains in the upcoming years, a decrease in population growth for Finland may become inevitable.

6.3. FURTHER RESEARCH AREAS

The forecasting scheme followed in this study is integrating the fuzzy modeling with a Bayesian approach, and the forecast accuracies are depending on the prior beliefs related to the distributions of model parameters. However, the MCMC algorithm used in estimations assumes a rather weak dependency to the past observations as the number of iterations in the simulation grows and the prior beliefs start to lose their impacts on the posterior distributions of the model parameters as the model converges. In addition to the prior beliefs driven by the data, judgments of a group of experts can also be elicited in determination of prior distributions for the model parameters in following studies.

The ultimate model selection in forecasting future time-variant fuzzy parameters is based on posterior odds criterion, however, it is worth mentioning that there are several other selection approaches. The posterior odds criterion is assumed to be a data-driven technique and commonly used in migration forecasting. Among the model selection methods, *deviance information criterion* or *inference pooling* [143] may be alternative approaches.

In a recent report by OECD [150], it is argued that quantitative analysis based on historic observations frequently ignores cannot reflect the impacts of unpredictable events which results in the necessity of combining such models with qualitative scenarios. As a matter of fact, although the general socio-economic profile of the country of concern and the response of age cohorts in migration behaviors are represented in FMM, the proposed FMM strictly relies on historic observations. The model does not include an explanatory variable standing for an extreme major event such as war, natural disaster, or an unpredictable economic depression which may influence migration behaviors of individuals directly. However, prediction of such sudden events is almost impossible or too complex and requires hybrid approaches that combine quantitative models with deterministic scenarios.

To examine the impacts of such exogenous effects through fuzzy what-if scenarios, Equ. (4.11) is modified as:

$$\tilde{Y}_{x,t} = [\tilde{A}_x \oplus_{T_w} \tilde{B}_x \otimes_{T_w} \tilde{K}_t] \oplus_{T_w} \tilde{C}_{i,x,t} \oplus_{T_w} \tilde{E}_{x,t} \quad (6.1)$$

where $\tilde{E}_{x,t}$ is the fuzzy age and time specific exogenous factor that represents the effect of extreme deviations from the historic trends of determinants of migration on age cohort behaviors. The inclusion of such exogenous variables to the model may provide insights in evaluating what-if scenarios. In this study, this exogenous factor is set to be zero, which corresponds to a scenario in which the deviations from the historic trends for determinants of migration are insignificantly small.

Even with such efforts, the inherent uncertainty about future migration values cannot be decreased due to the multi-dimensional aspects in migration phenomenon. However, stating the level of uncertainty in future forecasts are vital in socioeconomic decision making regarding migration behaviors, thus it should not be ignored in modeling migration.

As a future study, the impacts of this fuzzy exogenous factor in modeling and forecasting age-specific migration values can be analyzed through several scenarios for the near future. Moreover, a complete fuzzy population estimation method which models age-and-sex-specific mortality, fertility and migration and forecasts the future values through fuzzy forecasting techniques instead of Bayesian inference can be developed. Such kind of a study would eliminate the statistical assumptions of Bayesian forecasting. FMM can also be modified by including the second and/or third singular values and their corresponding eigenvectors to diminish the discrepancies between the actual and the estimated migration values. However, inclusion of more singular values increases the number of fuzzy parameters in unconstrained nonlinear optimization model, which may result in inefficiencies in estimating these parameters.

The proposed FMM involves some constraints to ensure model identifiability while computing the fuzzy parameters via SVD. Recently, there are several studies on the model identifiability issue as discussed in Mitchell *et al.* [29] and Beutner *et al.* [133]. The analysis of different model identifiability constraints or efforts to remove the dependency of the method on these constraints may be interesting research topics.

The dimension reduction idea embedded in FMM, which corresponds to the representation of observed demographic indicators through their largest singular value and its associated eigenvectors can be extended to other disciplines. Here, demographic modeling of

mortality, fertility, and migration is implemented on the age-time structure of the data. The proposed FMM can be assumed to perform well on any kind of data expressed as two dimensions if the data display regularities for one of the dimensions over the other like the regularities in demographic rates of age groups over time. Such application areas may be energy consumptions by energy type over time, currency parities, and basic statistics expressed as space and time and etc.

Last but not least, the computational performance of the proposed FMM may be compared for different software utilizations as a further research. In this study, the modeling of observed demographic indicators of mortality, fertility, and migration are accomplished through GAMS and MATLAB software; while the future values are forecasted using OpenBUGS software. The implementation of the FMM method in R, which is becoming popular for demographic analysis, may enable the comparison of the computational efficiencies of these softwares in population modeling and forecasting.

7. CONCLUSION

In this study, a fuzzy bi-level method for modeling age-specific demographic indicators (FMM) is proposed. The demographic indicators to be modeled and forecasted are age-specific mortality and fertility rates in addition to emigration and immigration counts. The proposed method extends the existing fuzzy mortality modeling method by incorporating two explanatory factors accompanied by implementation of singular value decomposition, fuzzy regression and unconstrained nonlinear optimization. The future migration values are forecasted using time series models based on a Bayesian approach. Moreover, the future population levels are forecasted through a fuzzy aggregation model in which the fuzzy forecasts for age-specific mortality, fertility and migration values are used.

The demographic indicators are modeled through a fuzzy technique due to inconsistent demographic data associated with under/over recordings and data collection errors. Such issues result in ambiguities and vagueness in population modeling and forecasting. Therefore, the mortality, fertility, migration and population values are expressed as fuzzy numbers to include the inherent uncertainty within the data.

The first level of FMM reflects the general characteristics of the country of concern; while the second level is dedicated to cluster impacts on age-group demographic behaviors. In the second level of FMM, age groups are clustered into classes such that the age groups in a single class possess similar demographic patterns through time; whereas distinct classes display diverse characteristics. This bi-level structure enables the model to capture the fluctuations and nonlinear patterns in demographic components.

The proposed FMM is applied to Finland mortality, fertility, emigration, and immigration data. The mortality and fertility datasets that are used in modeling consist of rates for twelve five-year time periods of 1940-1944 to 1995-1999. Mortality rates are expressed for females and males while fertility rates are provided for only females. Emigration and immigration datasets include annual counts for 1990-2010 period for females and males separately. The numerical findings show that the FMM gives reasonable fits to the observed data by generating small errors. The mortality and fertility rates for the time periods of 2000-2004 to 2020-2024 and migration values for years 2011 to 2024 are forecasted via fitting time series models on time-variant parameters through Bayesian

approach. Modeling and forecasting results are compared with the outcomes of the existing Bayesian method of Wiśniowski *et al.* [17]. The numerical findings display that the proposed fuzzy method generates more accurate point forecasts than the Bayesian approach. In addition, the proposed FMM covers more actual observations within its fuzzy interval than the prediction interval of the Bayesian method. Similarly the population forecasts obtained via aggregating the mortality, fertility, and migration forecasts of FMM for the years 1995 to 2025 exhibit more consistent patterns to the actual population trends in terms both level and age distribution when compared to the BMM. The outcomes of this study has been published in a research article [151], a proceedings paper [152], and two book chapters [153,154].

The main contribution of this study is that it shows that fuzzy modeling can be an efficient approach in demographic analysis and population modeling and forecasting. Furthermore, the bi-level structure embedded in the proposed method makes it possible to capture the strong correlations among some age groups in exhibiting similar demographic patterns. This two stage model is necessary to capture the nonlinearities in demographic patterns, especially for migration. The fuzzy model outputs are combined with Bayesian inference for forecasting future demographic values and population, so that the inherent uncertainties are explained through both fuzziness and randomness.

REFERENCES

1. Keyfitz N. *Applied mathematical demography*. New York: Wiley; 1977.
2. Hyndman RJ, Ullah MS. Robust forecasting of mortality and fertility rates: A functional data approach. *Computational Statistics and Data Analysis*. 2007;51(10):4942–56.
3. United Nations. *Manual VIII: Methods for projections of urban and rural population*. Department of Economic and Social Affairs, Population Studies, 55. New York: United Nations Publishing; 1974.
4. Lindh T. Demography as a forecasting tool. *Futures*. 2003;35(1):37–48.
5. Ahmadi SS, Li JSH. Coherent mortality forecasting with generalized linear models: A modified time-transformation approach. *Insurance: Mathematics and Economics*. 2014;59:194–221.
6. Danesi IL, Haberman S, Millosovich P. Forecasting mortality in subpopulations using Lee–Carter type models: A comparison. *Insurance: Mathematics and Economics*. 2015;62:151–61.
7. French D. International mortality modelling—An economic perspective. *Economics Letters*. 2014;122(2):182–6.
8. Caimei L, Yonghong H, Xuemeng W. China's population projections based on GM(1,1) metabolic model. *Kybernetes*. 2009;38(3–4):417–25.
9. Rowland DT. *Demographic methods and concepts*. Oxford, NY: Oxford University Press; 2003.
10. Bijak J. *Forecasting international migration: selected theories, models, and methods*. Warsaw: Central European Forum For Migration Research; 2006.
11. Booth H. Demographic forecasting: 1980 to 2005 in review. *International Journal of Forecasting*. 2006;22(3):547–81.

12. Cairns AJG, Blake D, Dowd K. Modelling and management of mortality risk: a review. *Scandinavian Actuarial Journal*. 2008;(2–3):79–113.
13. Shang HL. Selection of the optimal Box–Cox transformation parameter for modelling and forecasting age-specific fertility. *Journal of Population Research*. 2015;32(1):69–79.
14. Stoeldraijer L, van Duin C, van Wissen LJ, Janssen F. Impact of different mortality forecasting methods and explicit assumptions on projected future life expectancy: The case of the Netherlands. *Demographic Research*. 2013;29:323–54.
15. Lee RD, Carter LR. Modeling and forecasting U.S. mortality. *Journal of the American Statistical Association*. 1992;87(419):659–71.
16. Koissi M-C, Shapiro AF. Fuzzy formulation of the Lee–Carter model for mortality forecasting. *Insurance: Mathematics and Economics*. 2006;39(3):287–309.
17. Wiśniowski A, Smith PWF, Bijak J, Raymer J, Forster JJ. Bayesian population forecasting: Extending the Lee-Carter method. *Demography*. 2015;52(3):1035–59.
18. Lee RD, Miller T. Evaluating the performance of the Lee-Carter method for forecasting mortality. *Demography*. 2001;38(4):537–49.
19. Booth H, Maindonald J, Smith LEN. Population investigation committee applying Lee-Carter under conditions of variable mortality decline. *Population Studies*. 2002;56(3):325–36.
20. Lee R. The Lee-Carter method for forecasting mortality, with various extensions and applications. *North American Actuarial Journal*. 2000;4(1):80–91.
21. Renshaw AE, Haberman S. Lee-Carter mortality forecasting with age-specific enhancement. *Insurance: Mathematics and Economics*. 2003;33(2):255–72.
22. Renshaw AE, Haberman S. A cohort-based extension to the Lee-Carter model for mortality reduction factors. *Insurance: Mathematics and Economics*. 2006;38(3):556–70.

23. Russolillo M, Giordano G, Haberman S. Extending the Lee–Carter model: a three-way decomposition. *Scandinavian Actuarial Journal*. 2011;2011(2):96–117.
24. Debón A, Montes F, Martínez-Ruiz F. Statistical methods to compare mortality for a group with non-divergent populations: an application to Spanish regions. *European Actuarial Journal*. 2011;1(2):291–308.
25. Li N, Lee RD. Coherent mortality forecasts for a group of populations: An extension of the Lee-Carter method. *Demography*. 2005;42(3):575–94.
26. Li JS-H, Hardy MR. Measuring basis risk in longevity hedges. *North American Actuarial Journal*. 2011;15(2):177–200.
27. Dowd K, Cairns AJG, Blake D, Coughlan GD, Khalaf-Allah M. A gravity model of mortality rates for two related populations. *North American Actuarial Journal*. 2011;15(2):334–56.
28. De Jong P, Tickle L. Extending Lee-Carter mortality forecasting. *Mathematical Population Studies*. 2006;13(1):1–18.
29. Mitchell D, Brockett P, Mendoza-Arriaga R, Muthuraman K. Modeling and forecasting mortality rates. *Insurance: Mathematics and Economics*. 2013;52(2):275–85.
30. Cairns AJG, Blake D, Dowd K. A two-factor model for stochastic mortality with parameter uncertainty: Theory and calibration. *Journal of Risk and Insurance*. 2006;73(4):687–718.
31. Plat R. On stochastic mortality modeling. *Insurance: Mathematics and Economics*. 2009;45(3):393–404.
32. Haberman S, Renshaw A. A comparative study of parametric mortality projection models. *Insurance: Mathematics and Economics*. 2011 Jan;48(1):35–55.
33. Rueda C, Rodríguez P. State space models for estimating and forecasting fertility. *International Journal of Forecasting*. 2010 Oct;26(4):712–24.

34. Alho JM, Spencer BD. *Statistical demography and forecasting*. New York: Springer-Verlag; 2005.
35. Shang HL. Point and interval forecasts of age-specific life expectancies: A model averaging approach. *Demographic Research*. 2012;27:593–644.
36. Box GEP, Jenkins GM, Reinsel GC, Ljung GM. *Time series analysis: Forecasting and control*. 5th ed. Hoboken, New Jersey: John Wiley and Sons, Inc.; 2015.
37. Gupta A, Pasupuleti SSR. A new behavioural model for fertility schedules. *Journal of Applied Statistics*. 2013;40(9):1921–30.
38. Hoem JM, Madsen D, Nielsen JL, Ohlsen E-M, Hansen HO, Rennermalm B. Experiments in modelling recent Danish fertility curves. *Demography*. 1981;18(2):231–44.
39. George MV, Smith SK, Swanson DA, Tayman J. Population projections. *The methods and materials of demography*. 2nd Edition. San Diego: Elsevier Academic Press; 2004:561–601.
40. De Iaco S, Maggio S. A dynamic model for age-specific fertility rates in Italy. *Spatial Statistics*. 2016;17:105–20.
41. Gilje E. Fitting curves to age-specific fertility rates: some examples. *Statistical Review of the Swedish National Central Bureau of Statistics III*. 1969;7:118–34.
42. De Beer J. A new relational method for smoothing and projecting age-specific fertility rates: TOPALS. *Demographic Research*. 2011;24:409–54.
43. Chandola T, Coleman DA, Hiorns RW. Recent European fertility patterns: Fitting curves to ‘distorted’ distributions. *Population Studies*. 1999;53(3):317–29.
44. Coale AJ, Trussell TJ. Model fertility schedules: Variations in the age structure of childbearing in human populations. *Population Index*. 1974;40(2):185–258.
45. Peristera P, Kostaki A. Modeling fertility in modern populations. *Demographic Research*. 2007;16(6):141–94.

46. Gompertz B. On the nature of the function expressive of the law of human mortality, and on a new mode of determining the value of life contingencies. *Philosophical Transactions of the Royal Society of London*. 1825;115:513–83.
47. Goldstein J. A behavioral Gompertz model for cohort fertility schedules in low and moderate fertility populations. *MPIDR Working Papers*. 2010;49:1–20.
48. Brass W. Perspectives in population prediction: Illustrated by the statistics of England and Wales. *Journal of the Royal Statistical Society A*. 1974;137(4):532–83.
49. Yi Z, Zhenglian W, Zhongdong M, Chunjun C. A simple method for projecting or estimating and β : An extension of the brass relational Gompertz fertility model. *Population Research and Policy Review*. 2000;19(6):525–49.
50. McNeil DR, Trussell TJ, Turner JC. Spline interpolation of demographic data. *Demography*. 1977;14(2):245–52.
51. Hoem JM, Rennermalm B. On the statistical theory of graduation by splines. University of Copenhagen, Laboratory of Actuarial Mathematics. Working Paper No 14; 1978.
52. Schmertmann CP. A system of model fertility schedules with graphically intuitive parameters. *Demographic Research*. 2003;9:81–110.
53. Kostaki A, Moguerza J, Olivares A, Psarakis S. Graduating the age-specific fertility pattern using support vector machines. *Demographic Research*. 2009;20:599–622.
54. Rueda-Sabater C, Alvarez-Esteban P. The analysis of age-specific fertility patterns via logistic models. *Journal of Applied Statistics*. 2008;35(9):1053–70.
55. Durbin J, Koopman SJ. *Time series analysis by state-space models*. Oxford: Oxford University Press; 2001.
56. Nasir JA, Tahir MH, Riaz M. Measuring and modeling the fertility profile of indigenous people in Pakistan: A study of the Arians. *Pakistan Journal of Commerce and Social Sciences*. 2010;4(2):132–46.

57. Lee RD, Tuljapurkar S. Stochastic population forecasts for the United States: Beyond high, medium, and low. *Journal of the American Statistical Association*. 1994;89(428):1175–89.
58. Ramsay JO, Silverman BW. *Functional data analysis*. New York: Springer-Verlag; 2005.
59. Chen K, Delicado P, Müller HG. Modelling function-valued stochastic processes, with applications to fertility dynamics. *Journal of the Royal Statistical Society Series B: Statistical Methodology*. 2017;79(1):177–96.
60. Pantazis A, Clark SJ. A parsimonious characterization of change in global age-specific and total fertility rates. *PLOS ONE*. 2018;13(1):1–19.
61. Bernard A, Bell M. Smoothing internal migration age profiles for comparative research. *Demographic Research*. 2015;32:915–48.
62. Raymer J, Wiśniowski A. Applying and testing a forecasting model for age and sex patterns of immigration and emigration. *Population Studies*. 2018;1–17.
63. Rogers A, Raquillet R, Castro LJ. Model migration schedules and their applications. *Environment and Planning A: Economy and Space*. 1978;10(5):475–502.
64. Rees PH. *Migration and settlement*. Laxenburg: International Institute for Applied Systems Analysis; 1979.
65. Rogers A, Castro LJ. *Model migration schedules*. Laxenburg: International Institute for Applied Systems Analysis; 1981.
66. Bates J, Bracken I. Estimation of migration profiles in England and Wales. *Environment and Planning A*. 1982;14(7):889–900.
67. Wilson T. Model migration schedules incorporating student migration peaks. *Demographic Research*. 2010;23:191–222.
68. Rogers A, Watkins J. General versus elderly interstate migration and population redistribution in the United States. *Research on Aging*. 1987;9(4):483–529.

69. Rogers A, Jones B. Inferring directional migration propensities from the migration propensities of infants in the United States. *Mathematical Population Studies*. 2008;15(3):182–211.
70. Rogers A, Jones B, Ma W. *Repairing the migration data reported by the American Community Survey*. Boulder: University of Colorado at Boulder, Institute of Behavioral Science; 2008.
71. Ishikawa Y. Migration turnarounds and schedule changes in Japan, Sweden and Canada. *Review of Urban and Regional Development Studies*. 2001;13(1):20–33.
72. Rees P. Projecting the national and regional populations of the European Union using migration information. *International migration in Europe: Data, models and estimates*. Chichester: Wiley; 1996:175–92.
73. Rogers A. Parameterized multistate population dynamics and projections. *Journal of the American Statistical Association*. 1986;81(393):48–61.
74. Congdon P. Statistical graduation in local demographic analysis and projection. *Journal of the Royal Statistical Society Series A (Statistics in Society)*. 1993;156(2):237–70.
75. Rogers A, Castro LJ, Lea M. Model migration schedules: Three alternative linear parameter estimation methods. *Mathematical Population Studies*. 2005;12(1):17–38.
76. Rees P, Bell M, Dukw-Williams O, Blake M. Problems and solutions in the measurement of migration intensities: Australia and Britain compared. *Population Studies*. 2000;54(2):207–22.
77. Bernard A, Bell M, Charles-Edwards E. Improved measures for the cross-national comparison of age profiles of internal migration. *Population Studies*. 2014;68(2):179–95.
78. Pagan A, Ullah A. *Nonparametric econometrics*. Cambridge: Cambridge University Press; 1999.
79. Rogers A, Little J, Raymer J. *The indirect estimation of migration: methods for*

- dealing with irregular, inadequate, and missing data*. Dordrecht: Springer; 2010.
80. Carter DB, Signorino CS. Back to the future: Modeling time dependence in binary data. *Political Analysis*. 2010;18(3):271–92.
 81. Ruppert D, Wand MP, Carroll RJ. *Semiparametric regression*. Cambridge: Cambridge University Press; 2003.
 82. Beck N, Katz JN, Tucker R. Taking time seriously: Time-series-cross-section analysis with a binary dependent variable. *American Journal of Political Science*. 1998;42(4):1260–88.
 83. Sharef E, Strawderman RL, Ruppert D, Cowen M, Halasyamani L. Bayesian adaptive B-spline estimation in proportional hazards frailty models. *Electronic Journal of Statistics*. 2010;4:606–42.
 84. Peristera P, Kostaki A. An evaluation of the performance of kernel estimators for graduating mortality data. *Journal of Population Research*. 2005;22(2):185–97.
 85. Moguerza JM, Olivares A, Kostaki A, Psarakis S. Comparing smoothing techniques on fertility data. *2010 Ninth Mexican International Conference on Artificial Intelligence*; 2010: IEEE.
 86. Marron JS, Nolan D. Canonical kernels for density estimation. *Statistics and Probability Letters*. 1988;7(3):195–9.
 87. Rogers A, Raymer J, Willekens F. Capturing the age and spatial structures of migration. *Environment and Planning A*. 2002;34(2):341–59.
 88. Raymer J, Bonaguidi A, Valentini A. Describing and projecting the age and spatial structures of interregional migration in Italy. *Population, Space and Place*. 2006;12(5):371–88.
 89. Raymer J, Rogers A. Using age and spatial flow structures in the indirect estimation of migration streams. *Demography*. 2007;44(2):199–223.
 90. Rogers A, Raymer J, Willekens F. Imposing age and spatial structures on inadequate

- migration-flow datasets. *The Professional Geographer*. 2003;55(1):56–69.
91. Azose JJ, Raftery AE. Bayesian probabilistic projection of international migration. *Demography*. 2015;52(5):1627–50.
 92. Wiśniowski A, Forster JJ, Smith PWF, Bijak J, Raymer J. Integrated modelling of age and sex patterns of European migration. *Journal of the Royal Statistical Society: Series A (Statistics in Society)*. 2016;179(4):1007–24.
 93. Raymer J, Wiśniowski A, Smith PWF, Bijak J. *Applying and extending the Lee-Carter model to forecast migration*. Southampton: ESRC Centre for Population Change, University of Southampton; 2012.
 94. Nawrotzki R, Jiang L. *Community demographic model international migration (CDM-IM) dataset : Generating age and gender profiles of international migration flows*. Boulder: National Center for Atmospheric Research; 2014.
 95. Smith SK. Accounting for migration in cohort-component projections of state and local populations. *Demography*. 1986;23(1):127.
 96. Isserman AM. The right people, the right rates: Making population estimates and forecasts with an interregional cohort-component model. *Journal of the American Planning Association*. 1993;59(1):45–64.
 97. Billari FC, Graziani R, Melilli E. Stochastic population forecasts based on conditional expert opinions. *Journal of the Royal Statistical Society Series A: Statistics in Society*. 2012;175(2):491–511.
 98. KC S, Barakat B, Goujon A, Skirbekk V, Lutz W. Projection of populations by level of educational attainment, age, and sex for 120 countries for 2005-2050. *Demographic Research*. 2010;22:383–472.
 99. Jackson N, Cameron M, Cochrane B. *2014 Review of demographic and labour force projections for the Waikato region for the period 2013 - 2063*. Hamilton, New Zealand: Commissioned Report. University of Waikato, National Institute of Demographic and Economic Analysis; 2014.

100. Nowatzki J, Moller B, Demers A. Projection of future cancer incidence and new cancer cases in Manitoba, 2006-2025. *Chronic Diseases in Canada*. 2011;31(2):71–8.
101. Wu JM, Kawasaki A, Hundley AF, Dieter AA, Myers ER, Sung VW. Predicting the number of women who will undergo incontinence and prolapse surgery, 2010 to 2050. *American Journal of Obstetrics and Gynecology*. 2011;205(3):230.e1-230.e5.
102. United Nations. *Manuel X: Indirect techniques for demographic estimation*. New York: Department of International Economic and Social Affairs, Population Studies, United Nations Publication; 1983.
103. China Population and Development Research Center. Development history of PADIS-INT [cited 2016 20 September]. 2011. Available from: <http://www.padis-int.org/index.php?c=main&a=view&id=124&lan=en>
104. China Population and Development Research Center. *User guide: PADIS-INT: A web-based software for population projections version 1.0*. Digital China Co.; 2011.
105. Stover J, Kirmeyer S. *DemProj manual: A computer program for making population projections*. Atlanta: US Agency for International Development; 2007.
106. Booth H. Demographic forecasting: 1980 to 2005 in review. *International Journal of Forecasting*. 2006;22(3):547–81.
107. Özden Ç, Parsons CR, Schiff M, Walmsley TL. Global bilateral migration database, where on earth is everybody? The evolution of global bilateral migration, 1960-2000. *World Bank Economic Review*. 2011;25(1):12–56.
108. De Beer J, Raymer J, van der Erf R, van Wissen L. Overcoming the problems of inconsistent international migration data: A new method applied to flows in Europe. *European Journal of Population / Revue européenne de Démographie*. 2010;26(4):459–81.
109. Henning S, Hovy B. Data sets on international migration. *International Migration Review*. 2011;45(4):980–5.

110. Raymer J, de Beer J, van der Erf R. Putting the pieces of the puzzle together: Age and sex-specific estimates of migration amongst countries in the EU/EFTA, 2002–2007. *European Journal of Population / Revue européenne de Démographie*. 2011;27(2):185–215.
111. Abel GJ. Estimation of international migration flow tables in Europe. *Journal of the Royal Statistical Society Series A: Statistics in Society*. 2010;173(4):797–825.
112. Wilson T, Bell M. Australia's uncertain demographic future. *Demographic Research*. 2004;11:195–234.
113. Bijak J, Wiśniowski A. Bayesian forecasting of immigration to selected European countries by using expert knowledge. *Journal of the Royal Statistical Society: Series A (Statistics in Society)*. 2010;173(4):775–96.
114. Yang S, Xiong F, Wang F. Polynomial chaos expansion for probabilistic uncertainty propagation. *Uncertainty Quantification and Model Calibration*. 2017;13–47.
115. Chamberlain J, Gill B. Fertility and mortality. *Focus on people and migration*. Basingstoke: Palgrave Macmillan; 2005:71–89.
116. Nargund G. Declining birth rate in developed countries: A radical policy re-think is required. *Facts, Views and Vision in ObGyn*. 2009;1(3):191–3.
117. Härdle WK, Myšičková A. *Stochastic population forecast for Germany and its consequence for the German pension system*. SFB 649 Discussion Paper 2009–009. 2009;
118. García-Guerrero VM. A probabilistic method to forecast the international migration of Mexico by age and sex. *Papeles de Población*. 2016;22(88):113–40.
119. Yang D. Singular value decomposition for high dimensional data. Publicly Accessible Penn Dissertations. 595; 2012.
120. Zimmermann H-J. *Fuzzy set theory and its applications*. 3rd Edition. Boston: Kluwer Academic Publishers; 1996.

121. Zadeh LA. Fuzzy sets. *Information and Control*. 1965;8(3):338–53.
122. Hong DH. Shape preserving multiplications of fuzzy numbers. *Fuzzy Sets and Systems*. 2001;123(1):81–4.
123. Kumar M. Applying weakest t-norm based approximate intuitionistic fuzzy arithmetic operations on different types of intuitionistic fuzzy numbers to evaluate reliability of PCBA fault. *Applied Soft Computing*. 2014;23:387–406.
124. Shapiro AF. Fuzzy logic in insurance. *Insurance: Mathematics and Economics*. 2004;35(2):399–424.
125. Lin K-P, Wen W, Chou C-C, Jen C-H, Hung K-C. Applying fuzzy GERT with approximate fuzzy arithmetic based on the weakest t-norm operations to evaluate repairable reliability. *Applied Mathematical Modelling*. 2011;35(11):5314–25.
126. Diamond P. Fuzzy least squares. *Information Sciences*. 1988;46(3):141–57.
127. Leekwijck W Van, Kerre EE. Defuzzification: criteria and classification. *Fuzzy Sets and Systems*. 1999;108(2):159–78.
128. Golub GH, Reinsch C. Singular value decomposition and least squares solutions. *Handbook for automatic computation*. Berlin, Heidelberg: Springer Berlin Heidelberg; 1971:134–51.
129. Ahcan A, Medved D, Olivieri A, Pitacco E. Forecasting mortality for small populations by mixing mortality data. *Insurance: Mathematics and Economics*. 2013;54(1):12–27.
130. Lee R. The Lee-Carter method for forecasting mortality, with various extensions and applications. *North American Actuarial Journal*. 2000;4(1):80–91.
131. O. Chang Y-H, M. Ayyub B. Fuzzy regression methods – a comparative assessment. *Fuzzy Sets and Systems*. 2001;119(2):187–203.
132. Mandel J. Use of the singular value decomposition in regression analysis. *The American Statistician*. 1982;36(1):15–24.

133. Beutner E, Reese S, Urbain J-P. Identifiability issues of age–period and age–period–cohort models of the Lee–Carter type. *Insurance: Mathematics and Economics*. 2017;75:117–25.
134. Tanaka H, Uejima S, Asai K. Linear regression analysis with fuzzy model. *IEEE Transactions on Systems, Man, and Cybernetics*. 1982;12(6):903–7.
135. Agrawal S, Singh D. Modified Nelder-Mead self organizing migrating algorithm for function optimization and its application. *Applied Soft Computing Journal*. 2017;51:341–50.
136. Bazaraa MS, Jarvis JJ, Sherali HD. *Linear programming and network flows*. 2nd Edition. New York: John Wiley; 1990.
137. Mathews JH, Fink KD. *Numerical methods using MATLAB*. 4th Edition. New Jersey: Prentice Hall Inc.; 2004.
138. Pandi M, Premalatha K. An advanced Nelder Mead simplex method for clustering of gene expression dataTitle. *International Scholarly and Scientific Research and Innovation*. 2014;8(4):652–60.
139. Gao F, Han L. Implementing the Nelder-Mead simplex algorithm with adaptive parameters. *Computational Optimization and Applications*. 2012;51(1):259–77.
140. Li G, Wang Y, Zhang L, Zhu X. Similarity measure for time series based on piecewise linear approximation. *Wireless Communications and Signal Processing, 2009 IEEE International Conference on*; 2009: IEEE.
141. Li H, Guo C, Qiu W. Similarity measure based on piecewise linear approximation and derivative dynamic time warping for time series mining. *Expert Systems with Applications*. 2011;38(12):14732–43.
142. Keilman N, Pham DQ, Hetland A. *Norway's uncertain demographic future*. Oslo: Statistics Norway; 2001.
143. Hoeting JA, Madigan D, Raftery AE, Volinsky CT. Bayesian model averaging : A tutorial. *Statistical Science*. 1999;14(4):382–417.

144. Bijak J. *Forecasting international migration in Europe: A Bayesian view*. Dordrecht: Springer Netherlands; 2011.
145. United Nations Development Programme. Human development reports 2018 [cited 2019 25 Mar]. Available from: <http://hdr.undp.org/en/composite/HDI>
146. Liu S-T, Kao C. Fuzzy measures for correlation coefficient of fuzzy numbers. *Fuzzy Sets and Systems*. 2002;128(2):267–75.
147. Tsai C-C, Chen C-C. Tests of quality characteristics of two populations using paired fuzzy sample differences. *The International Journal of Advanced Manufacturing Technology*. 2006;27(5–6):574–9.
148. De Beer J, Alders M. Probabilistic population and household forecasts for the Netherlands. *European Population Conference EPC99*. 1999.
149. World Population Review. Finland population 2018 [cited 2018 31 Jul]. Available from: <http://worldpopulationreview.com/countries/finland/>
150. OECD. Four possible scenarios for international migration in 2030. *Perspectives on global development 2017: International migration in a shifting world*. Paris: OECD Publishing; 2016:47–73.
151. Demirel DF, Basak M. A fuzzy bi-level method for modeling age-specific migration. *Socio-Economic Planning Sciences*. 2018 (in publication).
152. Demirel DF, Basak M. A modified fuzzy Lee-Carter method for modeling human mortality. *Computational Intelligence, Proceedings of the 7th International Joint Conference on*; 2015: IJCCI.
153. Demirel DF, Basak M. Human mortality modeling with a fuzzy approach based on singular value decomposition technique. *Computational Intelligence*. 2017:197-215.
154. Demirel DF, Basak M. Migration modeling via higher order singular value decomposition. *International migration and challenges in the beginning of the twenty-first century*. London: Lexington Books; 2018:55–66.

APPENDIX A: GAMS CODE FOR SPREAD OPTIMIZATION

GAMS code used in finding the spread values in fuzzification of observed mortality rates for age 0 for females is given in this section. This code is used for computing the spread values for mortality and fertility rates as well as emigration and immigration counts of the remaining age and sex groups by changing the input data (observed demographic values, center value parameters, fuzzification indices) and time indices. The code is as follows:

Sets

i coefficients /1*2/

t time /1*17/

;

Parameters

y(t) log-mortality rates

/

1 -2.459426055

2 -2.668185465

3 -2.754026079

4 -2.798883417

5 -2.954436791

6 -3.464424763

7 -3.758186661

8 -4.056124349

9 -4.320743406

10 -4.572896625

11 -4.861095227

12 -5.131786496

13 -5.229911334

14 -5.364457169

15 -5.655278066

16 -5.886024035

17 -5.976772998

/

f(t) fuzzification index

/

1 23.62925483

2 21.67365062

3 19.96030697

4 19.92090337

5 14.56363877

6 6.616790063

7 2.52052295

8 -0.446221994

9 -1.847948497

10 -4.792391756

11 -8.804097846

12 -12.32792987

13 -12.73662699

14 -13.61539946

15 -16.09221047

16 -18.36402556

17 -19.85821513

/

c(i) regression coefficients

/

1 -4.230156408

2 0.079654563

/

;

scalar

h

/

0

/

;

Variable

```

z    total spread
;
Positive Variables
s(i)  spread of coefficient i
;
Equations
obj
equ1(t)
equ2(t)
*equ3(t)
;
obj..z=e=17*(s("1"))+(s("2"))*sum(t,abs(f(t)));
equ1(t)..c("1")+c("2")*f(t)+(1-h)*(s("1")+s("2")*abs(f(t)))=g=y(t);
equ2(t)..c("1")+c("2")*f(t)-(1-h)*(s("1")+s("2")*abs(f(t)))=l=y(t);
*equ3(t)..s("1")+s("2")*f(t)=g=0;
model projea /all/
option optcr=0.0;
solve projea using lp minimizing z;
display z.l, s.l;

```


APPENDIX B: MATLAB FUNCTION FOR NM ALGORITHM

MATLAB function representing the unconstrained nonlinear optimization problem to be minimized via NM Simplex algorithm for female emigration counts is given in this section. This function is also utilized in estimating the fuzzy parameters for the remaining demographic indicators by modifying the input data. The function is as follows:

```
function [ sum ] = finemigrationfc10( dd )

%age group averages as estimate for a
a=[5.97028    5.63140    5.27377    5.80970    6.83248    6.92860    6.56701    6.10647
    5.71879    5.36098    4.97258    4.60495    4.39238    3.84853    3.19963    3.50048];

%parameters to be estimated
b=dd(1:16);
k=dd(17:37);
alfa = dd(38:53);
beta=dd(54:69);
teta=dd(70:90);

%centers of fuzzified emigration counts
c=[5.41079    5.4093    5.48894    5.50826    5.78390    5.8518    6.02358    5.9072
6.00843    6.12433    6.27623    6.15364    6.16165    6.12949    6.24245    6.14689
6.09667    6.15667    6.24191    6.12903    6.12466;

5.2396    5.2386    5.29437    5.30790    5.50090    5.5484    5.66872    5.58723
5.65811    5.73926    5.8456    5.75978    5.76539    5.74287    5.82196    5.75506
5.71989    5.76190    5.8215    5.7425    5.7394;

4.87836    4.87735    4.9335    4.94724    5.14205    5.19008    5.31144    5.22919
5.30073    5.38264    5.49000    5.40336    5.4090    5.38629    5.46612    5.39859
5.36309    5.40550    5.46574    5.38596    5.38287;
```

5.43774 5.4367 5.48969 5.50254 5.68579 5.73097 5.84513 5.76776
5.83506 5.91211 6.01310 5.93160 5.93692 5.91554 5.99064 5.92711
5.89372 5.93361 5.99028 5.9152 5.9123;
6.36943 6.36825 6.43411 6.45010 6.67822 6.73447 6.87659 6.78027
6.86405 6.95997 7.08569 6.98423 6.99086 6.96424 7.05773 6.97864
6.93708 6.98674 7.05728 6.96386 6.96024;
6.33289 6.33137 6.4160 6.43666 6.73015 6.80251 6.98535 6.86143
6.96923 7.09262 7.25437 7.12383 7.13236 7.09812 7.21840 7.11665
7.06318 7.1270 7.21782 7.09763 7.09298;
5.87392 5.87216 5.97073 5.99466 6.33612 6.42031 6.63304 6.48886
6.61427 6.75784 6.94602 6.79415 6.80407 6.76423 6.90417 6.78579
6.72358 6.79791 6.90350 6.76366 6.75825;
5.39286 5.39104 5.49253 5.51717 5.86874 5.95542 6.17445 6.02600
6.15513 6.30295 6.49670 6.34033 6.35055 6.30953 6.45361 6.33173
6.26767 6.34420 6.45292 6.30894 6.30337;
5.18206 5.18070 5.25703 5.27556 5.53999 5.60519 5.76992 5.65827
5.75539 5.86657 6.01230 5.89469 5.90237 5.87152 5.97989 5.88822
5.84004 5.89760 5.97937 5.87108 5.86689;
4.84445 4.84313 4.91659 4.93443 5.18891 5.25165 5.41019 5.30274
5.39620 5.50320 5.64345 5.53026 5.53765 5.50796 5.61225 5.52403
5.47767 5.53306 5.61176 5.50754 5.50351;
4.25824 4.25642 4.35802 4.38268 4.73461 4.82138 5.04063 4.89203
5.02129 5.16926 5.36321 5.20668 5.21691 5.17585 5.32001 5.19807
5.13395 5.21055 5.31939 5.17526 5.16968;
3.89019 3.88837 3.99002 4.01470 4.36684 4.45366 4.67304 4.52434
4.65369 4.80175 4.99582 4.83919 4.84942 4.80834 4.95265 4.83057
4.76642 4.84307 4.95197 4.80775 4.80217;

3.38917 3.38662 3.52930 3.56393 4.05819 4.18004 4.48795 4.27926
 4.46079 4.66860 4.94098 4.72115 4.73551 4.67785 4.88040 4.70906
 4.61901 4.72659 4.87943 4.67702 4.66919;

3.13621 3.13439 3.23570 3.26030 3.61124 3.69776 3.91639 3.76821
 3.89711 4.04466 4.23806 4.08198 4.09217 4.05123 4.19505 4.07339
 4.00945 4.08584 4.19436 4.05064 4.04508;

2.37993 2.37784 2.49442 2.52272 2.92656 3.02613 3.27772 3.10720
 3.25553 3.42532 3.64788 3.46826 3.48000 3.43288 3.59838 3.45838
 3.38480 3.47276 3.59759 3.43220 3.42581;

3.20631 3.20556 3.24740 3.25756 3.40249 3.43822 3.52851 3.46731
 3.52054 3.58148 3.66135 3.59689 3.60110 3.58419 3.64358 3.59334
 3.56694 3.59848 3.64330 3.58395 3.58165];

%spreads for fuzzified emigration counts

e=[0.62480 0.625962 0.56113 0.54539 0.32084 0.26547 0.21242 0.22039
 0.20008 0.29449 0.41825 0.31837 0.32489 0.29869 0.39072 0.31287
 0.27196 0.32084 0.39028 0.29832 0.29476;

0.174 0.174 0.174 0.174 0.174 0.174 0.174 0.174 0.174 0.174 0.174 0.174
 0.174 0.174 0.174 0.174 0.174 0.174 0.174 0.174 0.174;

0.179 0.179 0.179 0.179 0.179 0.179 0.179 0.179 0.179 0.179 0.179 0.179
 0.179 0.179 0.179 0.179 0.179 0.179 0.179 0.179 0.179;

0.29390 0.29444 0.26472 0.25751 0.15459 0.12921 0.10490 0.10855
 0.09924 0.14251 0.19923 0.15346 0.15645 0.14444 0.18662 0.15094
 0.13219 0.15459 0.18642 0.14427 0.14264;

0.208 0.208 0.208 0.208 0.208 0.208 0.208 0.208 0.208 0.208 0.208 0.208
 0.208 0.208 0.208 0.208 0.208 0.208 0.208 0.208 0.208;

0.089 0.089 0.089 0.089 0.089 0.089 0.089 0.089 0.089 0.089 0.089 0.089
 0.089 0.089 0.089 0.089 0.089 0.089 0.089 0.089 0.089;

```
0.102 0.102 0.102 0.102 0.102 0.102 0.102 0.102 0.102 0.102 0.102 0.102
0.102 0.102 0.102 0.102 0.102 0.102 0.102 0.102 0.102;
```

```
0.13647 0.13660 0.12984 0.12820 0.10481 0.09905 0.09352 0.09435
0.09223 0.10207 0.11496 0.10455 0.10523 0.10251 0.11209 0.10398
0.09972 0.10481 0.11205 0.10247 0.10210;
```

```
0.124 0.124 0.124 0.124 0.124 0.124 0.124 0.124 0.124 0.124 0.124 0.124
0.124 0.124 0.124 0.124 0.124 0.124 0.124 0.124 0.124 ;
```

```
0.14395 0.14396 0.14326 0.14309 0.14065 0.14004 0.13947 0.13955
0.13933 0.14036 0.14171 0.14062 0.14069 0.14041 0.14141 0.14056
0.14011 0.14065 0.14140 0.14040 0.14036;
```

```
0.221 0.221 0.221 0.221 0.221 0.221 0.221 0.221 0.221 0.221 0.221 0.221
0.221 0.221 0.221 0.221 0.221 0.221 0.221 0.221 0.221;
```

```
0.232 0.232 0.232 0.232 0.232 0.232 0.232 0.232 0.232 0.232 0.232 0.232
0.232 0.232 0.232 0.232 0.232 0.232 0.232 0.232 0.232;
```

```
0.60079 0.60200 0.53447 0.51808 0.28416 0.22649 0.17122 0.17953
0.15837 0.25672 0.38563 0.28159 0.28839 0.26110 0.35696 0.27587
0.23325 0.28417 0.35650 0.26071 0.25700;
```

```
0.309 0.309 0.309 0.309 0.309 0.309 0.309 0.309 0.309 0.309 0.309 0.309
0.309 0.309 0.309 0.309 0.309 0.309 0.309 0.309 0.309;
```

```
0.278 0.278 0.278 0.278 0.278 0.278 0.278 0.278 0.278 0.278 0.278 0.278
0.278 0.278 0.278 0.278 0.278 0.278 0.278 0.278 0.278;
```

```
0.652 0.652 0.652 0.652 0.652 0.652 0.652 0.652 0.652 0.652 0.652 0.652
0.652 0.652 0.652 0.652 0.652 0.652 0.652 0.652 0.652];
```

```
%objective function evaluation
```

```
sum = 0;
```

```
for x = 1:16
```

```
for t = 1:21  
  
mx = max([alfa(x),abs(k(t))*beta(x),abs(b(x))*teta(t)]);  
  
sum = sum + (a(x)+b(x)*k(t)-c(x,t))^2 + ((a(x)+b(x)*k(t)- mx)-(c(x,t)- e(x,t)))^2 + ...  
  
((a(x)+b(x)*k(t)+ mx)-(c(x,t)+ e(x,t)))^2;  
  
end  
  
end  
  
end
```



APPENDIX C: CODE FOR BAYESIAN FORECASTING

OpenBUGS code used for forecasting future emigration counts for females is given in the following lines. By modifying the input values, this code is utilized in forecasting the future values of the remaining demographic indicators as well. The corresponding code is as:

```

model {
# Priors for variables
for (k in 2:5) { c[k] ~ dnorm(0,0.0001) } # priors for constants
phi[3] ~ dnorm (0.5,1); phi[5] ~ dnorm (0.5,1) # priors for AR coefficients
theta[4] ~ dnorm (0.5,1); theta[5] ~ dnorm (0.5,1) # priors for MA coefficients
for (k in 1:5) { tau[k] ~ dgamma(0.5,0.5) } # priors for random error precisions
e[1,4] ~ dnorm(0,tau[4]); e[1,5] ~ dnorm(0,tau[5]) # artificial MA error terms for t=1

# Models
# M[1]:  $m(t) = m(t-1) + e(t)$ 
# M[2]:  $m(t) = c[2] + m(t-1) + e(t)$ 
# M[3]:  $m(t) = c[3] + \text{phi}[3] m(t-1) + e(t)$ ;  $\text{phi}[3] < 0$  &  $\text{phi}[3] < 1$ 
# M[4]:  $m(t) = c[4] + u(t) - \text{theta}[4] e(t-1) + e(t)$ ;  $\text{theta}[4] < 0$ 
# M[5]:  $m(t) = c[5] + \text{phi}[5] m(t-1) + e(t) - \text{theta}[5] u(t-1) + e(t)$ ;  $\text{phi}[5] < 0$  &  $\text{theta}[5] < 0$ 

# Priors for models
mod ~ dcat(p[]) # categorical prior over the model space
p[1] <- 0.47059; p[2] <- 0.23529 ; p[3] <- 0.11765; p[4] <- 0.11765; p[5] <- 0.05882
# Prior probabilities based on Occam's razor principle
for (t in 1:n) { for (k in 1:5) { y[t,k] <- MR[t] }
yav[t] <- MR[t] }

# Estimation of the model parameters
for (t in 2:n) { ye[t,1] <- y[t-1,1]
ye[t,2] <- c[2]+y[t-1,2]
ye[t,3] <- c[3] + phi[3] * y[t-1,3]

```

```

ye[t,4] <- c[4] - theta[4] * e[t-1,4]
ye[t,5] <- c[5] + phi[5] * y[t-1,5] - theta[5] * e[t-1,5]
for (k in 1:5) { y[t,k] ~ dnorm(ye[t,k], tau[k]);
y.f[t,k] ~ dnorm(ye[t,k], tau[k]) }
e[t,4] <- y[t,4]-ye[t,4]
e[t,5] <- y[t,5]-ye[t,5]
yeav[t] <- ye[t,mod]; yeav.f[t] <- y.f[t,mod] # averaged model
}

# Future forecasts
for (t in n+1:N) { ye.f[t,1] <- y.f[t-1,1]
ye.new[t,2] <- c[2] + y.f[t-1,2]
ye.new[t,3] <- c[3] + phi[3] * y.f[t-1,3]
ye.new[t,4] <- c[4] - theta[4] * e[t-1,4]
ye.new[t,5] <- c[5] + phi[5] * y.f[t-1,5] - theta[5] * e[t-1,5]
for (k in 1:5) { y.f[t,k] ~ dnorm(ye.f[t,k], tau[k]) }
e[t,4] <- y.f[t,4]-ye.f[t,4]
e[t,5] <- y.f[t,5]-ye.f[t,5]}
for (k in 1:5) { prob[k] <- step(mod-k)-step(mod-k-1) } # posterior p(M|x)
}

# Data sets
# Data Finland Emigration Female - Level I tetat
list( n = 21, N = 36, MR = c(0.001151342, 0.001542264, -0.001092645, -0.001057872, -
0.002021348, -0.001921898, 0.00209408, 0.000228002, 2.95435E-06, -9.17541E-06, -
0.000799638, -0.002745758, 0.001283076, 8.90195E-05, 0.002380878, -0.000280956, -
0.000614448, -0.001568347, -0.001481576, -0.000972244, 0.000980961) )

# Data Finland Emigration Female - Level II class1
list(n = 21, N = 36, MR = c(0.187569703, 0.157768086, -0.65734193, -0.066991195,
0.1739997, 0.055005497, -0.078882251, 0.290352704, 0.375566792, -0.013905729, -
0.000416715, 0.335044458, 0.148336408, 0.052066411, -0.17306647, -0.066109589, -
0.009739194, -0.103235947, -0.242618559, -0.282548356, -0.080853825) )

```

```
# Data Finland Emigration Female - Level II class2
```

```
list( n = 21, N = 36, MR = c(0.218635387, 0.163421471, -0.095917718, -0.177986032, -  
0.034868783, -0.128077812, -0.064864691, -0.171214385, 0.060101928, 0.024002423,  
0.175865403, 0.187857912, 0.037016429, 0.046365534, -0.020246043, 0.09891833,  
0.021274631, -0.150082448, -0.075460769, -0.111737156, -0.003003612) )
```

```
# Data Finland Emigration Female - Level II class3
```

```
list( n = 21, N = 36, MR = c(0.185460886, -0.036253209, -0.100139321, -0.035503914,  
0.043669979, -0.155832071, -0.158332679, -0.006928797, 0.058536706, 0.13271952, -  
0.024258806, 0.259908424, 0.069129112, 0.104586815, -0.014661452, 0.080925905,  
0.048708605, -0.101954756, -0.162311021, -0.12794656, -0.059523367) )
```

```
# Data Finland Emigration Female - Level II class4
```

```
list( n = 21, N = 36, MR = c(0.125328303, -0.091365045, -0.159541783, 0.059896828,  
0.019477667, -0.018685804, 0.067821629, 0.054245445, 0.076945901, -0.019594238,  
0.021494092, 0.073389082, 0.025612354, -0.146073566, -0.067748243, -0.005015808,  
0.146708192, 0.008263018, -0.037602164, -0.079916292, -0.05363957) )
```

```
# Data Finland Emigration Female - Level II class5
```

```
list( n = 21, N = 36, MR = c(-0.051594067, 0.057107645, 0.112953142, -0.015681021,  
0.114218812, -0.047315417, 0.038351746, -0.116814607, -0.166711251, -0.044437745,  
0.14704891, 0.095615421, -0.070460354, 0.008107284, 0.101797979, -0.211807169, -  
0.161241895, -0.024983892, 0.152483778, 0.007906004, 0.075456698) )
```

```
# Data Finland Emigration Female - Level II class6
```

```
list( n = 21, N = 36, MR=c(0.041085394, -0.009267327, 0.096918346, 0.046740725, -  
0.131485611, -0.141278503, -0.018497797, -0.016770617, 0.011261127, 0.11872525,  
0.087710591, 0.172553695, 0.354840946, 0.128989315, -0.038755896, 0.053700891, -  
0.181221277, -0.038451489, -0.049082472, -0.217004023, -0.27071127) )
```

```
# Data Finland Emigration Female - Level II class7
```

```
list( n = 21, N = 36, MR = c(-0.642487348, -0.26371062, 0.628057668, 0.162476056,  
0.090167032, 0.271295378, -0.233739694, 0.177773906, -0.135337558, -0.403820369, -
```



```
0.331210639, -0.356400831, -0.133236757, 0.101675673, 0.007886126, 0.070754189,  
0.117084852, 0.329919968, 0.089901644, 0.436454248, 0.21984842) )
```

```
# Data Finland Emigration Female - Level II class8
```

```
list( n = 21, N = 36, MR = c(-0.097069619, -0.011418327, 0.177333586, 0.038119343, -  
0.258703061, 0.181364479, 0.464619507, -0.194167829, -0.263887928, 0.222786617, -  
0.125038635, -0.751492458, -0.414762472, -0.075890434, 0.140686851, -0.00489106,  
0.03490185, 0.097001285, 0.260338122, 0.391267902, 0.188902282) )
```



APPENDIX D: MIGRATION MODELING OUTPUTS

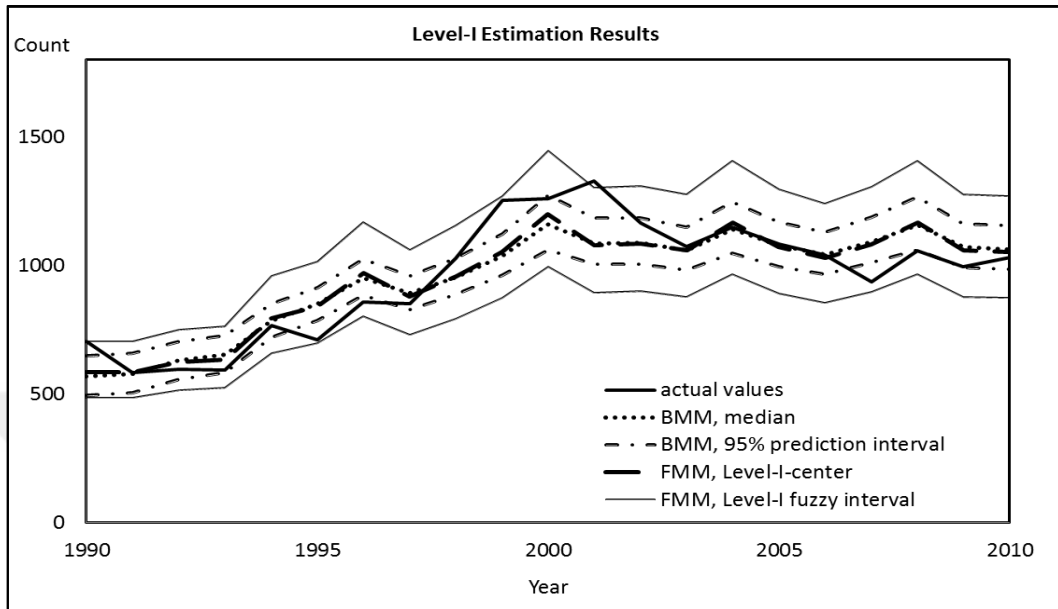


Figure D.1. Emigration modeling estimates for age group [20,25), males, using 1990-2010 data: FMM with Level I versus BMM

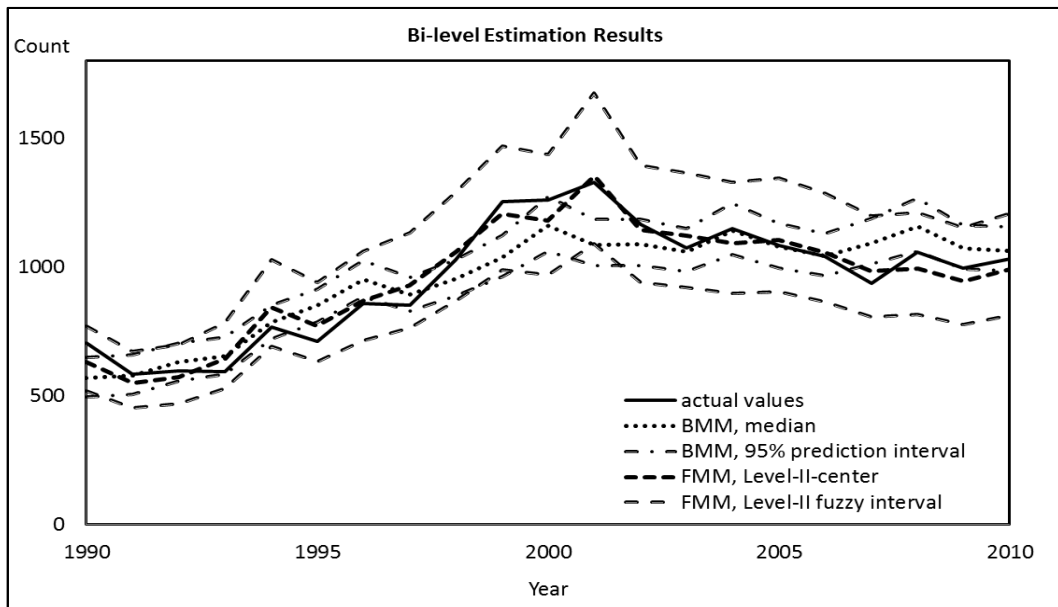


Figure D.2. Emigration modeling estimates for age group [20,25), males, using 1990-2010 data: bi-level FMM versus BMM

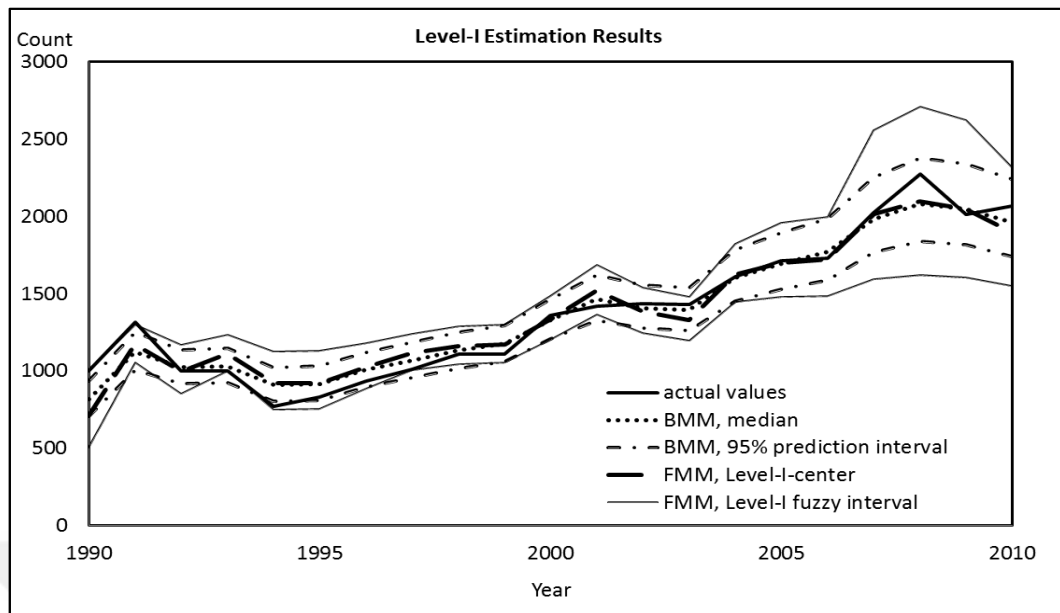


Figure D.3. Immigration modeling estimates for age group [20,25), females, using 1990-2010 data: FMM with Level I versus BMM

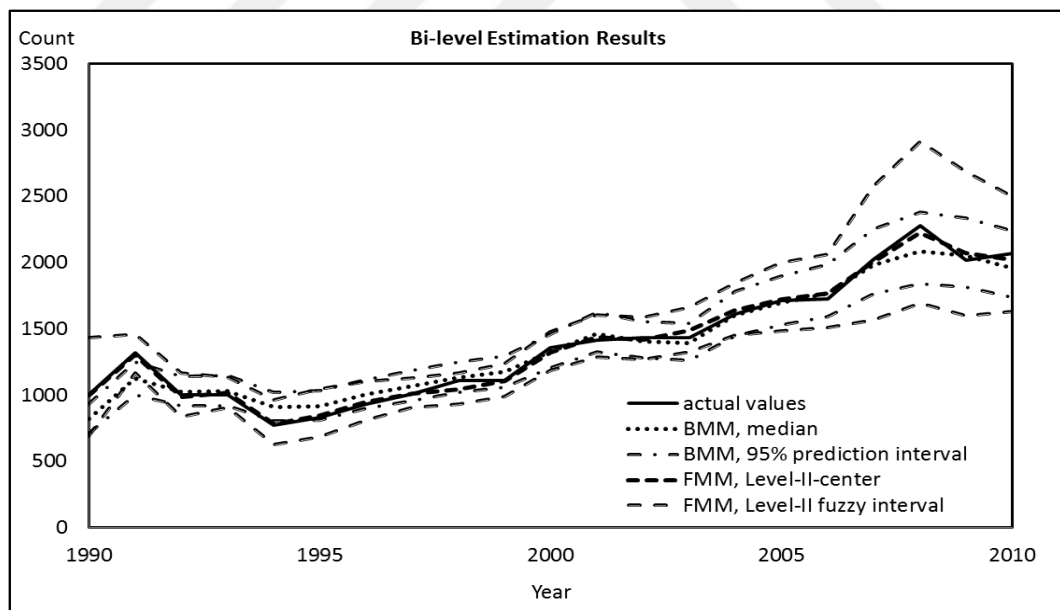


Figure D.4. Immigration modeling estimates for age group [20,25), females, using 1990-2010 data: bi-level FMM versus BMM

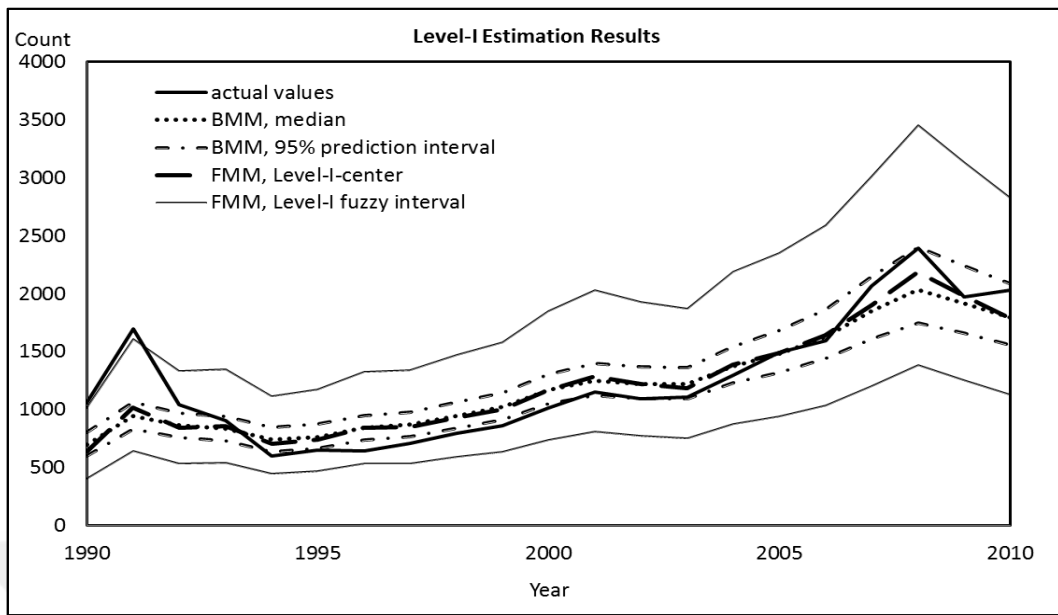


Figure D.5. Immigration modeling estimates for age group [20,25), males, using 1990-2010 data: FMM with Level I versus BMM

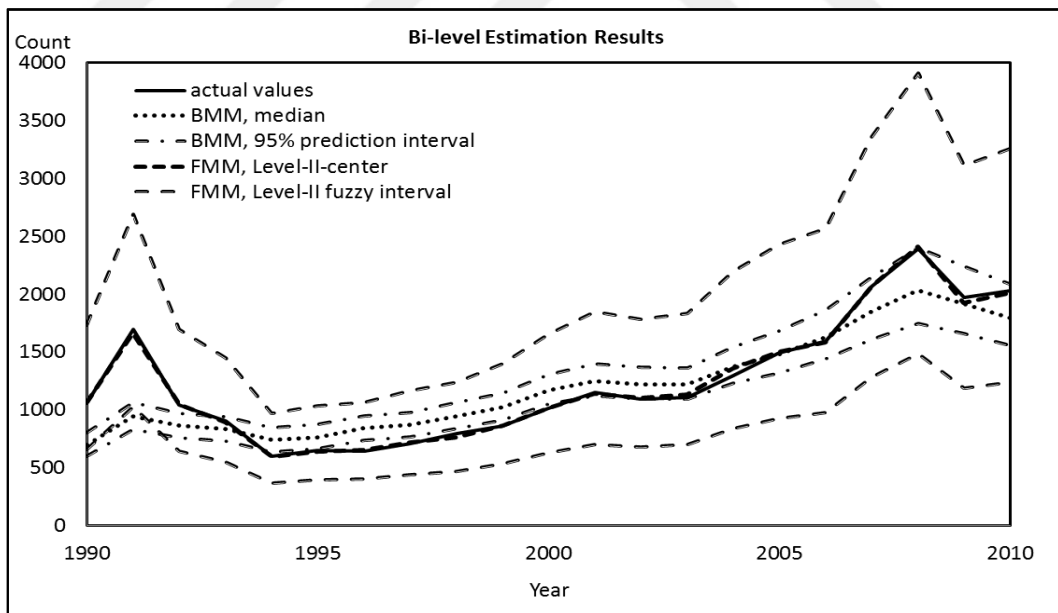


Figure D.6. Immigration modeling estimates for age group [20,25), males, using 1990-2010 data: bi-level FMM versus BMM

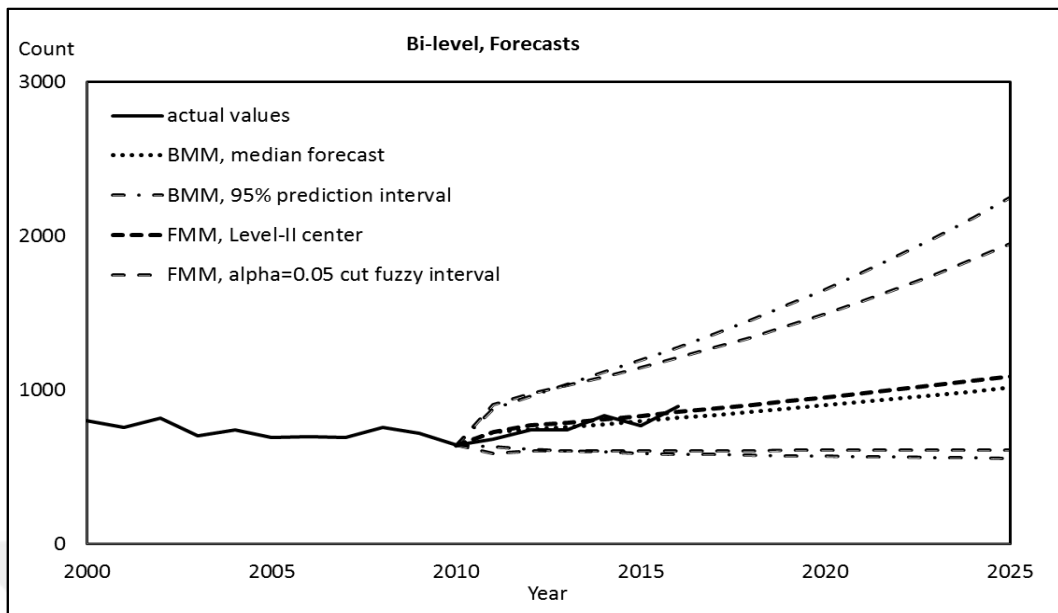


Figure D.7. Emigration forecasts for age group [20,25), males

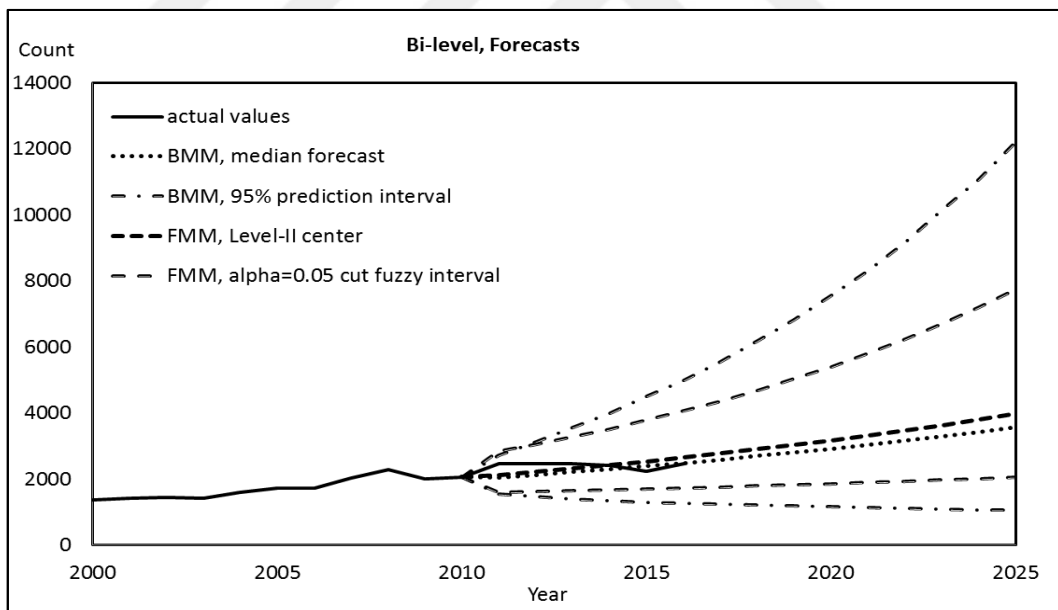


Figure D.8. Immigration forecasts for age group [20,25), females

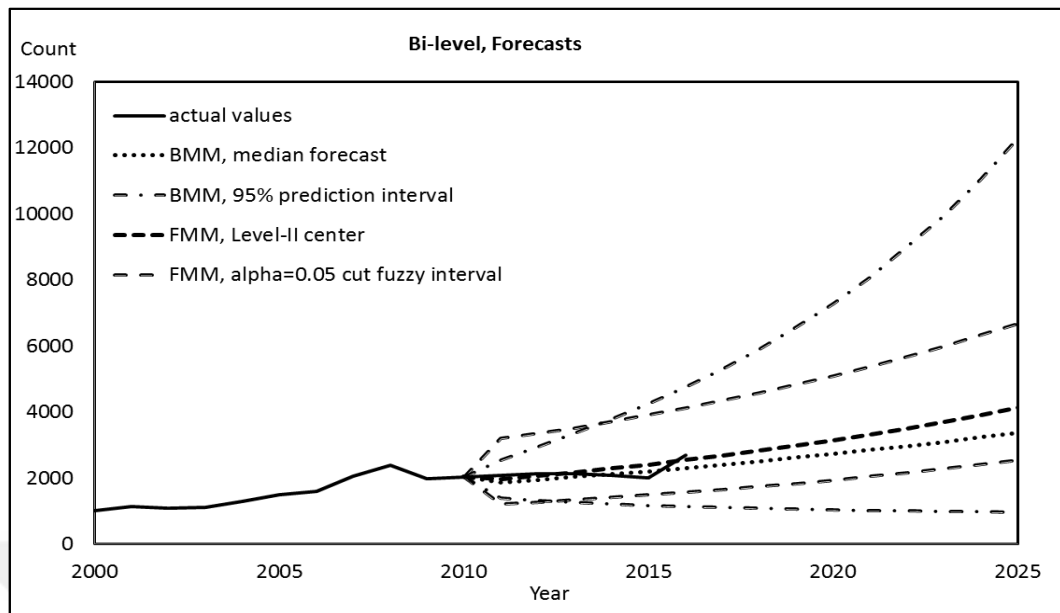


Figure D.9. Immigration forecasts for age group [20,25), males